ABSTRACT

Title of Dissertation / Thesis: A THERMODYNAMIC INVESTIGATION INTO THE ALLOSTERIC ACTIVATION MECHANISM OF THE BIOTIN REPRESSOR

Patrick H. Brown, Ph.D., 2004

Dissertation / Thesis Directed By: Professor Dorothy Beckett, Department of Chemistry and Biochemistry

The biotin regulatory system of *Escherichia coli* serves as a model for investigating the regulatory mechanism of a non-classical allosteric transcription factor. The central protein, BirA, functions as both an essential metabolic enzyme in biotin retention and as a repressor of transcription initiation. In its repressor function, two BirA monomers bind a 40-base pair palindromic DNA sequence thereby blocking transcription initiation at the two divergent overlapping promoters of the biotin biosynthetic operon. Binding of the small molecule corepressor, biotinyl-5'-AMP, promotes the assembly of the transcription repression complex by driving the self-association of the repressor. Here, the effects of binding of four corepressors on the self-association and DNA binding properties of BirA have been measured utilizing sedimentation equilibrium and DNaseI footprinting analyses. The results of this study indicate that biotinyl-5'-AMP and an ester analog, biotinol-AMP, are strong allosteric activators of BirA dimerization. The enhancement observed in the energetics of DNA binding closely matches with the enhancement of self-assembly of the repressor. Biotin and a sulfamoyl corepressor analog are weak allosteric effectors of BirA dimerization. Binding of the weak effectors, results in an uncoupling of

the self-association and DNA binding processes. A detailed thermodynamic investigation of the effector binding process was performed utilizing isothermal titration calorimetry. Binding of all four corepressors to BirA is an enthalpically driven process. However, the higher affinities for binding of the strong effectors are characterized by a relatively moderate binding enthalpy and a favorable entropic term. Whereas binding of the weak effectors is comprised of a much larger enthalpic contribution and is entropically opposed. Heat capacity changes for binding of the four effectors to BirA were determined by measuring the temperature dependence of the binding enthalpy. Results of the analysis indicate that a negative heat capacity change is associated with binding of each effector. No correlation is observed between the magnitude of the heat capacity change and the magnitude of the effect the corepressor has on the self-assembly of BirA. Finally, conditions were identified and utilized for the crystaliztion of BirA·biotinol-AMP. The crystals obtained are currently being analyzed by X-ray diffraction in a collaborative effort.

A THERMODYNAMIC INVESTIGATION INTO THE ALLOSTERIC ACTIVATION MECHANISM OF THE BIOTIN REPRESSOR.

By

Patrick H. Brown

Dissertation submitted to the Faculty of the Graduate School of the
University of Maryland, College Park, in partial fulfillment
of the requirements for the degree of
Doctor of Philosophy
2004

Advisory Committee:

Professor Dorothy Beckett, Chair
Professor Jeffrey Davis
Assistant Professor Lyle Isaacs
Professor George Lorimer
Assistant Professor Sergei Sukharev

Table of Contents

List of Tables

List of Figures

I. General Introduction

The research outlined in this thesis is focused toward a better understanding of the physical mechanism of an allosterically regulated prokaryotic transcription repressor. Specifically, the goal is to elucidate the structural and dynamic changes that occur in the *E. coli* biotin repressor upon binding of a small molecule effector, which activates it for its repressor function. A brief introduction has been included to put this contribution into a broader context. The topics covered in the introduction are intended to provide the reader with a general background for understanding what a transcription repressor is and how it may be allosterically regulated. Brief reviews of specific prokaryotic transcription factors follow.

A. Repression of transcription initiation

In order to thrive, an organism must adapt rapidly and specifically to changes in its environment such as the flux in the concentration of available nutrients. This process may require the increased or decreased expression of appropriate genes that enable the organism to respond to those changes. For example, *C. diphtheriae* express iron-binding proteins to sequester iron from the environment for biological functions. An excess of iron in the cell however, would result in the formation of highly reactive hydroxyl radicals that damage DNA and many other biological molecules (*3*). Insufficient iron uptake however, is a signal for the cell to express virulence factors. It is important then, that expression of these iron-uptake genes is regulated such that the appropriate levels of products are present to respond to the specific environmental circumstance.

Gene expression occurs in two steps that together form the "central dogma" of biology: DNA makes RNA makes Proteins. Transcription is the process by which genes encoded in a DNA sequence are converted into RNA strands while translation is the conversion of the RNA into cognate proteins:

$$\text{DNA} \rightarrow \text{RNA} \rightarrow \text{Proteins}$$

$$\text{Transcription: DNA} \rightarrow \text{RNA}$$

$$\text{Translation: RNA} \rightarrow \text{Proteins}$$

The enzyme responsible for transcription, RNA polymerase, is about 500 kDa in size and contains 5 subunits ($\alpha_2\beta\beta'\sigma$). One of the subunits, the σ-factor, is loosely bound to the core enzyme and dissociates from the enzyme-DNA complex after the start of transcription. The primary function of the σ-factor is recognition of the promoter locus, which is the region of the operon that signals the start of transcription. Most promoter sequences contain A-T-rich regions of base pairs and often occur 35 and 10 base pairs upstream from the start of transcription. Initiation requires the binding of the holoenzyme (the core polymerase plus σ-factor), and the unwinding of the double helix forming an "open complex" for incorporation of nucleoside triphosphates. Elongation of the RNA strand proceeds as a transcription bubble moves along the DNA sequence to be copied. Termination of transcription occurs at termination sequences and results in the release of the completed RNA strand from the complex.

Transcription initiation in prokaryotic organisms is regulated by the action of two classes of transcription factors: activators and repressors. Activators function to enhance

transcription initiation, while repressors inhibit the process. Activators bind DNA at or immediately upstream of promoters which are usually near or overlapping operator sequences. Binding of the activator to the promoter region leads to stabilization of the polymerase-DNA interaction. The bound polymerase inhibits the repressor from binding at the overlapping operator sequence and prompts the initiation of transcription. Conversely, repressors bind to the operator sequence and partially block the binding site for the polymerase, thereby preventing transcription initiation.

Many transcription factors function in DNA binding either as monomers(*4*) or as higher order homo- and hetero- oligomers(*5*). However, an analysis of structural data, reported between January 1999 and November of 2001, revealed that most prokaryotic transcription factors are homodimers that bind to palindromic or pseudopalindromic DNA sites (*6*). All but one of the transcription factors analyzed in that report contain a helix-turn-helix (HTH) DNA-binding motif (*6, 7*). This secondary structural element consists of two α-helices packed together at an angle of 120º (Figure 1). Linking them, is a four-residue turn in which the second position is usually a glycine. Finally, a third α-helix stacks against the first two and stabilizes the fold into one compact globular domain. The second helix, or the "recognition helix", binds within the major groove of DNA and is responsible for the specificity of the motif for a single half-site of a symmetric/pseudo symmetric transcription control sequence. Oligomerization of transcription factors provides for multiple recognition elements with which to stabilize the protein-DNA interaction.

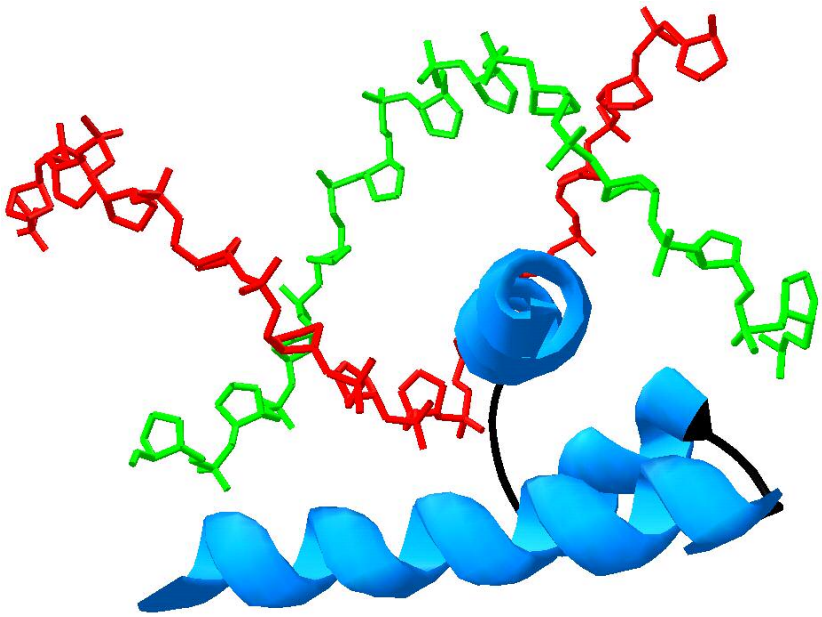

Figure 1. The helix-turn-helix motif. The recognition helix of the helix-turn-helix (HTH) motif fits within the major groove of the DNA backbone. This figure represents the N-terminal domain of the tryptophan repressor monomer (blue helices) bound in the major groove of its cognate operator sequence. For clarity, only the phosphate sugar backbone is shown (red and green strands). The model was generated using Deep View-The Swiss Pdb-Viewer (v. 3.7) and the Protein Data Bank file 1TRO as input (*1*).

B. Allosteric Regulation of Transcription Factors

The concept of regulating protein function through allostery surfaced from research on feedback inhibition in the 1960's (*8, 9*). It was suggested that there was a regulatory site on a protein that was distinct from the catalytic site. Further, the catalytic activity of a protein could be attenuated, by binding of an inhibitor at that distant regulatory site. This interaction at a distance could be explained by a mechanism in

which a conformational change in the protein accompanied binding at the regulatory site which inactivated the protein at the catalytic site (*10, 11*). Monod called this regulatory site an "allosteric" binding site (*12, 13*).

The DNA binding properties of many transcription factors are regulated through allosteric control. Generally, there are two classes of allosteric transcription repressors with respect to the influence the effector has on the repressor's affinity for site specific DNA binding (Figure 2). In the first class, the repressor exists as a preformed oligomer that has its affinity for DNA altered upon binding of an inducer or a corepressor. The altered affinity is a result of the effector having stabilized a conformational rearrangement of the DNA recognition elements in the repressor. A change in the population of the effector-bound conformer affects the level of occupancy of the operator site. The lactose (LacR), purine (PurR), and tryptophan repressor systems (TrpR) are all examples of this class of transcription regulators. In the second class, binding of the effector perturbs the self-assembly properties of the repressor. The altered oligomer equilibrium results in changes in the population of the active state of the protein, which in turn affects the level of occupancy of the operator site. Examples of this class of allosteric transcription regulators include the leucine responsive protein (Lrp), the diphtheria toxin repressor (DtxR) and the biotin repressor (BirA).

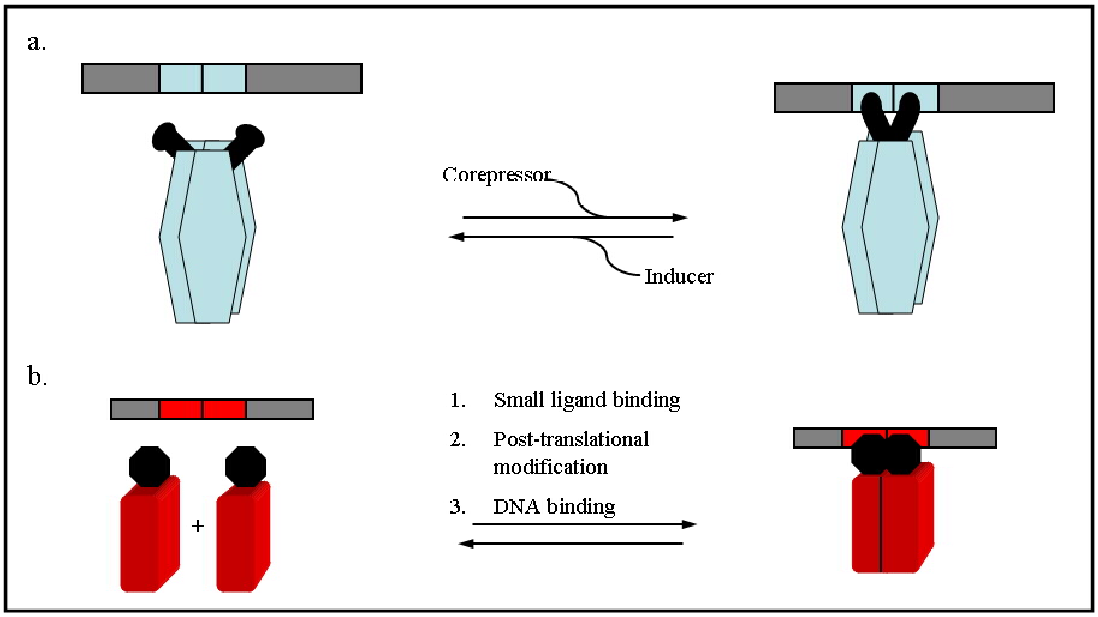

Figure 2. Classical *vs*. non-classical mechanism of allosteric regulation. A representation of the two classes of allosteric transcription regulators with respect to the influence the effector has on DNA binding affinity. In the classical paradigm of allostery (a) the repressor exists as a preformed oligomer. Binding of an effector alters the relative orientations of the repressor's DNA binding elements. In the second class (b) binding of an effector (or the input of some other allosteric signal) influences the self-assembly state of the repressor.

Because gene regulation is such a vital biological process for all organisms, much research has been focused toward its understanding and hence the role of allostery in transcription regulation. Many physical biochemists are interested in the mechanisms by which protein function is modulated- that is, how the structural and dynamic properties of a protein relate to its function. A combination of approaches is utilized to elucidate the changes that occur in the repressor throughout the allosteric transition. Structural information obtained from crystallography or nuclear magnetic resonance spectroscopy,

which often helps define initial and final states as well as intermediates, is utilized to formulate models that describe the mechanism of activation of the repressor. Solution biophysical methods further aid in testing and revising the proposed models.

1. Classical Mechanism

a. The Lactose Repressor (LacR)

The pioneering research of Jacob and Monod on the lactose Repressor led to the theory of gene regulation over 40 years ago (*14*). The Lac Repressor regulates expression of the *lac* operon (Figure 3) in response to the presence of lactose. Cellular conditions in which lactose is present result in the expression of the *lac* operon. Conditions in which lactose is not present result in the repression of transcription of the *lac* genes. The proteins encoded in the operon include thiogalactoside transacetylase (*lac*A), galactoside permease (*lac*Y), and β-galactosidase (*lac*Z). While the function of the transacetylase is not well understood, the permease mediates active transport of lactose into the cell, and β-galactosidase is responsible for hydrolysis of the glycosidic linkage between galactose and glucose, the component sugars of lactose. The physiologically active inducer however is not lactose but rather, allolactose a side product of its metabolism. Isopropyl-β- D-thiogalactoside (IPTG), a non-metabolizable mimic of allolactose, can be utilized in the laboratory to induce overexpression of genes that have been fused to the *lac* operator/promoter. The principal operator, O_1, has been determined to be a 27-base pair fragment with approximate dyad symmetry that is centered 11 base pairs downstream from the start of transcription of the *lac*Z gene (*15*). The *lac* operon has two auxiliary

operators O_2 and O_3; all three operators are necessary for maximum repression *in vivo* (*16*).

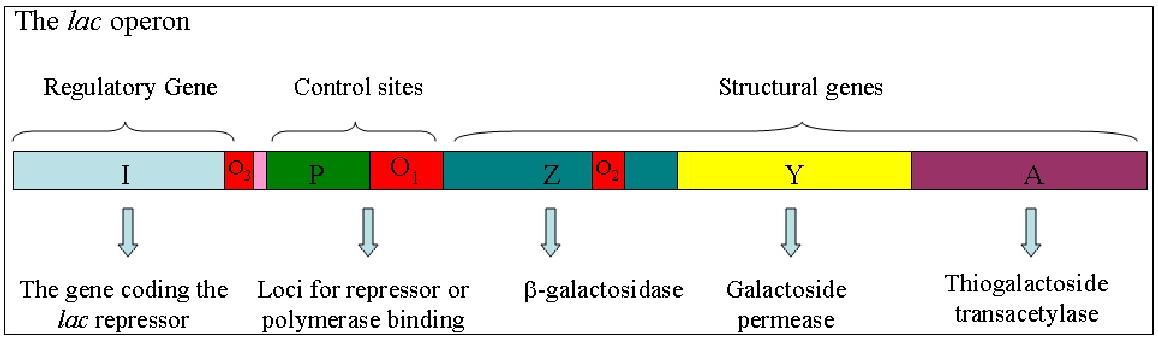

Figure 3. A schematic representation of the lac operon. In the absence of inducer, LacR, the product of the *lac*I gene, binds to the operator sequence (O_1-O_3) to block initiation of transcription of the operon. In the presence of lactose, LacR dissociates from the control site allowing access for RNA polymerase to bind at the promoter (P) to initiate transcription.

There is a vast amount of data from years of genetic and biochemical studies on this system, but only recently have structures of the repressor bound to the operator become available (*17, 18*). Several crystal structures have been obtained for various bound states of the repressor that help elucidate conformational changes that occur in the repressor upon inducer and DNA binding. An X-ray crystal structure is available for the intact LacR, the LacR bound to IPTG, and the LacR bound to a 21bp DNA sequence (4.8 Å) (*18*). Additionally, structures of a dimeric LacR in complex with an anti-inducer, orthonitrophenyl-fucoside (ONPF), and a symmetric operator sequence has been obtained at 2.6 Å resolution (*2*) (Figure 4).

The Lac Repressor is a 155 kDa tetrameric protein that can most conveniently be described as a dimer of dimers. Each monomer is composed of 5 separate structural units. The N-terminal "headpiece" (residues 1-49) domain has a helix-turn-helix (HTH) motif that binds in the major groove of the operator sequence. The "hinge" helix (residues 50-58) binds to the center operator (in the minor groove) inducing a 40º bend. In the absence of DNA, this hinge region is unfolded and residues 1-61 move freely with respect to the core. The core domain (residues 62-333) is divided into two subdomains: the NH_2-subdomain (residues 62-161 and 293-320) and the CO_2H-subdomain (residues 162-289 and 321-329), at the interface of these subdomains is where inducer binds. Finally, there is a C-terminal α-helix (residues 340-357) that associates to a four-helix bundle comprising the tetramerization domain. Deletion of this domain results in a stable dimeric repressor (*2*) (Figure 4).

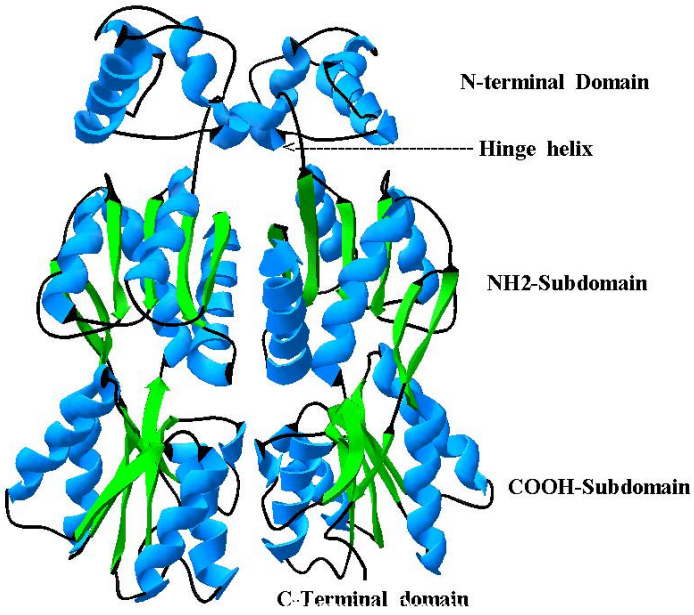

Figure 4. A model of the three-dimensional structure of the dimeric LacR determined by X-ray crystallography (*2*). For clarity, the operator sequence and ONPF ligands have been omitted. The model was generated using the graphics program DeepView-The Swiss-Pdb Viewer (v. 3.7) with the Protein Data Bank file 1JWL as input.

Comparison of the structure of the induced repressor (IPTG) with structure of the DNA-bound repressor led to a model that explained how IPTG binding destabilized the protein-DNA interaction (*18*). The model states that binding of the inducer sugar to the repressor results in a small hinge movement of the NH_2-subdomain of the central core in relation to the CO_2H-subdomain. This movement causes the hinge helices of the N-terminal domain to be displaced from the minor groove of the DNA operator sequence. This displacement destabilizes the protein-DNA interaction and results in dissociation of the repression complex. In the structure of the induced form of the repressor there are three electrostatic interactions in the NH_2-subdomain across the dimer interface that are

not present in the structure of the DNA-bound conformer. IPTG most likely stabilizes these electrostatic interactions in the induced form, which results in dissociation of the repression complex. This model is supported by a biochemical study wherein a disulfide bridge was introduced connecting the hinge helices of an engineered dimeric repressor in order to prevent the hinge motion upon inducer binding. This mutation disrupted the allosteric effect of IPTG (*19*).

Additional evidence suggests that the mechanism may involve more than just a simple hinge movement that displaces the hinge helix from the minor groove of DNA upon NH_2-subdomain reorientation. In one set of experiments, 1 to 3 glycine residues were introduced by mutation into the region between the hinge helix and the core domain, thereby extending the linker region between domains. These insertions were expected to uncouple the propagation of the allosteric signal from the two domains upon IPTG binding. However, the insertion mutants were still responsive to IPTG. This result suggests that other interactions between the two domains may also be involved in transmitting the allosteric signal (*20*).

Results from an additional set of experiments implicate the involvement of an ion pair between residues within the monomer-monomer interface in transmission of the allosteric signal (*21*). The His74-Asp278 interaction is present in the structure of the IPTG bound repressor but is not present in the DNA-bound structure (*18*). Mutation of the Asp278 residue resulted in a diminished response to the inducer.

Despite the availability of a large volume of genetic, biochemical, and structural data, there remains an incomplete picture of the physical mechanism governing the allosteric response of the Lac repressor to inducer. However, it is one of the most extensively utilized transcription factors and remains a model system for understanding protein-DNA interactions and allosteric control of transcription repressors.

b. The Tryptophan Repressor (TrpR)

The Trp Repressor regulates transcription of a series of operons encoding gene products responsible for aromatic amino acid biosynthesis in response to L-tryptophan (L-trp) levels. Expression of the *trp*EDCBA operon, which encodes the enzymes utilized in L-tryptophan biosynthesis from chorismate, is repressed in the presence of L-tryptophan. The structure of the apoTrpR was obtained in 1987 at 1.8 Å resolution (*22*). The TrpR was the first transcription factor for which a crystal structure was obtained for the protein:DNA complex (*1*). A second structure of the repressor bound to DNA was available in 1993 (*23*). In addition to this structure, several other X-ray structures of the apo repressor and holo repressor are available (*24*, *25*). Additionally, NMR structures for the apo, holo, and operator-bound repressor are available (*26-28*). TrpR is a 12.2 kDa (107 residues) protein that functions as a homodimer. Each monomer is composed of a C-terminal domain and an N-terminal HTH DNA binding domain (Figure5). A hydrophobic core stabilizes the dimerization interface formed by packing of the three α-helices of the C-terminal domain of each monomer.

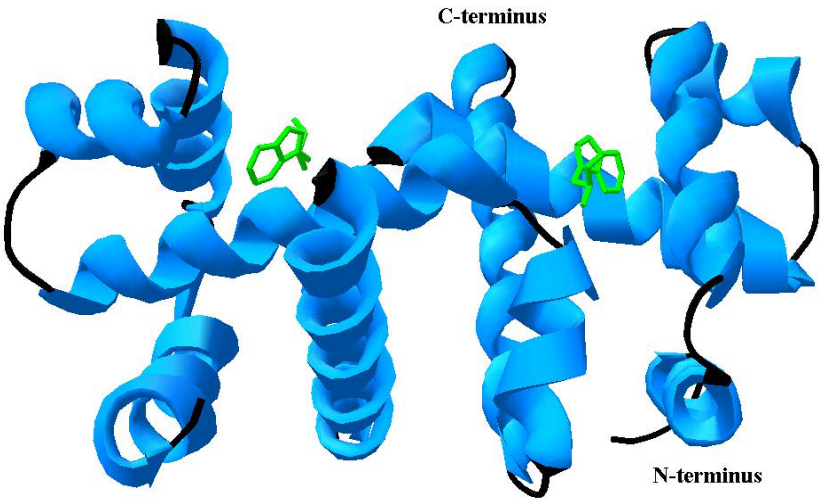

Figure 5. A model of the three-dimensional structure of TrpR bound to L-tryptophan determined by X-ray crystallography (*1*). The model was generated using the graphics program DeepView-The Swiss-Pdb Viewer (v. 3.7) and the Protein Data Bank file 1TRO as input.

Comparison of the apo and holoTrpR structures led to a model for the mechanism of L-trp activation of the TrpR. The model states that the effector binds to the repressor and acts like a wedge between the core domain and the DNA binding domain positioning the recognition helix of each monomer in the proper geometry for tight, complimentary alignment with the two operator half-sites (*22*). Other experimental evidence indicates that the mechanism may be more complicated than the L-trp acting as a wedge. NMR studies indicate that the HTH domain exists in a partially folded state in the apo repressor but is completely folded upon binding of L-trp. This results suggests that protein folding accompanies effector binding (*28*). Calorimetric measurements indicate a heat capacity change for L-trp binding that is larger than that expected from calculations for a rigid

body association, a result consistent with folding coupled to binding (*29*). A spectroscopic and calorimetric investigation of superrepressor mutants further supports the mechanism of a folding transition coupled to L-trp binding. The investigators suggest that L-trp binding induces the folding of portions of the HTH domain which alters the conformation of the recognition helix and leads to tighter DNA binding (*30*). Binding of L-trp to the repressor is energetically favorable (ΔG^o = -6.4kcal/mol) due to contributions from a large favorable enthalpy (ΔH^o = -11.7kcal mol) and an unfavorable entropy term (-$T\Delta S^o$ = 5.3 kcal/mol). In contrast, binding of L-trp to a superrepressor mutant exhibits a more favorable entropic contribution (-$T\Delta S^o$ = 1.5 kcal/ mol). This entropic difference suggests that the mutation structurally preorganizes the superrepressor for tighter DNA binding relative to wild type. Therefore a smaller entropic penalty is paid for binding of the corepressor.

In summary, the Lac Repressor functions in DNA binding as a homotetramer. Binding of inducer sugars results in the movement of the hinge helices from the minor groove of the transcription control region of the operon. This movement destabilizes the protein-DNA interaction and results in dissociation of the tetrameric repressor from the operator sequences. Dissociation of the repressor results in transcription of the operon. The TrpR functions in DNA binding as a homodimer. Binding of L-trp to the protein dimer results in the movement of the recognition helix of each monomer. The effector-bound conformation of the repressor has a higher affinity for the operator than does the unliganded conformer. An increase in the population of holorepressor results in a higher occupancy of the operator and thus repression of transcription of the operon. In both

cases it is the orientation of the repressor's DNA binding elements that is modulated by effector binding and not its oligomeric state.

2. Non-Classical Mechanism

In contrast to the classical allosteric transcription regulatory systems are the diphtheria toxin repressor, the leucine responsive protein, and the biotin repressor. In these systems binding of a small molecule effector alters the self-assembly properties of the repressor. The change in the assembly energetics of the oligomer is coupled to the overall assembly energetics of the transcription repression complex. Therefore, repressor self-assembly results in changes in the level of occupancy of the operator.

a. Diphtheria Toxin Repressor (DtxR)

The diphtheria toxin repressor is the best characterized member of a family of related proteins in bacteria that regulate metal-sensitive genes and is an example of a non-classical allosteric transcription regulator. DtxR controls transcription of the *tox* operator for production of diphtheria toxin and the siderophore corynebactin in response to iron levels. It has also been found to regulate a heme oxygenase (hmuO) and five other iron regulated operators (IRP1- IRP5). DtxR functions as a homodimer. In the presence of iron, DtxR forms a complex and binds to the *tox* operator to block transcription. The operator sequence, as identified in electrophoretic mobility-shift assays (EMSA), and DNaseI and hydroxyl radical footprinting techniques (*31-34*), is composed of an interrupted imperfect inverted palindrome spanning about 30-base pairs. While Fe^{2+} is

the physiological corepressor, several other divalent cations have been shown to allosterically activate DtxR *in vitro* including Ni^{2+}, Co^{2+}, Mn^{2+}, Cd^{2+} and Zn^{2+}.

Structural data are available from several X-ray studies of apoDtxR and holoDtxR (both wt and mutants) bound to various divalent metal ions (*35-40*). Additionally, structures of the holorepressor (Co^{2+}, Ni^{2+}) bound to a DNA sequence similar to the *tox* operator is available (*41, 42*). Each monomer is a 226-amino acid polypeptide with a molecular weight of 25.3 kDa that is composed of three domains (Figure 6). Domain 1 (residues 1-73) contains a HTH DNA binding motif. Domain 2 (residues 77-144) contains the dimerization domain and two metal binding sites. The metal in site 1 is tetrahedrally coordinated to the sidechains of His79, His98, Glu83, and the oxygen atom of a sulfate anion. The metal in site 2 is coordinated to a water molecule, the carbonyl oxygen of Cys102, and the sidechains of Glu105, His106. Interestingly, this site is not occupied in all available crystal forms. Domain 3 (residues 145-226) is less ordered in all structures indicating more mobility. This portion of DtxR exhibits a Src homology 3 (SH3)-like fold, and its function in repressor activity is a topic of debate (*40, 43*).

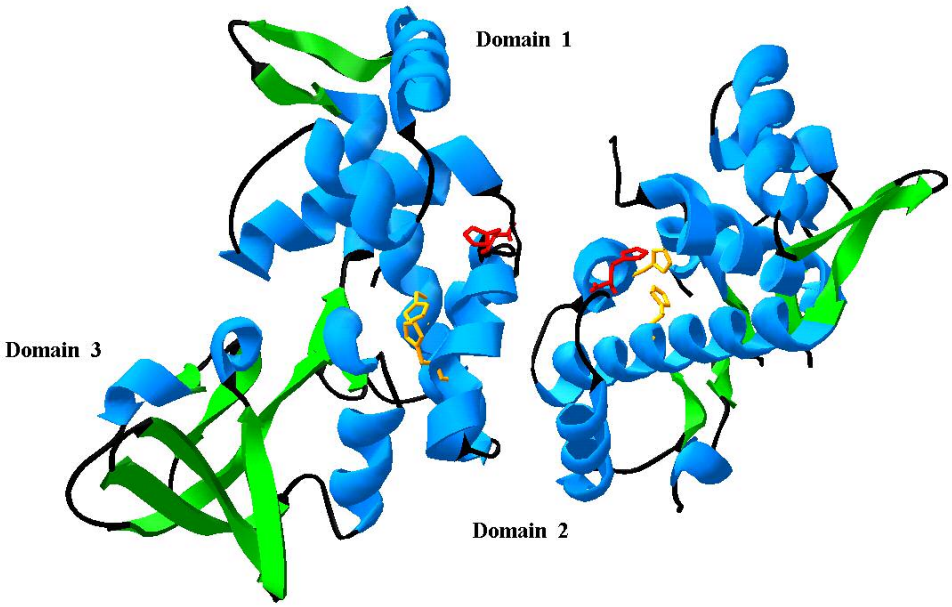

Figure 6. A model of the three-dimensional structure of the diphtheria toxin repressor bound by Co^{2+} obtained from X-ray crystallography (*41*). The histidine side chains in the metal binding sites are shown in orange (site 1) and in red (site 2). The figure was generated using DeepView- The Swiss-Pdb Viewer (v. 3.7) with the Protein Data Bank file 1COW as input.

In contrast to the structural model proposed from X-ray diffraction data, NMR studies indicate that the N-terminal portion of the repressor (Domains 1 and 2) appears less ordered in solution than what has been observed in the solid state (*44*, *45*). While resonances for the first 124 amino acids of apoDtxR(C102D) are not observed at 30 ºC, some are visible at 4 ºC. Moreover, when Cd^{2+} is present, substantial changes in the NMR spectrum occur including the sharpening of some resonances and the appearance of additional well-defined peaks. These results suggest that the aporepressor exchanges

between different conformational substates on an intermediate time scale, and that metal binding results in the ordering of the N-terminal domains.

An analysis of the self-association properties of the apo and Co^{2+}-bound repressor was performed using sedimentation equilibrium measurements (*46*). Although, the data could not be described by a monomer-dimer equilibrium model, the dimerization constant of the unliganded repressor was estimated to be in the low micromolar concentration range. The average apparent molecular weight calculated from this data (39 kDa) was independent of loading concentration, below 4 μM, and non-ideal behavior was observed to occur at higher protein loading concentrations. The authors indicated that metal contamination within the charcoal-epon centerpieces contributed to slight dimerization of the apo repressor, despite the addition of the chelator, EDTA. The estimated value for the K_d therefore must be considered a lower limit. Finally, data obtained for sedimentation of Co^{2+}-DtxR was fit to a monomer-dimer equilibrium model and indicated that metal binding shifts the dimer dissociation constant from low micromolar to 33 nanomolar (*46*). Additionally, non-denaturing polyacrylamide gel electrophoresis (PAGE) was utilized to probe the self-assembly properties of the repressor in the presence and in the absence of saturating amounts of Ni^{2+} (*44*). These studies indicated that the apo repressor, DtxR(C102D), had a significant dimer component at a loading concentration of 10 μM. The addition of 30 mM Ni^{2+} resulted in essentially complete dimerization of the repressor. Together, these results indicate that metal binding promotes self-assembly of the repressor.

Comparison of the apo and holoDtxR X-ray structures has provided evidence of only slight conformational changes that might be essential for corepressor-regulated repressor function. Two mechanistic models however have emerged from these structural analyses. The "caliper" model proposed by Schiering *et al*(*37*) states that binding of effector brings about a transition in the dimer where the monomers rotate toward each other by 2º with the metal binding sites being near the axis of rotation. This rotation causes the N-terminal recognition helices to move closer to each other to a distance of about 30 Å. Alternatively, the "hinge" model is proposed to consist of a bending motion of the DNA binding domain with respect to the dimerization domain as a result of metal binding (*40*). This rigid-body motion results in movement of the recognition helices respective to each other and is proposed to be critical for obtaining an optimal conformation for interacting with its cognate DNA.

Comparison of circular dichroism spectra of apo and Ni^{2+}-DtxR(C102D) and DtxRwt, with and without Ni^{2+}, indicates the absence of any significant structural differences between the metal-bound and unliganded forms. This result is consistent with the crystallographic data where only minor structural changes were observed. However, the NMR studies indicate that metal binding drives a disorder-to-order transition in the N-terminal domains. This transition does not include a change in secondary structural elements but rather a transition from a mobile globular state to a more ordered conformation that is responsible for enhanced dimerization and DNA binding (*44*).

In summary, the DtxR dimer has been shown to be the physiologically active form of the repressor. Metal binding drives the dimerization of the repressor. Comparison of crystal structures of the apoDtxR dimer and several holoDtxR dimers indicates only small conformational differences in the unbound and bound forms, while solution studies indicate the activation process is more complicated.

b. Leucine Responsive Protein (Lrp)

The leucine responsive protein (Lrp) serves as a global regulatory protein in prokaryotes (*47*). It serves to regulate several operons, often in response to L-leucine levels. The genes that are regulated by Lrp mainly code for proteins involved in transport, degradation, or biosynthesis of amino acids. A recent DNA microarray analysis indicates that Lrp affects transcription of at least 10% of all *E. coli* genes (*48*). It can serve as an activator of transcription in some cases or as a repressor in others. It appears to stimulate expression of operons involved in biosynthetic pathways and to repress transcription of operons that function in catabolic pathways.

The structure of the Lrp protein from *P. furiosus* (LrpA) has recently been determined by X-ray crystallography to 2.9 Å resolution (*49*). The crystal structure indicates that the protein folds into two domains and is octameric. The N-terminal domain contains an HTH motif that is proposed to be responsible for DNA binding (Figure 7). The C-terminal domain has a four-stranded antiparallel beta sheet flanked on one face by two alpha helices and a short C-terminal beta strand. A beta strand separates the two domains. The octamer is best described as a tetramer of dimers. The dimer

interface consists primarily of a hydrophobic core formed by stacking of the beta sheets of the C-terminal domain of each monomer. Additional contacts are made in the N-terminal domain and between the domain-linking beta strands. The C-terminal domain is also the region of contact for the assembly of dimers to form octamers.

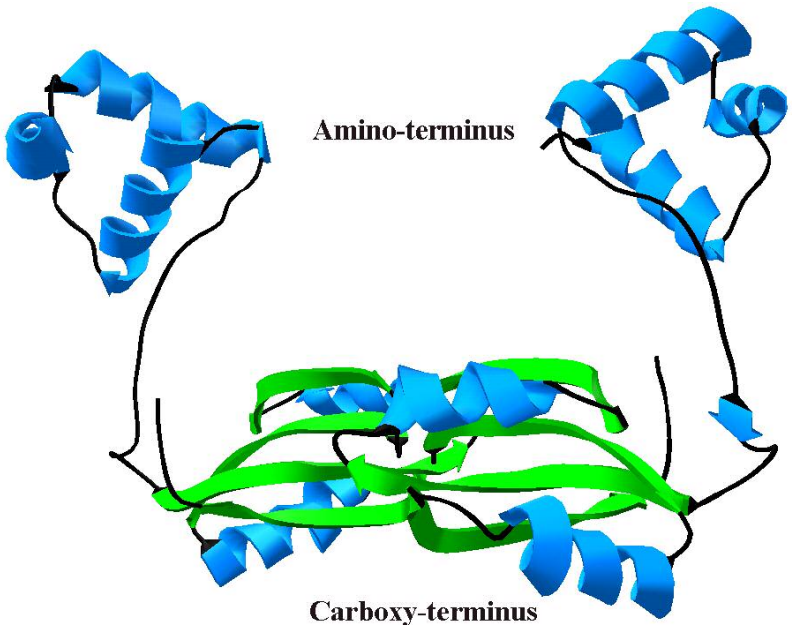

Figure 7. A model of the three-dimensional structure of the LrpA dimer from *P. furiosis* obtained from X-ray crystallography (*49*). The figure was generated using DeepView-The Swiss-Pdb Viewer (v. 3.7) with the Protein Data Bank file 1I1G as input.

Initially *E. coli* Lrp was isolated and purified and reported to exist as adimer in the cell (*50*). The evidence for the dimeric species was obtained from gel filtration of the purified protein extract. It was later reported to undergo self-association to a higher order oligomeric state and that the physiologically active species, at relevant cellular concentrations, is predominantly the hexadecamer in equilibrium with the octameric

species (*51*). Further characterization of the assembly state of Lrp was carried out with techniques including sedimentation equilibrium and velocity as well as dynamic light scattering (*51*).

Dynamic light scattering experiments were performed on Lrp in the presence and in the absence of leucine at a range of concentrations from low to high micromolar. Light scattering data provided an estimate of the hydrodynamic radius (R_h), which was used to obtain a molecular weight. The results indicate that the R_h of apoLrp is 6.3 nm while that for Lrp in the presence of leucine was 5.2 nm. The interpretation of the data indicated that apoLrp existed as a species with a molecular weight that is consistent with it being a hexadecamer in the absence of leucine. It was further concluded that while the R_h of Lrp in the presence of leucine didn't change considerably, the decrease is consistent with a lower molecular weight species.

Sedimentation equilibrium was performed on Lrp at multiple loading concentrations and multiple rotor speeds to probe the assembly properties of the protein in the presence and absence of leucine. Results of a global analysis indicated that the data was best described by a hexadecamer-octamer equilibrium with the equilibrium strongly favoring the 16-mer ($K_d = 10^{-8}$ M) in the absence of L-leucine. In the presence of the effector, the hexadecamer-octamer dissociation constant shifts 330-fold towards the formation of more octamer ($K_d = 10^{-5}$ M). There was also some evidence of small amounts of 32-mer present.

Sedimentation velocity experiments were performed at micromolar concentrations of 6HisLrp in the presence of millimolar concentrations of leucine. The data were well described by a single Gaussian distribution as would be expected for a rapidly equilibrating self-associating system. Sedimentation coefficients and diffusion coefficients were used to calculate an average molecular weight for the sedimenting species (155 kDa). A molecular weight that is consistent with Lrp being octameric in the presence of saturating amounts of leucine. A further investigation revealed that deletion of the C-terminal 11 residues resulted in the inability of the Lrp to form higher order oligomers than the dimer as revealed by dynamic light scattering and chemical crosslinking followed by SDS-PAGE (*51*). Interestingly, an attempt to delete the C-terminal 31 or 61 residues resulted in destabilization of the protein and nonspecific aggregation. This result supports the data from the crystal structure in which the C-terminal domain is involved in both the stabilization of the dimer and the stabilization of the octamer.

While the physical mechanism by which the Lrp protein is activated for function is not completely understood, it is apparent that leucine does affect the assembly properties of the regulator. It is proposed that the leucine-responsive self-association of Lrp is a mechanism by which the activity of Lrp can be regulated. The equilibrium is utilized to regulate the concentration of free Lrp available for site-specific DNA binding. In conditions of low leucine concentration, the growth rate of cells is slow, the concentration of free Lrp is high and the hexadecamer is the predominant species in solution. The hexadecamer binds its target sites to initiate transcription of the

biosynthetic operons and to repress transcription of those genes in the degradative pathway. In contrast, in conditions of high leucine concentration, growth rate is relatively fast, the concentration of free Lrp is low and the predominant Lrp species is the leucine-bound octamer. This shift in the equilibrium distribution means that less Lrp hexadecamer is available to activate transcription of the biosynthetic operons and the degradative pathway is derepressed.

c. The Biotin Repressor (BirA)

The *E. coli* biotin regulatory system provides an excellent model for examining the physical mechanism of an allosteric activation process (Figure 8). The central protein of this system, BirA or the biotin repressor, is bifunctional and is both an essential metabolic enzyme and a repressor of transcription initiation (*52, 53*). In its function as an enzyme, BirA catalyzes the two-step biotinylation of the Biotin Carboxyl Carrier Protein (BCCP), a subunit of acetyl-CoA carboxylase (*54*). The first step is the synthesis of biotinyl-5'-AMP (bio-5'-AMP) from the substrates biotin and ATP. The second step is the covalent linkage of the biotin moiety of bio-5'-AMP to the ε-amino group of a specific lysine residue of BCCP. The biotinylated carrier protein is utilized for the first committed step of fatty acid synthesis. Biotin is therefore, an essential cofactor. BirA is responsible for this post-translational modification of a single biotin dependent carboxylase in *E. coli*. However, other bacteria have three biotin-dependent enzymes, while eukaryotes have 4-5 biotin dependent carboxylases (*52, 55, 56*). Cross biotinylation of each family of biotin dependent carboxylases by a biotin ligase from a different family has been observed experimentally, and is attributed to the conserved

sequence homology in the respective biotinylation domains. This result illustrates the evolutionary importance of this interaction.

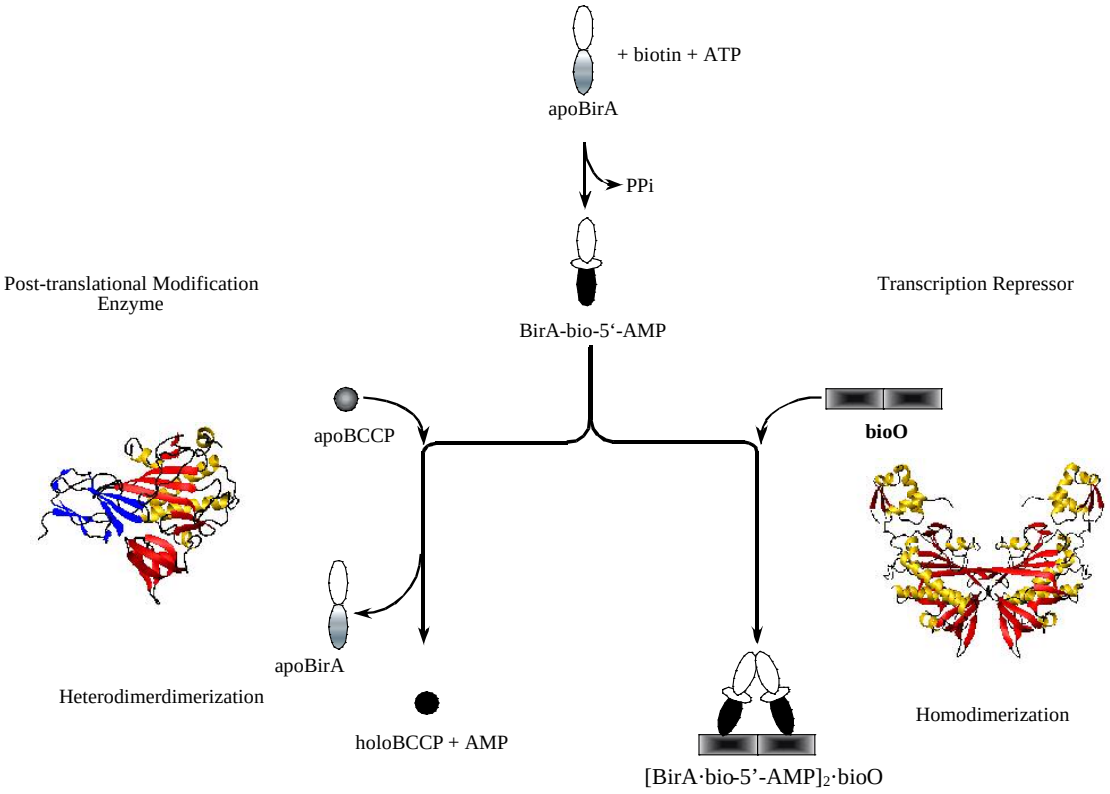

Figure 8. A schematic representation of the biotin regulatory system. The activated enzyme, BirA-bio-5'-AMP, switches between functioning as a biotin holoenzyme ligase and a transcriptional repressor.

In its function as a transcription regulator, two BirA monomers bind to the biotin operator, a 40 base pair DNA sequence, blocking access to two divergent overlapping promoters and represses transcription of the biotin biosynthetic operon. However, apoBirA is not the active species in bioO binding. Rather it is the adenylate-bound

protein that binds site-specifically and with high affinity to DNA. Eisenberg's laboratory reported that bio-5'-AMP is the physiologically active corepressor and is 1000-fold more effective in activating BirA for DNA binding than is biotin in *vitro* (*57*). Thus, in this system bio-5'-AMP serves both as the intermediate in enzyme-catalyzed biotin transfer and as the corepressor in transcription repression.

The mechanism of allosteric activation in the biotin repressor has been studied in great detail using a variety of thermodynamic, kinetic and structural approaches (*58-65*). DNaseI footprinting measurements indicate that binding of the repressor to the two operator half-sites is a cooperative process and that the dimer is the active species for DNA binding (*58*). Time-resolved DNaseI digestions indicate that dimerization precedes DNA binding (*62*). Results of a sedimentation equilibrium analysis of apoBirA and BirA-bio-5'-AMP indicate that binding of the effector enhances the energetics of repressor self-association by –4 to –5 kcal/mol (*59*). In a separate analysis, biotin was shown to be a weak activator of dimerization (*63*). Studies with repressor mutants indicate that drastic defects in bioO binding are correlated with a drastically weakened dimerization affinity of the repressor (*60*).

Models of the apoBirA structure as well as the holorepressor bound by either biotin or biocytin were obtained from X-ray diffraction studies (*64, 65*). The structure of the 321 amino acid polypeptide is comprised of three domains (Figure 9). The N-terminal domain contains a wHTH DNA binding domain. The central domain contains a 7-stranded mixed beta-sheet packed against 5 alpha helices, and four loops that appear as

partially disordered in the crystal structure. Biochemical data indicate that this domain is directly involved in dimerization and ligand binding and indirectly involved in DNA binding (*60, 66*). The C-terminal domain contains a β-sandwich motif. Its function in repression is not known. However it is believed to be important in ligase activity (*67*).

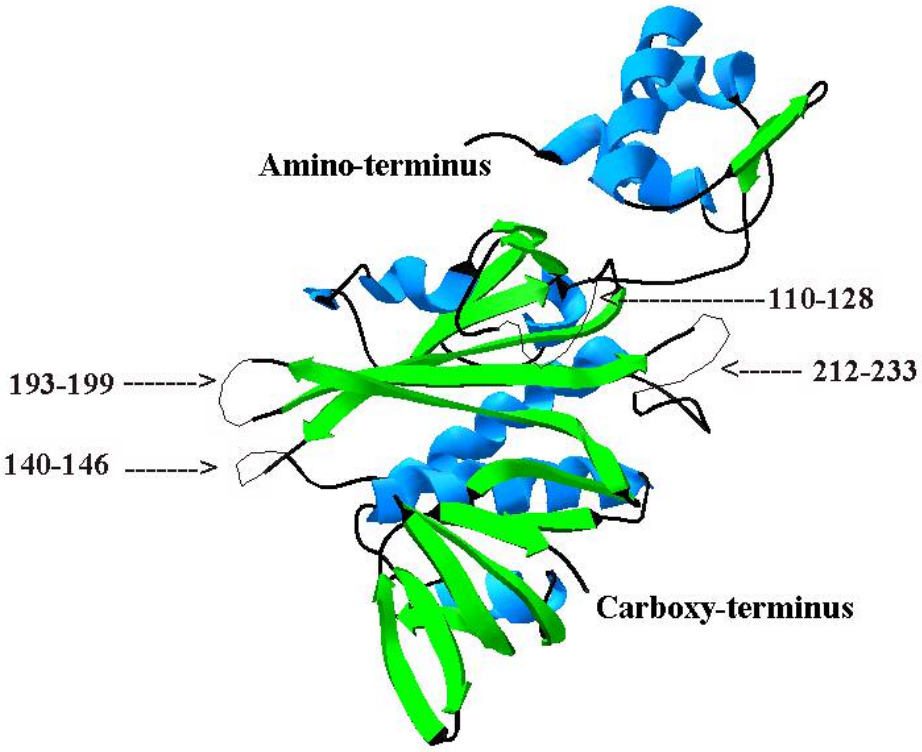

Figure 9. A model of the three-dimensional structure of apoBirA obtained from X-ray crystallography (*64*). The residues within the four partially disordered loops are indicated with arrows. The model was generated using Deep View- The Swiss-Pdb Viewer (v. 3.7) with the Protein Data Bank file 1BIA as input.

The crystal structure of biotin bound form of the repressor is dimeric (*65*). The dimerization interface is composed of a side-by side alignment of the beta sheet of the central domain of each monomer to form an extended beta sheet (Figure 10). The most striking feature of this structure is that 3 of the 4 surface loops that were disordered in the apo structure appear ordered in the biotin-bound structure and they are located at the dimer interface. The overall structures of the aporepressor and a monomer unit of the biotin-bound dimer are very similar. The main differences between them are localized to the regions of loops 110-128, 140-146, and 193-199. Superposition of the structures yielded a root-mean-square difference between α-carbons of 1.23 Å, 0.89 Å, 0.70 Å, and 1.26 Å for the N-terminal domain, the central domain, the C-terminal domain, and the overall molecule, respectively (*65*). This result suggests that biotin binding to the repressor does not bring about a large conformational change other than in the loop regions.

The structure of the repressor bound by bio-5'-AMP is likely to be different than the structure of the apo repressor and the repressor bound by biotin. Results of partial proteolysis and hydroxyl radical footprinting of the BirA backbone as a function of biotin or bio-5'-AMP binding demonstrated that bio-5'-AMP protects the remaining 212-233 loop from cleavage (*61, 68*). It is likely that this last loop becomes ordered upon binding of the physiological corepressor and that this ordering of the final loop is what brings about the enhanced dimerization and repression properties of BirA.

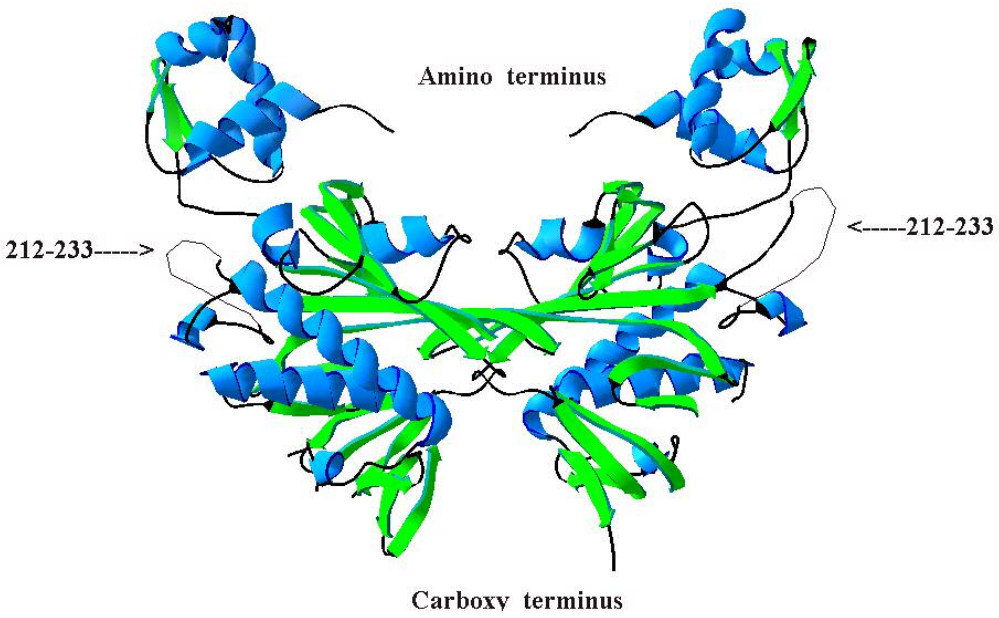

Figure 10. A model of the three-dimensional structure of BirA bound by *d*-biotin determined by X-ray crystallography (*65*). For clarity, the biotin ligand is not shown. The remaining partially disordered loop is labeled. The model was generated using the Protein Data Bank file 1HXD as input into the graphics program Deep View- The Swiss-Pdb Viewer (v. 3.7).

The model for the mechanism of allosteric activation of the biotin repressor obtained from analysis of all the data is that bio-5'-AMP drives the self-assembly of the repressor by organizing the surface loops upon binding the repressor. The organization of the loops results in more favorable self-association. The enhanced dimerization energetics in turn, lead to a more favorable free energy of assembly of the transcription repression complex. The resulting higher occupancy of the operator results in repression of transcription initiation at the two divergent promoters.

Thus, in contrast to the classical allosteric repressors, the leucine responsive protein, and the diphtheria toxin and biotin repressors have their affinity for DNA modulated by their self-assembly properties. Binding of the effector stabilizes a conformational transition in the protein that alters the oligomeric state of the repressor and thus its affinity for DNA. Binding of leucine to Lrp destabilizes the hexadecamer, which has the higher affinity for DNA, and shifts the equilibrium toward the leucine-bound octamer. Binding of a corepressor to the diphtheria toxin or the biotin repressor results in an enhancement of the energetics of dimerization. This, in effect, regulates the supply of repressor dimer and dictates the level of occupancy of the respective operator sites.

C. Organization of the Dissertation

The first chapter of this dissertation is a general introduction to important terms and concepts concerning the function of transcription repressors. A literature review of specific systems is included as background to put into a broader context the work described in the following chapters. The second chapter represents a body of work performed in this laboratory that was published in the Journal of Molecular Biology in 2003. Though the principal investigator served an important role in the process, this graduate student was primarily responsible for acquiring the data, interpreting the results, and made significant contributions toward writing of the manuscript. In this manuscript, the linkage of repressor dimerization to DNA binding was investigated utilizing corepressor analogs. As indicated in the materials and methods section of the chapter, the analogs were obtained through collaborators or were purchased commercially. Results of

sedimentation equilibrium measurements indicate that the corepressors can be divided into two classes with respect to the affect the ligand has on dimerization. Weak allosteric activators show an uncoupling between dimerization and DNA binding, while no such uncoupling is associated with binding of strong activators. The accumulated data indicate that the allosteric signal is not transmitted solely through the dimer interface, and that the critical species in the activation process is the liganded monomer. Therefore, in order to further delineate the mechanism of allosteric activation it is necessary to obtain information about the structural and dynamic changes that occur in the repressor monomer concomitant with effector binding.

The third chapter describes the strategy applied toward subjecting the effector binding process to a detailed thermodynamic analysis. Isothermal titration calorimetry was used to dissect the energetics of the interaction of the BirA monomer with four allosteric activators. Results of these measurements indicate that while the process is spontaneous in all cases, binding of the strong effectors to BirA exhibits less favorable enthalpy than does binding of the weak effectors. The heat capacity changes associated with the binding process were determined by measuring the temperature dependence of the binding enthalpy for all four binding processes. No correlation is observed between the magnitude of the heat capacity change and the magnitude of the allosteric effect associated with binding of a ligand. The interpretation of the results of this investigation suggests that an enthalpically costly transition is required to activate the protein for dimerization.

The fourth chapter describes work that remains in progress. Crystals have been obtained for BirA bound by the corepressor analog, biotinol-AMP (btnOH-AMP), and are currently being analyzed by X-ray diffraction in the laboratory of Dr. Brian Mathews at the University of Oregon. The chemical lability of the mixed anhydride linker in bio-5'-AMP has hindered further structural analysis of the physiologically relevant holorepressor. However, solution properties of the BirA·btnOH-AMP complex suggest that its three-dimensional structure may closely resemble that of BirA·bio-5'-AMP. This structural model is important for deciphering features of the repressor that are critical in transmission of the allosteric signal.

The final chapter summarizes the how the results obtained from this research contribute to a further understanding of the allosteric activation mechanism regarding the biotin repressor. It also discusses how these results contribute to a broader perspective of allosteric regulation. The chapter concludes with a prospectus of experiments that should be performed in order to further develop the working model.

II. The Biotin Repressor: Modulation of Allostery by Corepressor Analogs

A. Introduction

Allosteric regulation of protein-protein interactions is a hallmark of the complex macromolecular circuitry that functions in cellular processes including signal transduction and transcription initiation (*5, 69*). The *Escherichia coli* biotin regulatory system provides an excellent model for examining the physical mechanism of an allosteric activation process (Figure 11-A). The central protein of the system, BirA or the biotin repressor, is bifunctional and is both an essential metabolic enzyme and a repressor of transcription initiation (*70, 71*). As an enzyme the protein catalyzes the two-step biotinylation of the biotin-dependent enzyme, acetyl-CoA carboxylase. BirA utilizes the substrates biotin and ATP to catalyze synthesis of biotinyl-5'-AMP (*54*). In the second step of the reaction this adenylate serves as the biotin donor to a single lysine residue of the biotin carboxyl carrier protein subunit (BCCP) of the carboxylase. In its transcription repression function two biotin repressor monomers bind to the biotin operator sequence to repress transcription initiation at the two promoters of the biotin biosynthetic operon (Figure 11-B)(*58, 72*). However the unliganded enzyme, apoBirA, is not the active species in bioO binding. Rather, it is the adenylate-bound protein or holoBirA that binds tightly and site-specifically to DNA (*57*). Thus in this system not only is the protein bifunctional but bio-5'-AMP serves both as the intermediate in enzyme-catalyzed biotin transfer and as the corepressor in transcription repression.

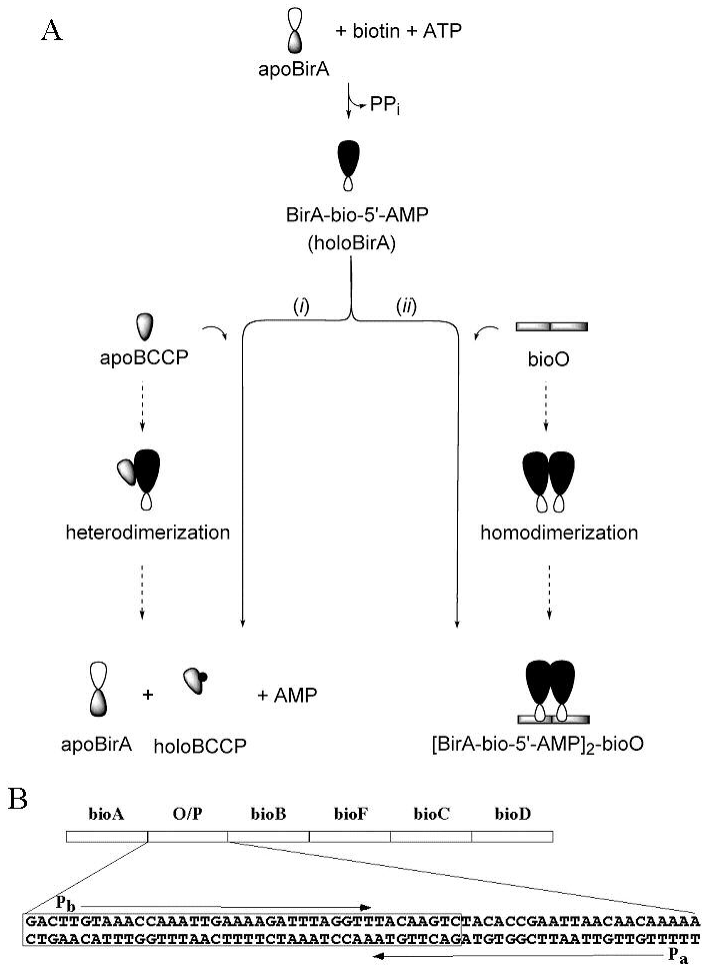

Figure 11. Schematic representation of the biotin regulatory system. (A) The activated enzyme, BirA·bio-5'-AMP, switches between functioning as (i) a biotin holoenzyme ligase and (ii) a transcriptional repressor. (B) Schematic representation of the biotin biosynthetic operon and the detailed sequence of the biotin operon transcriptional control region: *bioA* through *bioF* are the genes that encode the biotin biosynthetic enzymes, O/P is the transcriptional control region for the operon, and P_a and P_b are the promoters for leftward and rightward transcription, respectively indicated by the arrows. The boxed region represents the biotin operator sequence.

The mechanism of allosteric activation of the biotin repressor has been studied in great detail using equilibrium thermodynamic, kinetic, and structural approaches (*58-65*). As indicated above, two holorepressor monomers bind to the bioO sequence, a forty base- pair imperfect inverted palindrome (Figure 11-B)(*58, 72*). Moreover, results of studies of repressor mutants indicate that a defect in repressor dimerization is correlated with drastically weakened affinity of the protein for bioO (*60*). Finally, analysis of sedimentation equilibrium data indicates that binding of bio-5'-AMP to apoBirA renders the dimerization energetics of the protein more favorable by -4 to -5 kcal/mole (*59, 63*). A model of the apoBirA structure determined by X-ray crystallography is shown in Figure 12-A (*64*). The protein consists of three domains, an N-terminal wHTH DNA binding domain, the central domain that functions in both catalysis and DNA binding, and the C-terminal domain that is thought to function in the interaction between holoBirA and apoBCCP in the biotin transfer reaction. A significant feature of the apoBirA structure is the lack of structure in four surface loops of the central domain. Single-site mutations in these disordered loops have been shown to primarily impair the DNA binding and dimerization function of the protein (*60, 66*). A structure of the BirA dimer bound to the weak corepressor, biotin, is also available and is shown in Figure 12-B (*65*). The dimer is formed by side-by-side alignment of the β-sheets of the central domains of each monomer. A striking feature of the structure is the ordered appearance of three of the four unstructured loops of the aporepressor in the monomer-monomer interface. Moreover, the mutations that have been demonstrated to disrupt both DNA binding and dimerization are localized to these interface loops. The combined results of multiple solution and structural studies of the system has prompted formulation of a model for

allosteric activation of the biotin repressor by bio-5'-AMP. Upon binding to the aporepressor monomer, the bio-5'-AMP corepressor induces disorder-to-order transitions in the surface loops of the repressor central domain. The stabilization of these loops enhances dimerization by lowering the entropic penalty associated with self-assembly. The enhanced dimerization energetics in turn render overall assembly energetics of the transcription repression complex more favorable.

A detailed investigation of the thermodynamics of allosteric activation of BirA has been performed. One prediction of the model for allosteric activation is that the total assembly energetics of the repression complex is controllable by modulating the energetics of repressor dimerization. This prediction has been tested by examining the energetics of dimerization and DNA binding of three repressor species; apoBirA, BirA·biotin and BirA·bio-5'-AMP (*63*). The results of these studies reveal that the difference in dimerization energetics for the apoBirA and BirA·bio-5'-AMP species does indeed track precisely with the difference in the total assembly energetics (dimerization plus DNA binding) for their respective repression complexes. However, results of comparison of any pair of species that includes the biotin complex reveals a mismatch in the enhancement of dimerization and the total assembly energetics, suggesting that there is decoupling of the two processes in the substrate-bound species. These findings suggest, moreover, that the structure of the repressor-biotin complex may not accurately reflect the structure of the true holorepressor complex.

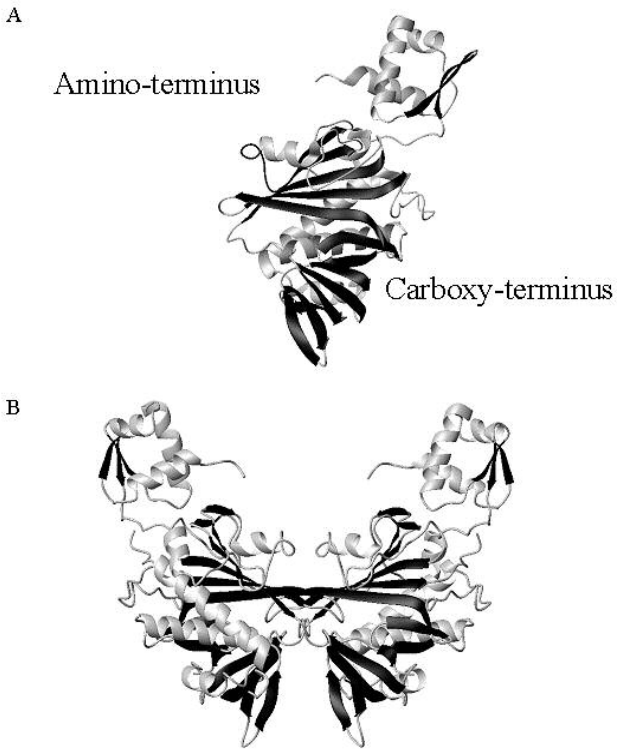

Figure 12. The biotin repressor. (A) Model of the three-dimensional structure of *apo*BirA determined by X-ray crystallography (*64*). (B) Model of the three dimensional structure of the BirA·biotin dimer (*65*). For clarity, the biotin ligand is not shown. The models were generated using the graphics program MOLMOL (*73*) with the Protein Data Bank files 1BIB and 1HXD, respectively, as input.

A second focus of interest in the biotin regulatory system is the mechanism of functional switching from transcription repressor to biotin ligase. *In vivo* studies indicate that it is not the level of biotin, *per se*, that dictates switching. Rather, the level of apoBCCP or acceptor protein is the significant factor. Indeed, in bacterial cultures in which transcription from the biotin promoters is fully repressed the induction of synthesis of apoBCCP87, the domain of the acceptor protein that is biotinylated, results in

derepression (*74*, *75*). Results of combined structural modeling and solution biochemical and biophysical studies have led to formulation of a competitive model for functional switching in the system. First, kinetic studies reveal that the biotin acceptor protein does not actively promote dissociation of the holoBirA·bioO complex (*62*). Second, structural modeling suggests that the heterodimeric complex of apoBCCP with holoBirA forms using the same surface of holoBirA as that used in homodimerization (*76*). This structural model is supported by low-resolution NMR studies, and biochemical studies of BirA and BCCP mutants (*74*, *76*, *77*). Finally, kinetic measurements of binding of holoBirA to bioO reveal that the repressor undergoes dimerization prior to associating with DNA (*62*). The accumulated evidence supports a mechanism for functional switching in the system in which the acceptor protein, when present at sufficiently high intracellular concentrations, prevents dimerization and thus DNA binding by sequestering the holoBirA surface that is utilized in self-assembly. Testing of this model requires direct kinetic and equilibrium thermodynamic measurements of homo- and heterodimerization of holoBirA.

The chemical lability of bio-5'-AMP, a mixed anhydride, presents a significant obstacle to further structural and solution analysis of the biotin repressor. For example, although crystals of the protein bound to bio-5'-AMP were obtained, handling of these crystals and their exposure to the x-ray beam resulted in hydrolysis of the adenylate (Kwon & Beckett, unpublished observations). Consequently, structural information was obtained for only the biotin-bound protein (*65*). Furthermore, the coupling of formation of the heterodimeric complex between holoBirA and apoBCCP to chemical transfer of

the biotin moiety prevents structural, thermodynamic and kinetic characterization of this complex. One potential route for overcoming these difficulties lies in the development of non-labile analogs of biotinyl-5'- AMP.

The reaction catalyzed by biotin holoenzyme ligases bears similarity to that catalyzed by the amino-acyl tRNA synthetases (AARS, (*78*)). Like the biotin ligases the AARS's utilize ATP and the amino acid to catalyze formation of a mixed anhydride, the amino acyl-adenylate, with release of pyrophosphate. In the second step of both reactions nucleophilic attack at the carbon of an acyl group occurs with release of AMP. This similarity between the enzymes extends in a few cases to structure (*79-81*). Indeed, the structures of two Class II amino acyl tRNA synthetases resemble that of the *E.coli* biotin ligase. In efforts to characterize the structures of the adenylate-bound tRNA synthetase species, several nonhydrolyzable amino acyl adenylate analogs have been developed. One class of analogs that have been utilized is the sulfamoyl derivative in which the phosphate that bridges the amino acid and nucleoside is replaced by a sulfamoyl group (*82, 83*). A second type of analog is the ester in which the α-carboxyl moiety of the amino acid is reduced to the alcohol and then joined to the 5'-phosphate of AMP *via* an ester linkage (*84, 85*). Similar compounds may be useful for studies of the biotin ligase system.

In this work the synthesis and characterization of two analogs of bio-5'- AMP are described. The ester and sulfamoyl derivatives of the intermediate were synthesized, and results of fluorescence measurements indicate that both bind to the biotin repressor. The

inability of the analogs to function as substrates in the biotin transfer reaction was verified using a combination of fluorescence spectroscopy and mass spectrometric measurement. Finally the dimerization and bioO binding properties of complexes of the biotin repressor bound to each analog were measured. The resolved equilibrium dimerization constants and DNA binding energetics indicate that while the sulfamoyl derivative is a relatively weak allosteric activator the ester exhibits properties that closely resemble those of the physiological corepressor, bio-5'-AMP. The results obtained with the derivatives mirror previous observations that while weak allosteric activators allow uncoupling of DNA binding and self-assembly no such uncoupling is associated with strong activators.

B. Materials and Methods

1. Chemicals and biochemicals

All chemicals used in the preparation of buffers were at least reagent grade. The d-biotin, ATP, and isopropyl β-D-thiogalactoside (IPTG) were purchased from Sigma. DNase I was purchased from Worthington Biochemicals. The [α-^{32}P]dATP and dGTP used in the radio-labeling of DNA were obtained from Amersham Biosciences. Bio-5'-AMP was synthesized in this lab (by K. Kwon) using a published procedure (*58*). The btnSA was synthesized as described below or obtained from RNA-Tec (Leuven, Belgium). The apoBCCP87 was purified as described in Nenortas & Beckett (*86*).

2. Synthesis of 5'-O-[N-(biotinyl)sulfamoyl]adenosine (btnSA)

The synthesis of 2',3'-*O*-Isopropylidene-5'-*O*-sulfamoyladenosine was as described by Kristinson (*87*), with slight modifications, from the commercially available 2',3'-*O*-isopropylideneadenosine. The productwas purified by silica gel chromatography with an elution gradient of methanol in ethyl acetate (0-5%). The resulting white powder (0.5 g, 1.3 mmol) was reacted with biotin-N-hydroxysuccinimide ester (0.4 g, 1.3 mmol) and 1,8-diazabicyclo[5.4.0]undec-7-ene (195µl, 1.30 mmol) in dimethylformamide (8 ml) with stirring and exclusion of moisture for 4 hours at room temperature. The crude product obtained after evaporation of the solvent was purified by column chromatography on Florisil and eluted with a gradient of ethanol in dichloromethane (0 - 15%). Finally, the isopropylidene group was removed with 3:1 trifluoroacetic acid/water. The solvent was evaporated and the crude product was purified using a semi-preparative RP-18 column (Millipore Delta Pak, 15µ) with a linear gradient (0 - 60%) of water (0.1% TFA) in acetonitrile (0.1% TFA). The final product was determined to have the correct mass of 572.8 Da as determined by ES/MS (calculated, $C_{20}H_{27}N_8O_8S_2$, 571.7). The product was also characterized by ^{1}H NMR spectroscopy; ^{1}H NMR (250 MHz, DMSO-d_6): 1.1-1.65(m, 6H, CH(CH_2)$_3$), 2.05(t, 2H, COCH_2), 2.54 and 2.82(m, 2H, SCH_2), 3.05(m, 1H, SC*H*), 4.05-4.17(m, 5H, H-3', H-4', H5' and CHC*H*NH), 4.28(m, 1H, CH_2C*H*NH), 4.58(m, 1H, H-2'), 5.91(d, 1H, H-1'), 6.36 and 6.62(2 x s, 2H, 2x CON*H*), 7.28 (br s, 2H, NH_2), 8.14(s, 1H, H-2) and 8.37(s, 1H, H-8).

3. Synthesis of biotinol-adenylate (btnOH-AMP)

Biotinol was made by reduction of biotin methyl ester with $LiBH_4$ in tetrahydrofuran-methanol (*88*) and purified by crystallization from methanol-ether (mp 173-174^o). The synthesis of 2',3'-isopropylidene-adenosine-5'-phosphate was as described by Tener (*89*) from the commercially available 2',3'-*O*-isopropylidene adenosine. It was purified using Sephadex A-25 with an elution gradient of ammonium carbamate (0.0 – 0.2 M). Fractions containing 2',3'-isopropylidene-adenosine-5'-phosphate were dried by rotary evaporation. The resulting residue was dissolved in water and passed through a DOWEX-50W-X8 resin (pyridinium form). The flow through and a pyridine (5%) wash of the resin were combined, evaporated to dryness, and twice resuspended in dry pyridine and dried by evaporation to obtain the pyridinium salt of 2',3'-isopropylidene-adenosine-5'-phosphate. This salt (1.3 g, 2.7 mmol) was combined with biotinol (0.5 g, 2.3 mmol) in dry pyridine and dried by rotary evaporation. This residue was taken up in dry pyridine (20 mL) containing N,N'-dicyclohexylcarbodiimide (0.6 g, 3.0 mmol). The flask was tightly stoppered and the reaction was stirred for 24 hours at room temperature. Finally, the isopropylidene group was removed by the addition of acetic acid to a final concentration of 20% (v/v) and refluxed for 2 hours. The mixture was filtered and washed with water, and the resulting filtrate and washings were combined and evaporated to dryness. The product was purified on Sephadex A25 as described for bio-5'-AMP (*54, 58*), followed by an HPLC step. A Synergi Polar RP column (Phenomenex) with buffers A: 50 mM ammonium acetate, pH 4.75, and B: acetonitrile (0.1% TFA) was used with a gradient of: 0% B for 10 min, then 0-60% B over the next 30 min. BtnOH-AMP eluted (as detected by UV absorbance at 260 nm) at

23 min (25% B). The final product gave a single UV-absorbing spot on TLC, stained with dimethylaminocinnamaldehyde (a reaction specific for cyclic ureides), and was determined to have the correct mass by ES/MS of 558.1 Da (calculated, $C_{20}H_{30}N_7O_8PS$, 559.5). The btnOH products was also subjected to proton NMR spectroscopy: ^{1}H NMR (400 MHz, DMSO-d_6): 8.43 (s, 1H, H-8), 8.14 (s, 1H, H-2), 7.32 (br s, 2H, N*H*$_2$), 6.61 and 6.37 (2 x s, 2H, 2x CON*H*), 5.90 (d, 1H, H-1'), 5.55 and 5.54 (2 x br s, 2H, 2x CHO*H*), 4.58 (m, 1H, H-2'), 4.28 (m, 1H, CH$_2$C*H*NH), 4.19 (m, 1H, H-4'), 4.12 (m, 1H, CHC*H*NH), 4.00 (m, 1H, H-3'), 3.80 (m, 2H, H-5'), 3.59 (m, 2H, C*H*$_2$OP), 3.06 (m, 1H, SC*H*), 2.80 and 2.56 (m, 2H, SC*H*$_2$), 1.19-1.61 (m, 8H, CH(C*H*$_2$)$_4$).

4. Expression and purification of the biotin repressor

BirA was expressed in an *E. coli* strain (BL21(λDE3)) that had been transformed with a plasmid (pHBA) carrying the *E. coli birA* gene under the control of the T7*lac* promoter (*67*). Cells were grown using methods previously reported(*58*), with the exceptions that growth was performed at 23 °C and glucose was added to the LB to 2% (w/v). Following lysis and precipitation steps, BirA was separated from other cellular proteins in three chromatography steps. First, the protein mixture was dialyzed against 50 mM potassium phosphate pH 6.5, 5% glycerol, and 0.1 mM dithiothreitol (DTT), loaded onto a HA-Ultragel (Sepracor) hydroxyapatite column (200mm x 10mm), and eluted with a linear potassium phosphate pH 6.5 gradient (0.0-0.5 M) containing 5% glycerol, and 0.1 mM DTT. Fractions containing BirA were pooled, dialyzed, and passed through a Q-Sepharose (Amersham Biosciences) column (105 mm x 10 mm) that had been equilibrated with 50 mM Tris-HCl pH 7.5 at 4 °C, 50 mM KCl, 5% glycerol, and

0.1 mM DTT. The flowthrough and the wash containing BirA were combined and loaded directly onto a SP-Sepharose (Amersham Biosciences) column (330 mm x 25 mm) and eluted in a linear KCl gradient (0.0 – 0.8 M) in 50 mM Tris-HCl pH 7.5 at 4 °C, 5% glycerol, and 0.1 mM DTT. Fractions containing BirA were pooled and dialyzed against 50 mM Tris-HCl pH 7.5 at 4 °C, 200 mM KCl, 5% glycerol, and 0.1 mM DTT. The protein was stored in this buffer at –70 °C. The total yield of BirA was 17 mg/ L of culture. The final protein sample was judged be > 98% pure by Coomassie staining of samples electrophoresed on SDS-PAGE gels, and was determined to be 95% active by stoichiometric titrations with bio-5'-AMP (*58*) .

5. Fluorescence spectroscopy

Steady state fluorescence measurements were made using an ISS-PC1 spectrofluorimeter (ISS, Champaign, IL) equipped with a VWR Scientific 1160 constant temperature bath (PolyScience, Niles, IL) maintained at 20.0 ± 0.1 °C. The excitation wavelength was 295 nm, a wavelength at which BirA but not the ligands or apoBCCP absorbs light, and emission was monitored from 310 - 450 nm. Excitation and emission slit widths were set at 4 nm. All measurements were made in the ratio mode using rhodamine B as a quantum counter. For binding measurements, a fluorescence spectrum of a 2 μM solution of apoBirA in standard buffer [10 mM Tris-HCl (pH 7.5 ± 0.02 at 20 ± 0.1 °C), 200 mM KCl, 2.5 mM $MgCl_2$] was recorded. A second spectrum was recorded two minutes after the addition of a concentrated ligand solution (freshly prepared in standard buffer) was added to a final concentration of 2.2 μM. The integrated area of each emission spectrum (310 – 450 nm) was obtained using ISS PC1 software. For

biotinylation studies, an aliquot of a concentrated BCCP87 solution was added to the cuvette containing the BirA·ligand complex to a final concentration of 10 μM, and the resulting fluorescence spectrum was obtained after a two-minute equilibration period. All integrated areas were corrected for buffer contribution and volume changes due to addition of ligand or protein.

6. Mass spectrometry

Mass spectra of products of biotin transfer to BCCP87 were determined following a protocol previously reported (*86*), using a Kratos (Manchester, UK) Kompact MALDI 4 time-of-flight mass spectrometer equipped with a 337 nm nitrogen laser and pulsed-ion extraction. BirA (1 μM) and BCCP87 (100 μM) in 10 mM Tris, 200 mM KCl, 2.5 mM $MgCl_2$ (pH 7.5 ± 0.02 at 20 ± 0.1 °C) were incubated in the presence of 110 μM of each of the ligands biotin, bio-5'-AMP, btnSA, or btnOH-AMP, at 20 °C for 1 h. Each reaction mixture was then dialyzed exhaustively against 5% (v/v) acetic acid in water to remove salts and buffer components. The resulting solution was then lyophilized to dryness, resuspended in 1:1 water (0.1% TFA)/ CH_3CN (0.1% TFA) and spotted onto a stainless steel slide with 3,5-dimethoxy-4-hydroxycinnamic acid as the matrix and horseheart cytochrome c as the external calibration standard.

7. Sedimentation equilibrium

The dimerization properties of the BirA-analog complexes were determined by analytical ultracentrifugation using a Beckman Optima XL I analytical ultracentrifuge

equipped with a four-hole An-60 Ti rotor. Double sector cells with charcoal-filled epon centerpieces and sapphire windows with optical pathlengths of 3 mm or 12 mm were used (*59*). BirA was dialyzed extensively against standard buffer [10 mM Tris-HCl, 200 mM KCl, 2.5 mM $MgCl_2$ (pH 7.5 ± 0.02 at 20 ± 0.1 °C)], and the resulting protein concentration was determined spectrophotometrically using the extinction coefficient at 280 nm (ε_{280} = 47510 $M^{-1}cm^{-1}$ (*58*)). All samples for sedimentation were prepared with dialysis buffer under stoichiometric conditions where ligand was in slight excess over protein. Sample volumes were typically 150 μL for 12 mm cells and 50 μL for 3 mm cells. The solvent density (1.006 g/ mL) was determined pycnometrically, and the partial specific volume of the BirA monomer (0.755 mL/ g) has been previously reported (*59*). Absorbance *vs*. radial position scans were recorded at either 295 or 300 nm for samples prepared at multiple loading concentrations (5 μM – 100 μM) and centrifuged at multiple rotor speeds (22000, 26000, and 30000 rpm). Scans were acquired as an average of three measurements of absorbance at each radial position with a spacing of 0.001 cm. Data were analyzed using a version of the nonlinear least-squares program NonLin adapted for analysis of sedimentation equilibrium data (*90*). Initially, each scan was analyzed to obtain a σ-value that is related to the molecular weight of the sedimenting species by the following relationship (*91*):

$$\sigma = \frac{M(1-\bar{\nu}\rho)\omega^2}{RT} \qquad (1)$$

where $\bar{\nu}$ is the partial specific volume of the macromolecule in mL/ g , ρ is the density of the buffer used in g/ mL, ω is the angular velocity of the rotor, R is the gas constant,

and T is the absolute temperature in K. The data were also analyzed globally using the following model for a monomer-dimer association reaction (*91*):

$$c_t(r) = c_m(r_\circ)e^{\left[M(1-\bar{v}\rho)\frac{\omega^2\left(r^2-r_\circ^2\right)}{2RT}\right]} + K_a\, c_m^2(r_\circ)e^{\left[2M(1-\bar{v}\rho)\frac{\omega^2\left(r^2-r_\circ^2\right)}{2RT}\right]} \quad (2)$$

where, $c_t(r)$ is the total concentration as a function of radial position, r. The symbol r_o represents a reference radial position (first data point), c_m is the concentration of monomer species, and K_a is the monomer-dimer association constant. In analyses using a monomer-dimer model, the reduced buoyant molecular mass of a dimer was assumed to be twice the value for the monomer. The quality of each fit was assessed from the examination of the magnitudes of the square root of the variance and the distribution of the residuals.

8. DNase I footprinting

DNase I footprinting was performed as previously described (*58*) following a modification of the methods outlined by Brenowitz (*92*.) The reaction buffer contained 10 mM Tris-HCl (pH 7.5 ± 0.02 at 20 ± 0.1 °C), 200 mM KCl, 2.5 mM $MgCl_2$, 1.0 mM $CaCl_2$, 100 µg/ mL BSA, 2 µg/ mL sonicated calf thymus DNA and btnSA or btnOH-AMP (40 µM), or biotin (50 µM) and ATP (500 µM). Each 200 µL binding reaction was prepared in reaction buffer and contained 12000 cpm of radio-labeled DNA at a final concentration of approximately 20 pM, and BirA at a range of concentrations. Reaction mixtures were equilibrated for 1 h at 20 °C. DNase I digestion was initiated by addition

of 5 μL of a freshly prepared DNase I solution (3 μg/ mL) in 10 mM Tris-HCl (pH 7.5 ± 0.02 at 20 ± 0.1 °C), 200 mM KCl, 2.5 mM $MgCl_2$, 1 mM $CaCl_2$. After 2 min at 20 °C the digestion was quenched by the addition of 33 μL of a 50 mM Na_2EDTA solution. The DNA was precipitated by addition of 700 μL of 0.4 M NH_4OAc, 50 μg/ mL yeast phenylalanyl tRNA in EtOH, followed by incubation in a dry ice/ethanol bath for 20 min. After centrifugation, the pellets were washed twice with 500 μL of cold aqueous EtOH 80% (v/v), and lyophilized. The resulting pellets were resuspended in 7 μL of gel loading buffer containing 80% (v/v) deionized formamide, 1 x TBE (*93*), 0.02% (w/v) bromophenol blue, and 0.02% (w/v) xylene cyanol, and heated for 10 min at 90 °C. Products were separated by electrophoresis on a 10% denaturing polyacrylamide gel (19:1 acrylamide/ bisacrylamide in 8 M urea). The gels were dried, exposed to storage phosphor screens for $\geq$ 40 h, and directly imaged using the Storm phophorimaging system (Ammersham Biosciences). The optical densities of bands representative of the bioO binding site at each protein concentration were integrated and binding isotherms were generated as described by Brenowitz (*92*). All binding data were analyzed by nonlinear least-squares techniques using NonLin (*94*) using the following equation:

$$\bar{Y} = \frac{K_{Dim} K_{bioO} [holoBirA]^2}{1 + K_{Dim} K_{bioO} [holoBirA]^2} \qquad (3)$$

that relates the occupancy of the biotin operator site to the total repressor monomer concentration. For this analysis, the dimerization constant (K_{Dim}) of holoBirA was obtained from analysis of sedimentation equilibrium data. The concentration of free

BirA is assumed to be equal to the total BirA concentration. This assumption is valid because in all measurements the total protein concentration is much greater than the DNA concentration (*94*).

C. Results

1. Chemical structures of the analogs

The structures of bio-5'- AMP and the two analogs shown in Figure 13 illustrate the chemical differences between the physiological corepressor and its two putative non-labile derivatives. The sulfamoyl analog, 5'-O-[N-(biotinoyl)-sulfamoyl] adenosine or btnSA, is altered from bio-5'-AMP by replacement of the bridging phosphate with the isosteric sulfamoyl group. The ester, biotinol-adenylate or btnOH-AMP, is simply the product of formation of the phosphate-ester linkage of 5'-AMP with biotinol. In order to be useful in future structural and thermodynamic studies, the analogs must bind to BirA with reasonable affinity and be proven to be inactive substrates in biotin transfer. Moreover, like bio-5'-AMP, they must function in enhancing the affinity of BirA for bioO.

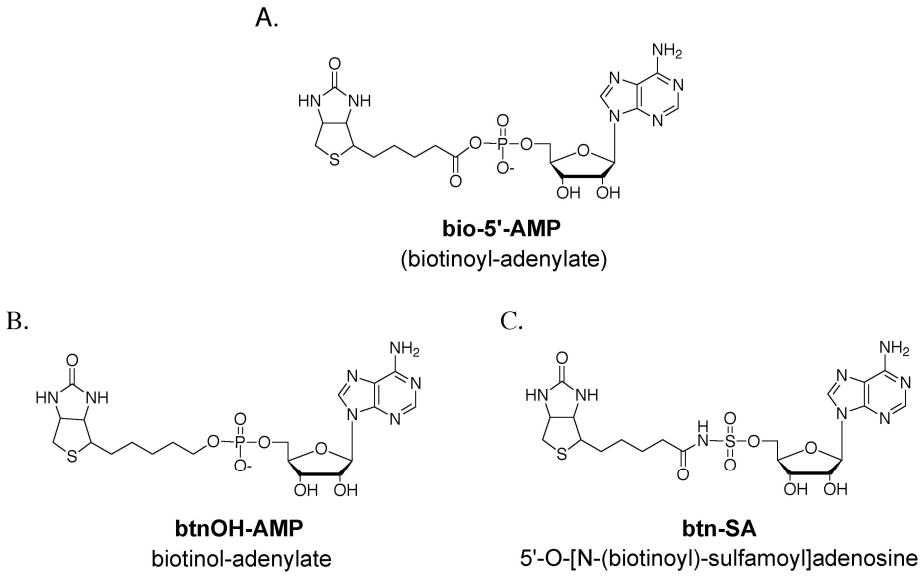

Figure 13. Chemical structures of the physiological corepressor and its analogs. (A) bio-5'-AMP (B) btnSA and (C) btnOH-AMP.

2. The analogs bind tightly to BirA

Fluorescence spectroscopy was used to determine if the two corepressor analogs bind to apoBirA. The intensity of the intrinsic fluorescence emission spectrum of BirA has been shown to be dependent on its state of ligation (*95*). While saturation of apoBirA with biotin results in a 15% decrease in the signal intensity, saturation with bio-5'-AMP leads to 40% quenching (Figure 14-A). In this study the effect of addition of saturating amounts of each adenylate analog on the intrinsic fluorescence emission spectrum of BirA was determined. In initial measurements a molar excess of each analog was added to a 2 μM solution of apoBirA. As observed for binding of bio-5'-AMP to apoBirA, addition of either analog resulted in an approximately 40% decrease in the intrinsic fluorescence of apoBirA (Figure 14-B) a result consistent with binding of both ligands to the protein. Furthermore, although no equilibrium dissociation constants for the binding interactions could be obtained, titrations of apoBirA with each analog provided a semi-

quantitative estimate of the affinity of the analogs for the protein as well as the stoichiometry of each binding process. Titration of 2 μM repressor with either ligand yielded a breakpoint titration, consistent with a tight binding process with upper limits for the equilibrium dissociation constants in the nanomolar range of concentration (Data not shown). Moreover, for either analog the stoichiometry obtained from analysis of the data was one ligand per protein monomer.

3. The bio-5'-AMP analogs are not substrates for biotin transfer

Two methods were used to assess the ability of BirA to catalyze biotin transfer from each analog to the biotin acceptor protein, apoBCCP87. This 87 residue protein constitutes the C-terminal domain of the acceptor protein subunit of *E.coli* acetyl-CoA carboxylase that has been shown to be as active as the intact acceptor protein in the biotin transfer reaction (*86*). Fluorescence spectroscopy was initially used to assess the activity of the analogs in the second step of the biotin ligation reaction. Upon addition of a molar excess of apoBCCP87 to a 1:1 repressor: adenylate complex transfer of biotin to the acceptor protein results in regeneration of apoBirA and concomitant return of the fluorescence spectrum to that of unliganded protein (*86*). However, when this same experiment was performed using either the BirA·btnSA or BirA·btnOH-AMP complex (Figure 14-B), no change in the emission spectrum occurred, consistent with a lack of transfer of biotin from either ligand to apoBCCP87.

Since post-translational addition of biotin to apoBCCP87 gives rise to an increase in the mass of the protein by 226 Da mass spectrometric analysis can also be used to measure the biotin transfer reaction (*86*). In this experiment, the apo-acceptor protein is incubated with catalytic amounts of BirA and a molar excess of bio-5'-AMP over acceptor protein. Analysis of the products of the reaction by MALDI-TOF yields the spectrum shown in Figure 15 and Table 1. The masses obtained from spectra acquired from samples in which the small ligand is replaced by biotin, btnOH-AMP or btnSA are also shown in the table. While incubation of apoBCCP87 with BirA in the presence of bio-5'-AMP leads to the expected increase in the mass of the acceptor protein, no mass shift is observed in the presence of the remaining three ligands, indicating that both analogs are indeed inactive in biotin transfer to apoBCCP.

4. Analog binding is positively linked to biotin repressor dimerization

In its function as a corepressor, bio-5'-AMP increases the affinity of BirA for the biotin operator by enhancing the energetics of repressor dimerization. Previously published studies indicate that while the apo repressor and repressor·biotin complex have no tendency to dimerize, the BirA·bio-5'-AMP complex undergoes a monomer-dimer transition with a K_D of approximately 10 μM, in standard buffer (200 mM KCl) at 20 °C (*59*).

The assembly properties of the two BirA-analog complexes were determined by sedimentation equilibrium measurements and compared to those of the adenylate-bound

repressor. Based on the information obtained from fluorescence titrations described above, the concentrations of protein and ligand utilized for all sedimentation measurements ensured saturation of repressor with ligand. Measurements were performed on each complex at multiple loading concentrations and samples were centrifuged at multiple rotor speeds. Sedimentation data were initially analyzed using a single species model and molecular weights obtained from the analyses are shown in Table 2. With the exception of the BirA·biotin complex, the average molecular mass resolved for each protein-ligand complex is significantly greater than the known mass of the monomer (35 kDa), consistent with self-association of the protein complexes. Additionally, single-species analyses performed on samples prepared at a range of loading concentrations indicated increases in the apparent molecular mass of the complex with increasing loading concentration (data not shown). These observations are also consistent with reversible association of each complex (*91*).

The sedimentation equilibrium data obtained from measurements performed on each complex were also analyzed using a monomer-dimer self-association model. Global analysis of six data sets obtained at multiple rotor speeds and loading concentrations was performed for each complex (Figure 16 and Table 2). The resolved dimerization constant for the BirA·bio-5′-AMP complex of 9 x 10^{-6} M is in excellent agreement with that obtained previously under the same conditions (*59*). Similarly, analysis of the data obtained with BirA·biotin did not return a reasonable dimerization constant. Moreover, the mass of this complex calculated from the reduced molecular weight (see Materials and Methods) is consistent with a monomeric complex. The complex of BirA bound to

the sulfamoyl-analog, btnSA, does undergo limited self- association, with an equilibrium dissociation constant in the millimolar range of monomer concentration. Finally, btnOH-AMP functions much like the physiological corepressor in driving dimerization of BirA. The resolved equilibrium dissociation constant determined for this complex of 38 μM is only four-fold greater than that measured for the BirA·bio-5'-AMP complex. Furthermore, the distribution of the residuals and the magnitudes of the square root of the variance obtained from the data analyses for the three complexes of BirA bound to bio-5'-AMP, btnSA, and btnOH-AMP, indicated that the assembly of each is best described by a monomer-dimer model.

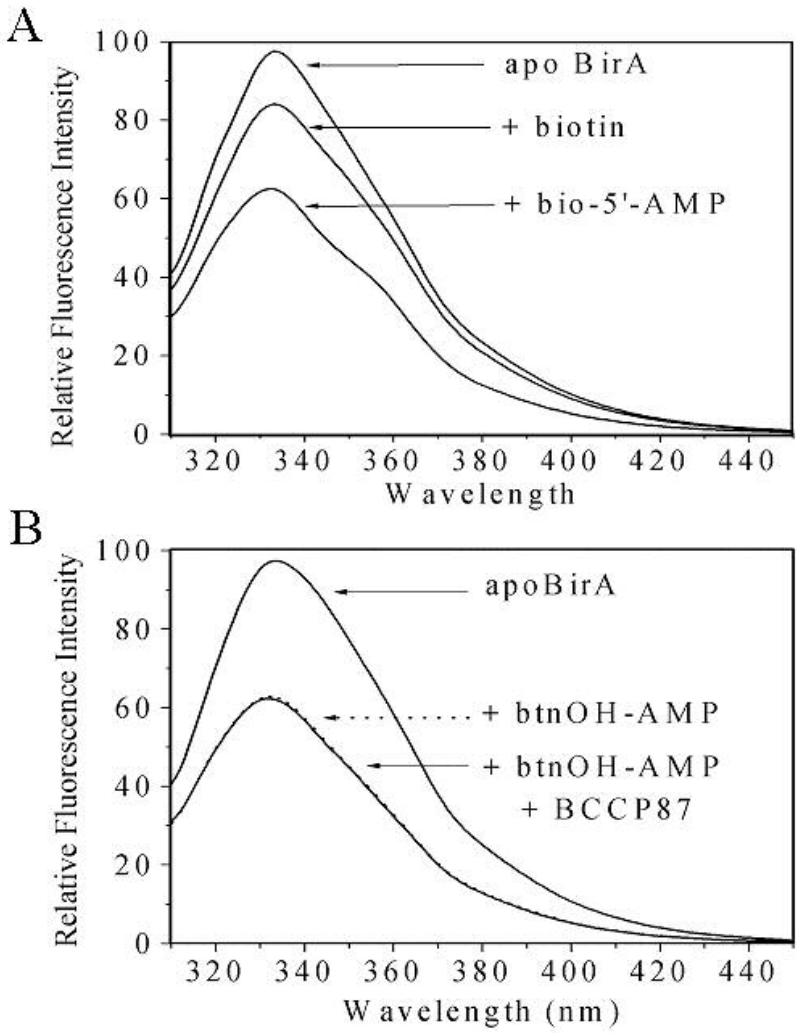

Figure 14. (A) Intrinsic fluorescence spectra of 2 μM apoBirA, 2 μM BirA + 2.2 μM biotin, and 2 μM BirA + 2.2 μM bio-5'-AMP. All spectra were acquired in 10 mM Tris-HCl (pH 7.50 ± 0.02 at 20.0 ± 0.1 °C), 200 mM KCl, 2.5 mM $MgCl_2$. Spectra were smoothed using an FFT filter within the Origin software package. (B) Monitoring biotin transfer by fluorescence; The cuvette contained either 2 μM ApoBirA, 2 μM BirA + 2.2 μM btnOH-AMP, or 2 μM BirA + 2.2 μM btnOH-AMP + 10 μM BCCP87 in buffer identical to that used in (A). Spectra were smoothed using an FFT filter within the Origin software package.

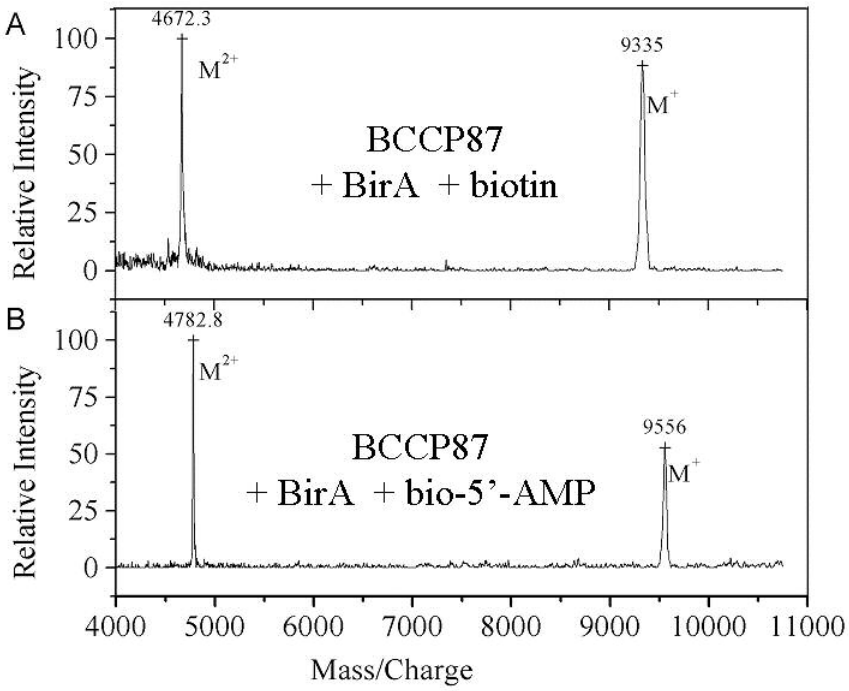

Figure 15. MALDI-TOF mass spectra of BCCP87 after incubation at 100 μM with (A) 1.0 μM BirA + 110 μM biotin or (B) 1.0 μM BirA + 110 μM bio-5'-AMP.

Table 1. Results of MALDI-TOF MS analysis of BCCP87 samples.

Condition[a]:	**Mass BCCP87 (Da)[b]**	**ΔMass (Da)[c]**	**Biotin Transfer[d]**
BirA + biotin	9335	2	-
BirA + bio-5'-AMP	9556	220	+
BirA + btnSA	9339	3	-
BirA + btnOH-AMP	9359	23	-

[a]Incubation of BCCP87 and catalytic amounts of BirA was performed in 10 mM Tris-HCl (pH 7.50 ± 0.02 at 20.0 ± 0.1 °C), 200 mM KCl, 2.5 mM $MgCl_2$, in the presence of the indicated ligand. [b]The mass of the BCCP87 sample determined by MALDI-TOF MS. [c]Difference in measured mass of BCCP87 sample incubated with the respective BirA complex from the calculated mass of *apo*BCCP87. [d]An observed mass shift of ~226 Da is consistent with biotinylation of BCCP87 (the masses of *apo*BCCP87 and *holo*BCCP87 are 9337 and 9562 Da, respectively).

5. Analog binding is positively linked to bioO binding

One of the physiological roles of the adenylate is to drive binding of the biotin repressor to bioO. As indicated above, this is achieved through enhancement of dimerization. Although binding of either analog is, indeed, positively linked to repressor dimerization, it is important to directly measure the affinities of the complexes for the biotin operator sequence. This was accomplished using DNaseI footprint titrations. Results of previous DNase I footprinting analyses (*63*), indicate that binding of bio-5'-AMP to apoBirA enhances the energetics of assembly of the protein-DNA complex by -4.5 kcal/ mole.

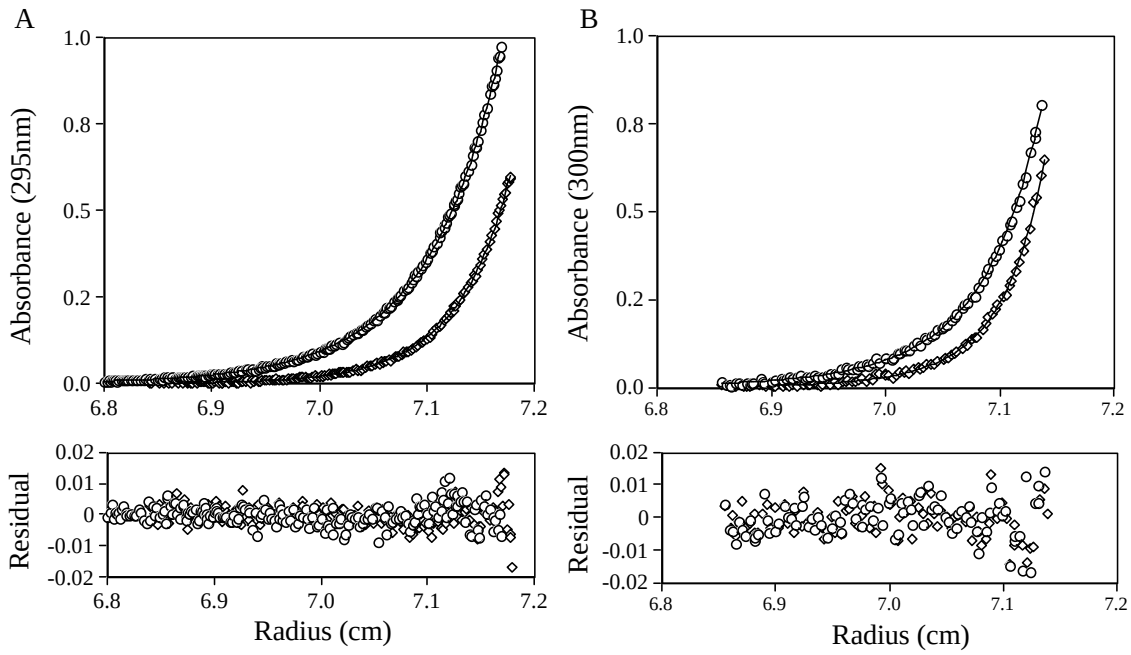

Figure 16. Absorbance vs. radial position profiles for (A) 30 μM BirA·btnSA and (B) 30 μM BirA·btnOH-AMP at 22k (◊) and 26 k (❍) rpm obtained in 10 mM Tris-HCl (pH 7.50 ± 0.02 at 20.0 ± 0.1 °C), 200 mM KCl, 2.5 mM $MgCl_2$. The solid lines are the best-fit curves generated from a global analysis of six data sets that were acquired from samples prepared at multiple concentrations and spun at multiple rotor speeds. A monomer-dimer model was utilized in the analysis. The lower panels illustrate the residuals of the fits.

Table 2. Sedimentation equilibrium measurements of the assembly properties of the BirA-ligand complexes.

Complex[a]	Single Species MW (Da)[b]	Monomer-Dimer K_{dim} (M)[c]	ΔG°_{dim} (kcal/mol)[d]	var$^{1/2}$	
				ss	m-d
BirA·biotin	35872 (34861, 36848)	-----	-----	0.005	0.005
BirA·bio-5'-AMP	56177 (54325, 57991)	9.0 (± 1.0) x 10^{-6}	-6.8 (± 0.1)	0.025	0.005
BirA·btnSA	39695 (39111, 40279)	1.0 (± 0.1) x 10^{-3}	-4.0 (± 0.1)	0.007	0.003
BirA·btnOH-AMP	51830 (48799, 54861)	3.8 (± 0.8) x 10^{-5}	-5.9 (± 0.1)	0.035	0.004

[a]All measurements were performed in 10 mM Tris-HCl (pH 7.50 ± 0.02 at 20.0 ± 0.1 °C), 200 mM KCl, 2.5 mM $MgCl_2$. Sufficient ligand to fully saturate the protein was present in all samples. [b]Resolved molecular masses were calculated from the best-fit values of the reduced molecular weight, σ, obtained from the single species fit of 25 μM BirA saturated with biotin, and 30 μM BirA saturated with btnSA, btnOH-AMP, or bio-5'-AMP. The values in parentheses provide the 65% confidence intervals. [c]Equilibrium dimerization constants were obtained from the global analysis of six data sets obtained at two rotor speeds and three loading concentrations. [d]Gibbs free energies of dimerization were calculated from the equilibrium dissociation constant using the relationship $\Delta G^{\circ}_{dim} = -RT \ln K_{dim}$. [e]Square root of the variance obtained from the global analysis of data fit to either a single species (ss) or monomer-dimer (m-d) model.

Figure 17-A shows an image of a gel for a typical footprint obtained from titration of bioO with the analog complex BirA·btnOH-AMP. The footprint is qualitatively identical to that obtained in experiments with BirA**.**bio-5'-AMP. Previously, equilibrium footprinting data obtained on this system have been analyzed using a two-site cooperative binding model (*58*). However, analysis of rapid kinetic measurements of the protein-DNA binding process indicates that the mechanism of binding entails dimerization of

holoBirA followed by DNA binding (*62*). Thus, the equilibrium footprinting data were analyzed using a binding model in which a preformed dimer associates with the DNA (see Equation 3 in Materials and Methods). For each complex the dimer concentration was calculated at each total monomer concentration using the equilibrium dissociation constant obtained from the sedimentation equilibrium studies. A binding isotherm obtained from titration of bioO with BirA·btnOH-AMP is shown in Figure 17-B. The data shown in the figure contains information about fractional saturation of each of the operator half-sites. Nonlinear least-squares analysis of the footprinting data obtained for the three BirA complexes bound to bio-5'-AMP and the two analogs yielded the parameters shown in Table 3. The magnitudes of both the total free energies of assembly of each protein DNA complex from two protein monomers, ΔG^{o}_{total}, as well as the free energies associated with binding of the dimer to bioO, ΔG^{o}_{bioO}, are provided. The total free energies of assembly of the dimer-DNA complexes from the free monomers and DNA range from -18.4 kcal/mole to -20.7 kcal/mole. Consistent with previous studies, the relative energetics of dimerization of a particular BirA-ligand complex predicts the relative magnitude of the total assembly energetics of the complex. However, comparison of the apparent affinities of the three dimers for bioO indicates they are not equivalent. While the dimers of BirA bound to either bio-5'-AMP or btnOH-AMP exhibit identical affinities for bioO, the BirA·btnSA dimer binds with significantly more favorable free energy to the operator site.

Table 3. Results of DNase I footprinting titrations of bioO with the BirA-ligand complexes.

Complex[a]	ΔG°_{bioO} (kcal/mol)[b]	ΔG°_{total} (kcal/mol)[c]
BirA·bio-5'-AMP	-13.9 (± 0.2)	-20.7 (± 0.2)
BirA·btnSA	-14.5 (± 0.2)	-18.4 (± 0.2)
BirA·btnOH-AMP	-13.7 (± 0.1)	-19.6 (± 0.1)

[a]All measurements were performed in 10 mM Tris-HCl (pH 7.50 ± 0.02 at 20.0 ± 0.1 °C), 200 mM KCl, 2.5 mM $MgCl_2$, 1 mM $CaCl_2$, 2 μg/mL sonicated calf thymus DNA, and 100 μg/ml BSA. [b]Binding free energies are calculated from the equilibrium binding constants obtained from least-squares analysis of the data using the relationship $\Delta G^{\circ}_{bioO} = -RT \ln K_{bioO}$. [c]Total free energies associated with assembly of each protein-DNA complex were calculated using the relationship $\Delta G^{\circ}_{total} = \Delta G^{\circ}_{bioO} + \Delta G^{\circ}_{dim}$. Dimerization free energies used were obtained from results of sedimentation equilibrium analysis of BirA-ligand complex.

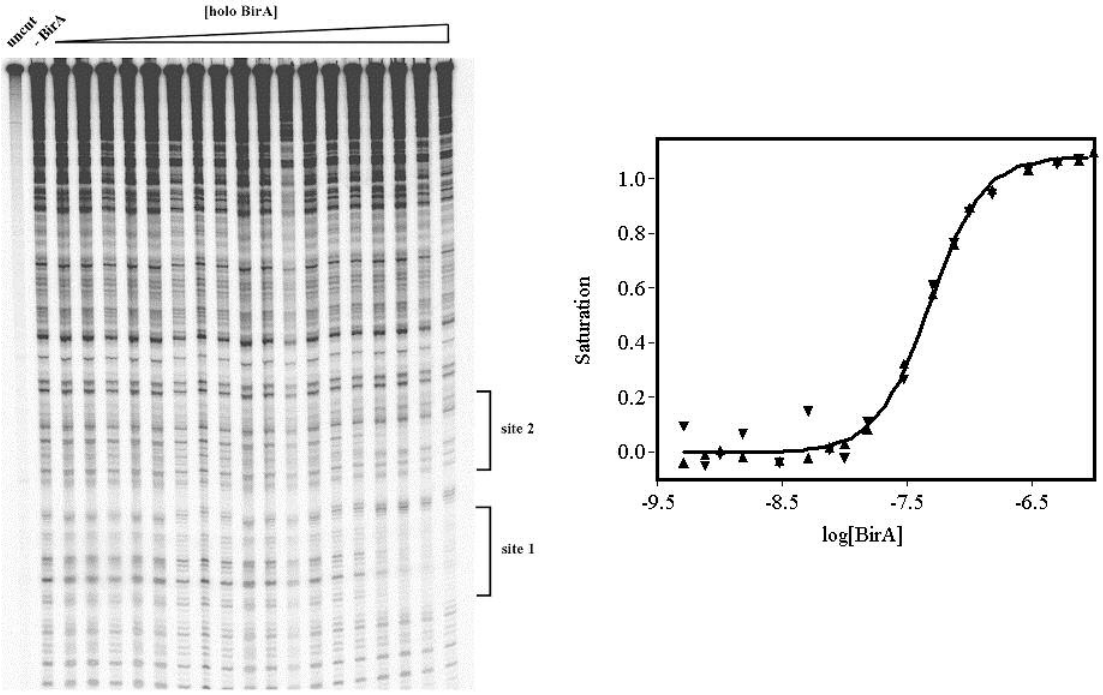

Figure 17. (A) DNase I footprint of bioO with BirA·btnOH-AMP. The footprint was obtained in buffer containing 10 mM Tris-HCl (pH 7.50 ± 0.02 at 20.0 ± 0.1 °C), 200 mM KCl, 2.5 mM $MgCl_2$, 1 mM $CaCl_2$, 2 μg/mL sonicated calf thymus DNA, and 100 μg/ml BSA. (B) Binding isotherm generated from quantitation of a DNase I footprint titration of bioO with BirA·btnOH-AMP. The solid line represents the best-fit curve from the analysis of the data. The data symbols represent the fractional saturation of the two operator half sites, 1 (▼) and 2 (▲), with the BirA·btnOH-AMP complex.

D. Discussion

The two analogs of bio-5'-AMP analyzed in this work are structurally very similar to the adenylate. However, although the sulfamoyl group is isosteric with a phosphate it lacks the negative charge. The btnOH-AMP analog retains the negatively charged phosphate group but lacks the carbonyl group of biotin. Participation of the biotin repressor in multiple processes and the availability of assays to measure these processes provide the means to thoroughly test the functional properties of the analogs. The protein binds to biotin and ATP and catalyzes synthesis of the biotinoyl-adenylate, bio-5'-AMP, which has been shown to bind with high affinity to BirA and its binding results in a conformational transition in the protein (*68*). The enzyme-intermediate complex functions both in transfer of biotin to the acceptor protein and site-specific binding to the biotin operator. The data obtained from fluorescence titrations indicate that both analogs bind to BirA in a 1:1 stoichiometry and that, although the exact equilibrium dissociation constants are not known, the upper limit for both ligands is in the nanomolar range of

concentration. This conclusion is supported by the observation that titration of 2 μM protein with either analog resulted in stoichiometric or break point binding curves. Furthermore, the observation that binding of either analog induces quenching of the intrinsic fluorescence of the repressor equivalent to that associated with bio-5'-AMP suggests induction of the same conformational change by binding of each ligand to BirA (*68*). It was also critical to demonstrate the lack of biotin transfer from either analog to apoBCCP. The fluorescence measurements and mass spectrometric analysis are consistent with the conclusion that both compounds are inert to the transfer process. While these results do not absolutely prove that given sufficient time some transfer would not occur, three observations contradict this notion. First, the analogs are chemically very stable as indicated by their lack of hydrolysis when subjected to acidic pH (See Materials and Methods). Second, complexes of the corresponding aminoacyl adenylate analogs bound to tRNA synthetases have been demonstrated to be stable to crystallization and X-ray diffraction studies (*83, 96, 97*). Finally the chemical structures (Figure 13) indicate that while the ester lacks the carbonyl carbon at which nucleophilic attack occurs in the second step of biotin transfer, the sulfamoyl is characterized by a very stable amide bond between the biotin and SA moieties.

The adenylate serves as the corepressor in repression of transcription initiation at the biotin biosynthetic operon and previous studies indicate that the ligand activates the repressor for biotin operator binding by promoting self-assembly of the repressor (*59*). The increased stability of the repressor dimer leads to a more favorable free energy of assembly of the repression complex. Thus in assessing the function of the analogs it was

important to measure both the dimerization and DNA binding properties of the repressor·analog complexes. Sedimentation equilibrium analysis of the complexes indicate that while the sulfamoyl analog is a relatively weak activator of dimerization, the ester analog acts similarly to bio-5'-AMP. In considering their function in dimerization it is instructive to calculate the enhancement to the dimerization affinity of the repressor that accompanies binding of each analog. Unfortunately, at a salt concentration of 200 millimolar KCl used for the measurements described in this work no dimerization of apoBirA can be detected. However, previous studies indicate that in low salt conditions, 50 mM KCl, binding of the adenylate to BirA renders repressor dimerization energetics more favorable by -4.2 kcal/mole (*63*). Assuming that the same difference in the dimerization energetics for apoBirA and BirA·bio-5'-AMP species is retained upon shifting the KCl concentration from 50 to 200 mM allows calculation of enhancement of the dimerization energetics linked to binding of each small ligand. Using this assumption, the calculated Gibbs free energy of dimerization of apoBirA at 200 mM KCl is -2.6 kcal/mole, consistent with an equilibrium dimerization constant of approximately 10 mM. This large dimerization constant is confirmed by inability to detect dimerization of apoBirA by sedimentation equilibrium as well as the observation of a monomer of this species in X-ray crystallographic studies (*59, 64*). Based on this calculated value of the dimerization free energy of apoBirA, binding of the btnSA and btnOH-AMP analogs are estimated to enhance the repressor dimerization by -1.4 and -3.3 kcal/mole, respectively. The change associated with btnOH-AMP binding compares favorably with the -4.2 kcal/mole enhancement linked to bio-5'-AMP binding.

The function of the analogs in promoting bioO binding was assessed using DNaseI footprint titration measurements. The data indicate that binding of either ligand to apoBirA renders the energetics of assembly of the repression complex more favorable. Again, the inability to measure binding of apoBirA to bioO in 200 mM KCl precludes direct calculation of the enhancement of repression complex assembly energetics associated with each ligand. However, assuming that in comparing apo and holoBirA species the $\Delta\Delta G^{o}$ for the assembly process remains the same upon increasing the salt concentration from 50 to 200 mM KCl allows calculation of the energetic advantage for the assembly process that is linked to binding of each ligand. While for bio-5'-AMP the enhancement is -4.5 kcal/mole (*63*), for btnSA it is -2.5 kcal/mole, and for btnOH-AMP -3.5 kcal/mole. As observed for the dimerization process, the ester is a considerably better functional mimic of bio-5'-AMP than is the sulfamoyl derivative. However, both are positive activators of the dimerization and DNA binding functions of BirA.

As indicated in the Introduction, the design of these analogs was based on similar analogs used in studies of the amino acyl-tRNA synthetases. A number of nonhydrolyzable analogs amino acyl adenylates of the sulfamoyl and ester classes have been synthesized (*82-85*). However, in the tRNA-synthetase context, the functional studies of these analogs are limited to inhibition measurements to obtain information about their apparent affinities for the enzymes (*98*). Moreover no information is available on how the binding affinity of each analog compares to that of the amino-acyl adenylate. Structures of several amino-acyl tRNA synthetases bound to the analogs have been obtained by X-ray crystallographic studies (*83, 96, 97*). The results of these studies are used to infer the affect of adenylate binding on conformational transitions in the

enzyme. In the absence of more extensive functional analysis of the analogs, the validity of these inferences is unclear.

The functional properties of the two analogs in promoting dimerization and bioO binding of the repressor provides further insight into the allosteric mechanism of this protein. Numerous studies of this system indicate that the adenylate functions in activating the repressor for DNA binding by enhancing its dimerization. Thermodynamic tests of this model indicate that for the physiological corepressor the total enhancement in the energetics of assembly of the protein-DNA complex closely matches the enhancement of dimerization afforded by binding of the ligand (*63*). This is consistent with the dimerization interface serving as the major conduit for transduction of the allosteric signal. However, the properties of the weak allosteric activator, biotin, indicate an uncoupling of dimerization and DNA binding. While binding of this ligand to apoBirA yields no enhancement of dimerization energetics it does increase the assembly energetics of the repression complex by- 1.6 kcal/mole. The data obtained in studies of the adenylate analogs mirror these results of previous studies (Figure 18). In transformation of the repressor from the btn-OH-AMP-bound species to the bio-5'- AMP complex the dimerization free energy is enhanced by -1.0 kcal/mole. The enhancement of the total free energy of assembly of the repression complex associated with this transformation is also -1.0 kcal/mole. However, if one compares the sulfamoyl complex with the adenylate complex there is a mismatch between the differences in dimerization energetics and total assembly energetics. As observed for the biotin-bound protein, the total free energy of assembly of the repression complex is considerably more favorable

than would be predicted from the dimerization energetics (Tables 2 and 3). The combined results indicate an uncoupling of dimerization and DNA binding with weak allosteric activators whereas strong activators exhibit no such uncoupling. The uncoupling observed for weak allosteric activators may indicate allosteric coupling within a monomer unit; perhaps between the catalytic or effector binding and the DNA binding domains.

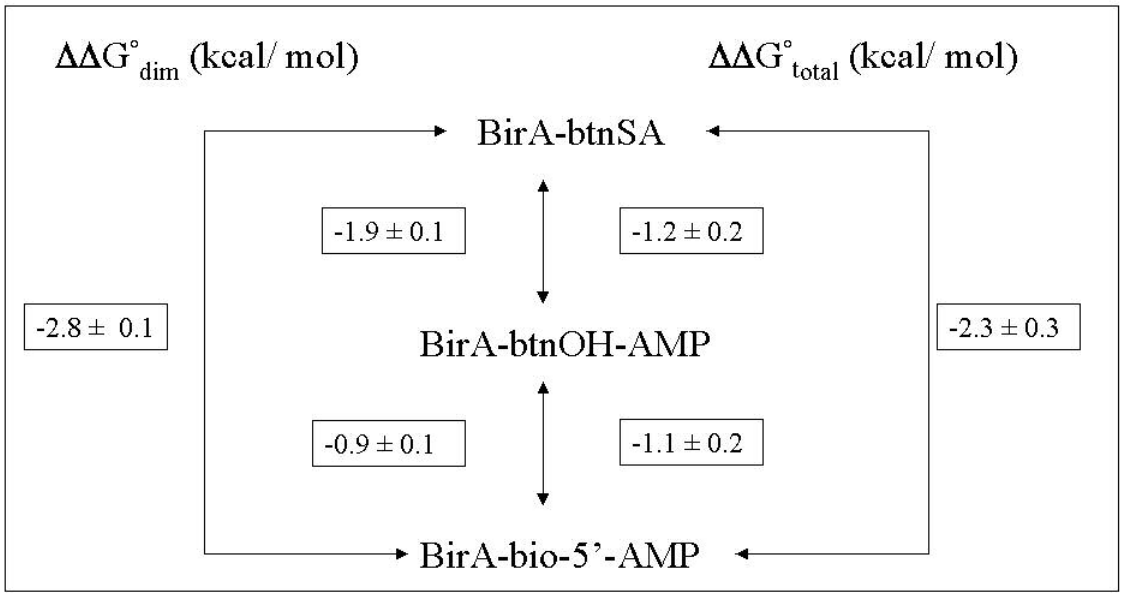

Figure 18. Effects of the physiological corepressor and its analogs in driving dimerization of BirA and assembly of the holorepressor-bioO complex. $\Delta\Delta G^{o}_{dim}$ is the pairwise difference in dimerization free energy of the indicated BirA-ligand complexes. $\Delta\Delta G^{o}_{total}$ is the pairwise difference in total free energy for formation of the indicated holorepressor-bioO complexes, $\Delta G^{o}_{total} = \Delta G^{o}_{dim} + \Delta G^{o}_{bioO}$.

The functional properties of the two adenylate analogs revealed in this study indicate that they will be useful in future solution and structural probing of the biotin regulatory system. Both ligands bind with reasonable affinity to the repressor and are inactive in biotin transfer. Moreover, the two ligands function in allosteric activation of the repressor. While the sulfamoyl derivative is a weaker allosteric activator it will undoubtedly prove useful in understanding the mechanism of allosteric activation in this system.

III. A thermodynamic investigation of corepressor binding to the biotin repressor

A. Introduction

Control of biological processes such as signal transduction and transcription is vital for the proper function of any organism. Allosteric regulation is one of the most frequently utilized mechanisms of control of macromolecular function (*5, 69*). In allosteric control of protein function binding of small molecule effectors, post translational modification or the binding of other proteins can serve to regulate the functional properties of a protein. In order to gain a mechanistic understanding of any allosteric process it is necessary to elucidate the structural and functional features of the states of the system and the rules governing their interconversion.

Many transcription regulatory proteins are subject to allosteric regulation. Classic examples include the lactose (LacR) and purine (PurR) repressors to which binding of a small ligand alters the affinity of the protein for its target DNA. In these systems the repressors are oligomers and effector binding has no impact on the oligomeric state of the protein. Rather, the relative orientations of the DNA binding domains respond to ligand binding thus altering the affinity of the protein for DNA. While in the lactose repressor system the affinity is decreased, the affinity of the purine repressor for DNA increases in response to effector binding. A second class of allosterically regulated transcription repressors include those for which DNA binding affinity is modulated via alteration of the assembly properties of the protein. In these systems effector binding may be positively coupled to the multimerization of the protein and thereby increases the

probability that a regulatory DNA site is occupied by protein. The diphtheria toxin repressor (DtxR) provides one example of this class of protein. In this system metal binding appears to enhance DNA binding by driving repressor dimerization. In contrast to the well-studied repressors systems such as LacR and PurR, which adhere to the "classical" allosteric mechanism, few of the transcription regulators in which the effector operates via its influence on protein assembly have been subjected to detailed physical-chemical analysis of the allosteric mechanism.

The *Escherichia coli* biotin regulatory system provides an excellent model for examining the physical mechanism of allosteric activation in the latter class of transcription regulators. The central component of this system, BirA or the biotin repressor is a 35.3 kDa protein that serves two biological functions (*70, 71*). First, the two-step catalysis of biotinylation of the biotin carboxyl carrier protein, a subunit of acetyl-CoA carboxylase, is essential for cell viability (*54, 70*). In the first step, BirA catalyzes the synthesis of biotinyl-5'-AMP (bio-5'-AMP) from the substrates*d*- biotin and ATP. In the second step the biotin moiety is transferred to a specific lysine residue of the carrier protein. The second function of BirA is to repress transcription of the genes coding biotin biosynthetic enzymes (Figure 19) (*72*). This function requires two repressor molecules to bind site-specifically to a 40-base pair palindromic DNA sequence, thereby blocking initiation of transcription at the two divergent promoters of the operon, bioO (*58, 72*). The affinity of the repressor for its target DNA sequence is modulated by binding of the small molecule corepressor, biotinyl-5'-AMP, to BirA. Binding of bio-5'-AMP to BirA promotes the dimerization of the holorepressor and

enhances the affinity of the repressor for the biotin operon. Notably, it is not the apo repressor but rather the holo or adenylate-bound BirA that is the active species in repression (*57*). Thus, biotinyl-5'-AMP serves as both the active intermediate in enzyme catalyzed biotin transfer and as the positive allosteric effector of DNA binding.

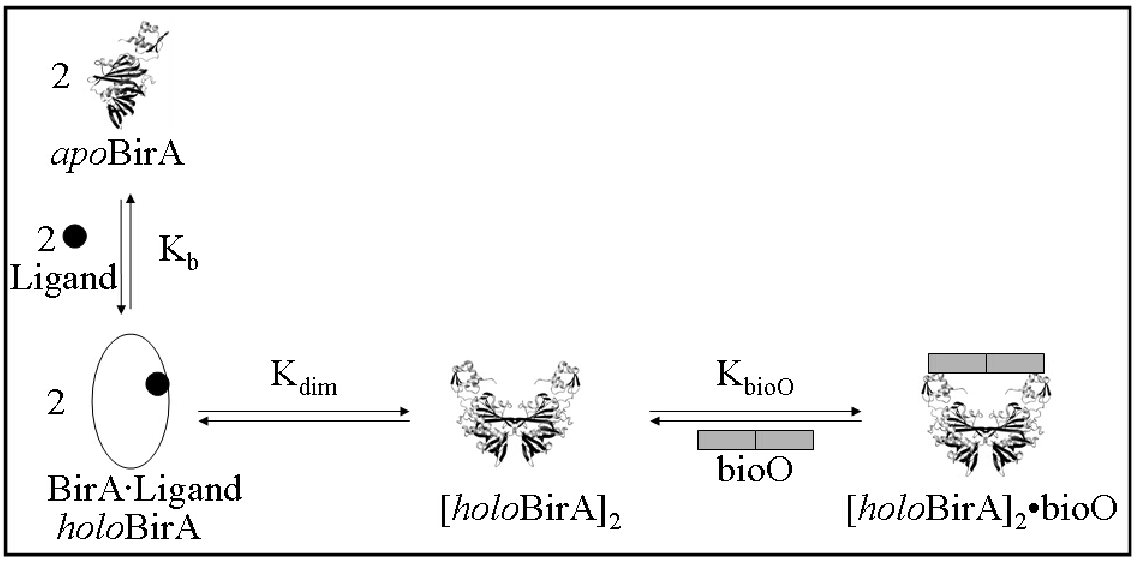

Figure 19. Allosteric activation of DNA binding. The biotin repressor (BirA) is a system in which binding of the small ligand, bio-5'-AMP, promotes DNA binding (bioO) by enhancing repressor dimerization.

The structure of the unliganded, or apo repressor, determined by X-ray crystallography (*64*) revealed that it is a monomer and is organized into three domains. The N-terminal domain adopts a winged helix-turn helix motif (*6*, *7*) and directly contacts the DNA in the repression complex. The central domain, which functions in both catalysis and in DNA binding, is folded into a seven-stranded beta-sheet and is also

characterized by four partially unstructured surface loops. The C-terminal domain, to which no function has been definitively assigned, adopts a beta-sandwich motif. As indicated above the unliganded protein is inactive in transcription repression.

The mechanism of allosteric activation of the biotin repressor has been studied in great detail using equilibrium thermodynamic, kinetic, and structural approaches (*58-64, 76*). First, as indicated above, two holorepressors bind to bioO (*58, 72*). Second, binding of the adenylate to apoBirA is positively coupled to dimerization of the protein (*59, 63*). Results of sedimentation equilibrium measurements indicate that binding of the physiological corepressor, bio-5'-AMP, enhances dimerization of BirA by -4 to -5 kcal/mol (*59, 63*). Moreover, the magnitude of this enhancement in dimerization energetics directly correlates with the enhancement in the total assembly energetics of the repression complex from free holoBirA monomers and bioO (*63*). Furthermore, single amino acid substitutions at positions in the disordered surface loops of apoBirA result in loss of repression in vivo and defects in both dimerization and DNA binding in vitro (*60*). Finally, results of time-resolved DNaseI footprinting measurements indicate that repressor dimerization precedes bioO binding (*62*). Thus corepressor bio-5'-AMP binding regulates the supply of repressor dimer, thereby dictating the probability of occupancy of bioO and therefore repression.

The structure of the repressor bound to *d*-biotin (*65*), a weak allosteric activator of BirA dimerization and DNA binding provides some insight into the structural origins of the activation mechanism. In this structure, BirA is a dimer in which the interface is

formed by side-by side alignment of the beta-sheets of the central domain of each monomer. Interestingly, three of the four loops that were disordered in the apo structure appear ordered at the monomer-monomer interface. This feature is consistent with studies of BirA mutants summarized above. Additionally, one of the loops is folded over and largely encloses the biotin molecule indicating that biotin binding to BirA is coupled to ordering of at least one of the surface loops that are disordered in the unliganded structure. The combined results of solution and structural studies of the biotin repressor have prompted formulation of a model describing the allosteric mechanism of activation of the repressor. Binding of bio-5'-AMP drives a disorder-to-order transition in the surface loops of BirA. This pre-organization of the loops results in more favorable dimerization energetics. The enhanced dimerization energetics in turn renders the overall assembly energetics of the transcription repression complex more favorable.

The linkage of repressor dimerization to DNA binding has further been investigated using corepressor analogs (*99*). The analogs have been designed to function as non-labile mimics of the physiological corepressor, bio-5'-AMP (Figure 20). Therefore, the mixed anhydride connection between the biotin and AMP moieties was replaced with either a phosphate ester (btnOH-AMP) or a sulfamoyl (btnSA) linking group. The analogs bind BirA with a 1:1 stoichiometry in the submicromolar concentration range and are inactive substrates in the BirA-catalyzed biotin transfer reaction.

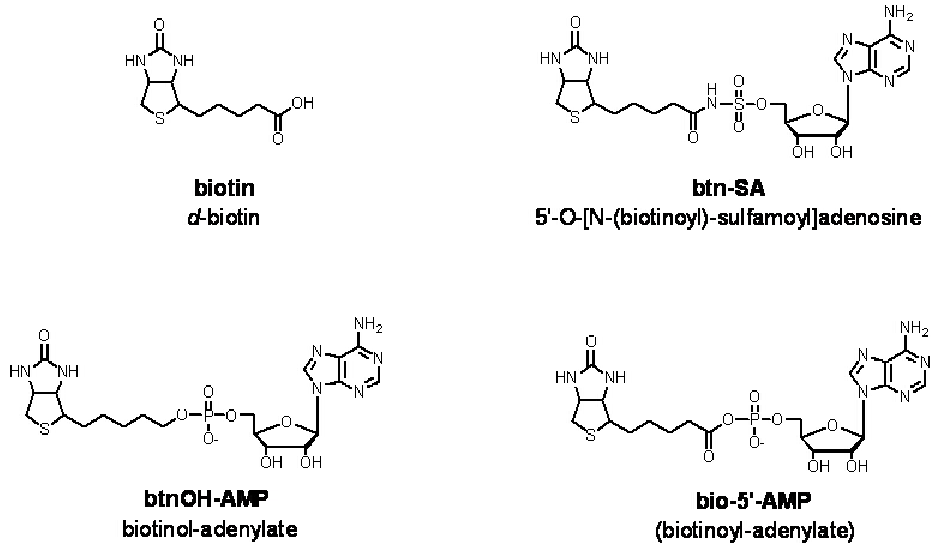

Figure 20. Chemical structures of the small molecule effectors (A) biotin, (B) btnSA, (C) btnOH-AMP, and (D) the physiological corepressor, bio-5'-AMP.

The analogs were further probed with respect to their properties in allosteric activation of the repressor by measuring the dimerization and bioO binding properties of complexes of BirA bound to each (*99*). Results of a global analysis of sedimentation equilibrium data indicate that the allosteric effectors fall into two classes. BtnSA, like *d*-biotin, is a weak allosteric activator of BirA dimerization. In contrast, btnOH-AMP functions more like bio-5'-AMP as a strong activator of dimerization. Furthermore, results of DNaseI footprinting measurements reveal a difference in the details of the allosteric mechanism for binding of the strong and weak effectors. For strong effectors the magnitude of the enhancement of repressor dimerization due to effector binding is equivalent to the magnitude of the enhancement in the overall assembly energetics of the repression complex. In contrast, binding of weak allosteric activators results in uncoupling of the two processes. The accumulated data indicate that the critical species

of the allosteric response is the liganded or activated monomer. Thus in order to further delineate the mechanism of allosteric activation it is necessary to obtain information about the structural and dynamic changes that occur in the repressor monomer concomitant with effector binding.

A potentially fruitful strategy for elucidating the mechanism of allosteric activation of the BirA monomer is to subject the effector binding process to a detailed thermodynamic analysis. In this work isothermal titration calorimetry has been utilized to dissect the energetics of the interaction of the BirA monomer with four allosteric activators. The Gibbs free energies, enthalpies, and entropies of binding have been determined. Results of these measurements indicate the effectors exhibit a range of Gibbs free energies of binding from -10 to -14 kcal/ mol. Moreover, the strong effectors exhibit enthalpic contributions to binding that are distinct from binding of weak effectors. While the interaction of BirA with the weak effectors is driven by a large favorable enthalpy component, binding of the strong effectors is characterized by a relatively modest enthalpic contribution. Binding of all four effectors to BirA is characterized by a small negative heat capacity change. However, no correlation is observed between the magnitude of the heat capacity change and the magnitude of the allosteric affect associated with binding of the ligand. In the context of the allosteric model, the contrasting enthalpic signatures of weak and strong effectors binding suggest that an enthalpically costly transition is required to activate the protein for dimerization and thus tight DNA binding.

Table 4. Allosteric Properties of the Small Molecule Effectors.

Ligand	K_{dim} (M)[a]	ΔG°_{dim} (kcal/mol)[b]	$\Delta\Delta G^{\circ}_{dim}$ (kcal/mol)[c]
biotin	[7.0 x 10^{-3}]	[-2.9 (±0.4)]	[-0.3 (± 0.3)]
btnSA	1 (±0.1) x 10^{-3}	-4.0 (±0.1)	-1.4 (± 0.2)
btnOH-AMP	3.8 (±0.8) x 10^{-5}	-5.9 (±0.1)	-3.3 (± 0.2)
bio-5'-AMP	9 (±1) x 10^{-6}	-6.8 (±0.1)	-4.2 (± 0.2)

a- Equilibrium dimerization constants were determined for each BirA·ligand complex from a global analysis of six data sets obtained at two rotor speeds and three loading concentrations using sedimentation equilibrium. Experiments were performed in 10 mM Tris-HCl (pH 7.50 ± 0.02 at 20.0 ± 0.1 ºC), 200 mM KCl, 2.5 mM $MgCl_2$. Biotin induced dimerization is not detected under these conditions, the tabulated value is assumed based on results obtained in low salt conditions (*63*). *b*- The dimerization free energy was calculated by the relationship $\Delta G^{o}_{dim} = -RT \ln K_{dim}$. *c*- Differences in dimerization free energy relative to apoBirA, assuming that the enhancement of dimerization associated with biotin and bio-5'-AMP binding is independent of [KCl] (*63*).

B. Materials and Methods.

1. Chemicals and biochemicals

All chemicals used in the preparation of buffers were obtained from commercial sources and were of at least reagent grade. The *d*-biotin was obtained from Sigma, and biotinoyl-5'-adenosinemonophosphate (bio-5'-AMP) was synthesized and purified in this

lab as described in Abbott & Beckett (*58*) using a modification of the procedure outlined in Lane *et al*. (*54*). The analogs, 5'-*O*-[*N*-(biotinoyl)-sulfamoyl]adenosine (btnSA) and biotinol-adenylate (btnOH-AMP) were synthesized as described in Brown & Beckett (*99*) or were obtained from RNA-Tec (Leuven, Belgium). The biotin repressor (BirA) was overexpressed in and purified from *Escherichia coli* BL21(λDE3)pHBA as described in Brown et al. (*99*). The purified protein was >95% pure as judged by SDS-PAGE, and >92% active as determined with fluorometric breakpoint titrations with bio-5'-AMP(*58*).

2. Isothermal Titration Calorimetry

All calorimetric binding measurements were performed using a VP-ITC microcalorimeter (1.44 mL cell) equipped with a thermovac sample degasser and a 250 μL syringe (MicroCal, Inc., Northampton, MA). Prior to performing measurements the protein stock was dialyzed extensively, unless otherwise indicated, against Standard Buffer [10 mM Tris-HCl (pH 7.50 ± 0.02 at 20.0 ± 0.1 ºC), 200 mM KCl, 2.5 mM $MgCl_2$]. The dialyzed protein was filtered through a 0.22 μm PTFE syringe filter, and its concentration determined spectrophotometrically using the extinction coefficient at 280 nm (ε_{280} = 47510 $M^{-1}cm^{-1}$) (*58*). Protein and ligand solutions were prepared from concentrated stocks using filtered dialysis buffer and were degassed for 10 min prior to use in titrations. In all experiments, the ligand was added to the protein in the sample cell. All heats of binding were corrected for the heat of ligand dilution by subtraction of the average heat associated with multiple injections of ligand performed after saturation of the protein. The binding data were analyzed using the Origin (7.0) software package.

a. Equilibrium Binding Titrations:

Direct Titrations. A direct titration method was utilized in calorimetric measurements of biotin and btnSA binding to BirA. A 5 μM BirA solution was titrated with 29 - 10 μL injections of either a 50 μM biotin or btnSA solution in Standard Buffer at 20.0 ±0.1 ºC. The calorimetric signals were integrated and nonlinear least-squares analysis of the resulting binding data using a single-site model was performed to determine the equilibrium association constant, K_A, binding enthalpy, ΔH°, and the stoichiometry of the interaction, *n*. The Gibbs free energy of binding ΔG° and the binding entropy term $-T\Delta S^{\circ}$ were calculated from the resolved parameters using the following relationships:

$$\Delta G^{\circ} = -RT \ln K_A \qquad (4)$$

$$\Delta G^{\circ} = \Delta H^{\circ} - T\Delta S^{\circ} \qquad (5)$$

Displacement titrations. The high affinities of BirA for BtnOH-AMP and bio-5'-AMP necessitated the use of a displacement titration method for measuring these two binding interactions. This procedure was performed in two steps. First, a BirA solution was titrated to saturation with 29 - 10 μL injections of a biotin stock solution. This titration was followed by a displacement titration with 29 - 10 μL injections of a btnOH-AMP or bio-5'-AMP solution. The concentrations of components used for the btnOH-AMP titrations were, 5 μM BirA, 50 μM biotin, and 50 μM btnOH-AMP. In the bio-5'-AMP titrations, BirA was present in the cell at 2 μM, while the biotin and bio-5'-AMP titrant concentrations were 20 μM each.

The raw calorimetric signal obtained for each displacement titration were integrated and corrected for the heat of ligand dilution. The resulting binding isotherm was subjected to nonlinear least-squares analysis using a single site model to obtain an apparent binding constant K_{app} and an apparent binding enthalpy ΔH_{app}. The binding constant K_A and enthalpy ΔH°_A for the higher affinity binding process are related to the apparent binding parameters by the following relationships (*100*):

$$K_{app} = \frac{K_A}{1 + K_B[B]} \qquad (6)$$

$$\Delta H_{app} = \Delta H^{\circ}_A - \Delta H^{\circ}_B \frac{K_B[B]}{1 + K_B[B]} \qquad (7)$$

where K_B, and ΔH°_B, refer to the equilibrium binding constant and the molar binding enthalpy for the ligand that binds to BirA with lower affinity, in this case biotin. The parameters K_A, and ΔH°_A correspond to the equilibrium binding constant and binding enthalpy for the ligand that displaces biotin, either btnOH-AMP or bio-5'-AMP. The total concentration of biotin in the cell is represented by [B].

b. Titrations at Total Association

An alternative calorimetric titration method was used to obtain information about the heat capacity changes and linked protonation events associated with the four protein:ligand interactions. The method requires a total of 15 injections of a concentrated

ligand solution into the calorimeter cell containing the protein. An initial 2 μL injection is followed by 5 - 5 μL injections, then a single 150 μL injection, and finally 8 - 5 μL injections. The 2 μL injection is performed as a precaution against any leakage of ligand solution that may have occurred during loading of the syringe into the calorimeter cell. Information obtained from this injection is discarded. Injections 2 thru 6 were performed to obtain 5 measurements of the uncorrected binding enthalpy. In these titration conditions the protein and ligand concentrations are in the range of stoichiometric binding. Thus, in each of these five injections all ligand binds quantitatively to the protein. The 150 μL injection is designed to fully saturate the protein so that the heat evolved in subsequent injections will be due only to ligand dilution. The final 8 injections were performed to obtain an average heat of ligand dilution. The average heat of these last 8 injections was subtracted from each uncorrected measured heat of binding for injection 2 thru 6 to obtain the corrected binding enthalpy, ΔH°_{bind}.

Using this method, one obtains 5 measurements of the binding enthalpy in one experiment. This strategy contrasts the single-point saturation method used previously (*101*), which provides one measurement of the enthalpy, and does not offer protection against leakage of the syringe during loading. The total association method was used to determine the binding enthalpy for formation of each effector complex as a function of temperature or the experimental buffer used.

c. Linkage of protonation to ligand binding.

The linkage of protonation (nH^+) to ligand binding was investigated by measuring the dependence of the binding enthalpy on the ionization enthalpy of the experimental buffering agent. A BirA solution was titrated with a ligand in Standard Buffer or in MOPS Buffer [10 mM MOPS (pH 7.50 ± 0.02 at 20.0 ± 0.1 ºC), 200 mM KCl, 2.5 mM $MgCl_2$]. The number of protons released or taken up in the binding process was calculated from the measured heats of binding using the following relationship (*102*):

$$\frac{\Delta H^{\circ}_{bind(A)} - \Delta H^{\circ}_{bind(B)}}{\Delta H^{\circ}_{ion(A)} - \Delta H^{\circ}_{ion(B)}} = nH^{+} \qquad (8)$$

Where $\Delta H^{\circ}_{bind(A)}$ and $\Delta H^{\circ}_{ion(A)}$ are the measured binding enthalpy in buffer A (TrisHCl) for formation of a specific BirA·ligand complex and the ionization enthalpy of buffer A [$\Delta H^{\circ}_{ion(Tris)}$ = +11.3 kcal/mol] (*103*). Similarly, $\Delta H^{\circ}_{bind(B)}$ and $\Delta H^{\circ}_{ion(B)}$ are the measured binding enthalpy in buffer B (MOPS) and the ionization enthalpy of buffer B [$\Delta H^{\circ}_{ion\ (MOPS)}$ = +5.3 kcal/mol].

d. Determination of heat capacity changes.

Heat capacity changes associated with formation of the protein·ligand complexes were determined by measuring the temperature dependence of the binding enthalpy for each process. With the exception of the bio-5'-AMP binding interaction, temperatures in the range of 5-30 ºC were used for all experiments. Because of complications associated with ligand-induced dimerization, measurements of bio-5'-AMP binding were limited to

the range of 5-20 ºC. The pH of each buffer was adjusted to 7.50 ±0.02 at the working temperature. The heat capacity change upon complex formation is related to measured binding enthalpies and temperature by the by the following equation:

$$\Delta C_p = \frac{\Delta H^\circ}{T} \qquad (9).$$

Assuming that the heat capacity change associated with each binding process is constant in the temperature range employed, linear least-squares analysis of the dependence of the measured binding enthalpy on temperature yields the ΔC^o_p for the binding process. Data analysis was performed using the Origin software package.

C. Results

1. Equilibrium Binding Titrations:

a. Direct titrations.

The relatively low affinities of the two weak allosteric activators, biotin and btnSA, for BirA allowed use of direct calorimetric titrations to determine the thermodynamic parameters governing these two protein-ligand interactions. Moreover, the weak dimerization of the resulting protein-ligand complexes eliminated (see Table 4) concern about any contribution of dimerization to the calorimetric signals obtained in titrations. Figure 21-A shows a typical ITC profile for binding of btnSA to BirA in Standard buffer [10 mM Tris-HCl (pH 7.50 ± 0.02 at 20.0 ± 0.1 ºC), 200 mM KCl, 2.5 mM $MgCl_2$]. The data were obtained from 29 - 10 μL injections of a concentrated stock of btnSA into the protein solution. Similar data were obtained in titrations of BirA with biotin. The binding isotherm generated is also shown in Figure 21-A along with the

curve generated from the best-fit parameters obtained from nonlinear least-squares analysis of the data using a single-site binding model. The thermodynamic parameters governing binding of biotin and btnSA to BirA are provided in Table 5. The equilibrium dissociation constant determined for the BirA·biotin interaction is 4.2 (±0.3) x 10^{-8} M. This value is in excellent agreement with that previously calculated from results of stopped-flow kinetic measurements of the kinetic parameters governing the interaction (4.2 (± 0.5) x 10^{-8} M, (*68*)). The equilibrium dissociation constant for the interaction of the repressor with the analog, btnSA, indicates that this ligand binds to BirA with approximately the same affinity as does biotin. Additionally, while binding of biotin and btnSA are characterized by large favorable enthalpies, both binding processes are also opposed by sizeable unfavorable entropic contributions to the binding free energy.

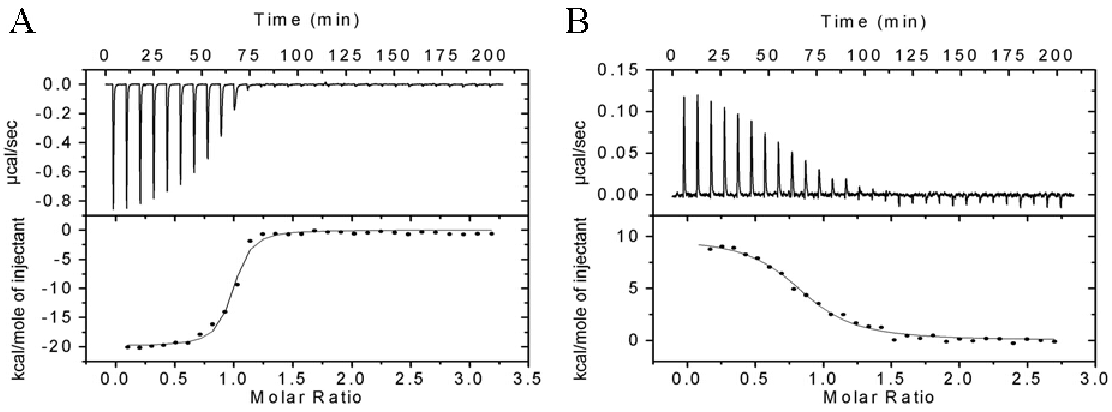

Figure 21. Calorimetric titrations of BirA. (A) Direct titration of BirA with btnSA. (B) Displacement titration of BirA·biotin with btnOH-AMP. These experiments were performed at 20 ºC in Standard Buffer [10 mM Tris-HCl (pH 7.50 ± 0.02 at 20.0 ± 0.1 ºC), 200 mM KCl, 2.5 mM $MgCl_2$]. In (A) 29 x 10 µL volumes of a 50 µM btnSA solution were injected into 5 µM BirA and (B) 29 x 10 µL volumes of a 50 µM btnOH-AMP solution were injected into 5 µM BirA saturated with biotin.

b. Displacement titrations.

Results of previous kinetic studies indicate bio-5'-AMP binds to BirA with an equilibrium dissociation constant of 5 ±2 x 10^{-11}M (*68*), a value beyond the utility of the direct titration method of calorimetric measurements (*104-106*). Moreover, results of preliminary measurements of the BirA-btnOH-AMP interaction indicated that this binding process is also not amenable to measurement by direct calorimetric titration. The displacement titration method has previously been applied to measure equilibrium dissociation constants in the picomolar range of concentration (*107*). In a displacement titration the protein is first saturated with a ligand characterized by a binding affinity sufficiently weak to measure by direct titration. In this case that ligand is biotin. The weaker binding ligand is then displaced by titration with a ligand that binds with a higher affinity. In the displacement titration the first ligand competes with the second ligand for a binding site and thereby yielding a reduced apparent affinity of the protein for the second ligand. Moreover, in the displacement titration, the measured heat of binding of the second ligand reflects both the intrinsic heat of binding of that ligand as well as the heat of displacing the first ligand. Therefore, in order to obtain a calorimetric signal that is characterized by an acceptable signal-to-noise ratio in a displacement titration, it is necessary that the enthalpic signatures for binding of the two ligands be sufficiently different. For a detailed analysis of ligand competition protocol by displacement ITC, see Sigurskjold (*100*).

Figure 21-B shows a typical displacement titration profile for the binding of btnOH-AMP to BirA. The raw data represents 29 injections of 10 μL of a concentrated

btnOH-AMP stock into the calorimeter cell containing BirA saturated with biotin in Standard Buffer at 20 ºC. The calorimetric signal initially appears to indicate the occurrence of an endothermic process with each injection, up to the point at which the ligand/protein ratio becomes greater than 1. In subsequent injections the signal becomes inverted indicating the occurrence of exothermic events. The protein is initially saturated with biotin and binding of each btnOH-AMP molecule to BirA is coupled to displacement of a biotin molecule. As indicated above, biotin binding to BirA occurs with a large favorable enthalpy of approximately -20 kcal/ mol. Therefore, the endothermic peaks associated with the first several injections in the displacement of biotin by btnOH-AMP indicate that the ester binds with less favorable enthalpy than does biotin. In subsequent injections, as more binding sites become occupied by btnOH-AMP, fewer biotin molecules are displaced and the contribution of the binding and displacement enthalpies to the observed calorimetric signal decreases while the contribution from dilution of the ligand becomes apparent. The raw data were utilized to generate the isotherm also shown in Figure 21-B. Nonlinear least-squares analysis of the data using a single-site model yielded the apparent binding enthalpy and equilibrium constant governing the reaction. The binding enthalpy of the high affinity ligand in the displacement titration can be related to the apparent binding enthalpy using equation 7 (see Materials and Methods). The resolved parameters governing binding of btnOH-AMP obtained from analysis of the displacement titration are shown in Table 5. The resolved equilibrium dissociation constant for the ester analog indicates that it binds to BirA approximately four-fold more tightly than does biotin.

Titrations of BirA with bio-5'-AMP were also performed using the displacement technique. However, of the four ligands examined in this work, bio-5'-AMP binding to BirA has been shown to induce the tightest dimerization of the repressor. The equilibrium dissociation constant for dimerization of the holorepressor in Standard Buffer at 20 ºC is approximately 10 μM (*59, 63, 99*). Additionally, results of a Van't Hoff analysis of the temperature dependence of the equilibrium dimerization constant indicates that dimerization of the holorepressor is an endothermic process (Brown & Beckett unpublished data). Therefore the potential contribution of the dimerization process to the calorimetric signal obtained in titrations with bio-5'-AMP must be considered. Consequently, a repressor concentration of 2 μM was employed for all bio-5'-AMP titrations. This concentration represents a compromise between minimizing the contribution of dimerization while optimizing the signal-to-noise ratio. However, in the conditions used for the titration even at 2 μM approximately 23% of the BirA·btnOH-AMP complex forms dimer. Thus, enthalpy values reported for bio-5'-AMP binding measured at 20 ºC must be considered an upper limit.

The displacement titration data obtained with bio-5'-AMP was analyzed in a manner identical to that obtained with btnOH-AMP and the parameters governing its interaction with BirA are provided in Table 5. The equilibrium dissociation constant obtained for the process ($4 \pm 2 \times 10^{-11}$M) agrees well with that calculated from kinetic measurements of the interaction (*68*). Moreover, binding of each ligand btnOH-AMP and bio-5'-AMP, to BirA is accompanied by a favorable enthalpic contribution. However, consistent with the endothermic peaks observed for the initial injections of

btnOH-AMP and bio-5’-AMP in displacement of biotin from BirA, the magnitude of the enthalpy for both ligands is approximately half of that observed for biotin and btnSA. Furthermore, binding of each of these strong activators is characterized by a small but favorable entropic contribution to the Gibbs free energy.

Table 5. Binding Thermodynamics of BirA·ligand Complexes.

Ligand[a]	**K_b (M)**[b]	**G° (kcal/mol)**[c]	**H° (kcal/mol)**[b]	**$-T\,S^\circ$ (kcal/mol)**[c]
Biotin	4.2 (± 0.3) x 10^{-8}	-9.89 (± 0.04)	-19.2 (± 0.1)	9.3 (± 0.1)
btnSA	6 (± 1) x 10^{-8}	-9.7 (± 0.2)	-19.9 (± 0.3)	10.2 (± 0.4)
btnOH-AMP	1.5 (± 0.2) x 10^{-9}	-11.82 (± 0.06)	-9.9 (± 0.3)	-1.9 (± 0.3)
Bio-5'-AMP	4 (± 2) x 10^{-11}	-13.9 (± 0.4)	-12.3 (± 0.9)	-1.6 (± 0.9)

a- All titrations were performed in 10 mM Tris-HCl (pH 7.50 ± 0.02 at 20.0 ± 0.1 ºC), 200 mM KCl, 2.5 mM $MgCl_2$ using a VP-ITC calorimeter (MicroCal, Inc, Northampton, MA). *b*- Binding parameters K_b and ΔH^o were obtained from the analysis of ITC data using a single-site binding model (biotin, and btnSA) or a displacement model (btnOH-AMP and bio-5'-AMP) using the Origin software package. *c*- Binding free energies and entropies were calculated using the relationships: $\Delta G^o = -RT\ \ln K$ and $\Delta G^o = \Delta H^o - T\Delta S^o$.

2. Titrations at Total Association:

In order to obtain information about heat capacity changes associated with the four binding interactions as well as the linkage of protonation to the binding processes, an alternative method was utilized to measure the binding enthalpy. This method is a modification of the single-point saturation method previously utilized (*101*). Figure 22 shows the raw data obtained from a titration of BirA (2 μM) with a concentrated biotin stock solution (20 μM) in Standard Buffer at 20 ºC. The first peak represents the heat evolved upon injection of a 2 μL volume of the syringe solution into the calorimeter cell containing the protein. The purpose of this injection is to expel any volume of air that may have been generated by vibration while inserting the syringe into the calorimeter cell. The actual volume of ligand delivered in this injection is at most 2 μL, but is

dependent upon the extent of the leakage that may have occurred from the syringe. Therefore, any heat measured for this injection is unreliable, and is not used in data analysis. The next five peaks and the final eight peaks each represents the heat evolved upon the addition of a 5 μL volume of the ligand solution. The large peak represents the heat evolved upon the addition of a 150 μL volume of the ligand solution into the calorimeter cell. Injections 2 thru 6 were performed to obtain several measurements of the heat of binding. Based on the equilibrium dissociation constant for biotin binding ($4.2 \pm 0.3 \times 10^{-8}$ M), in each injection, all of the biotin injected into the cell is bound to BirA. This stoichiometric binding condition has been termed *total association at partial saturation* (*108*). The observed signal associated with each of the injections, however, reflects a sum of the heat of binding and heat of dilution of the ligand. The large injection was performed to add sufficient biotin to fully saturate the protein. The remaining 8 peaks represent the heat evolved upon the addition of biotin after saturation of the protein, and therefore is simply the heat of dilution of the ligand. The integrated heat determined for each of the injections 2 thru 6 is corrected for ligand dilution by subtracting the average of the integrated heat associated with the final 8 injections. In this manner, one obtains 5 measurements of the binding enthalpy from one experiment.

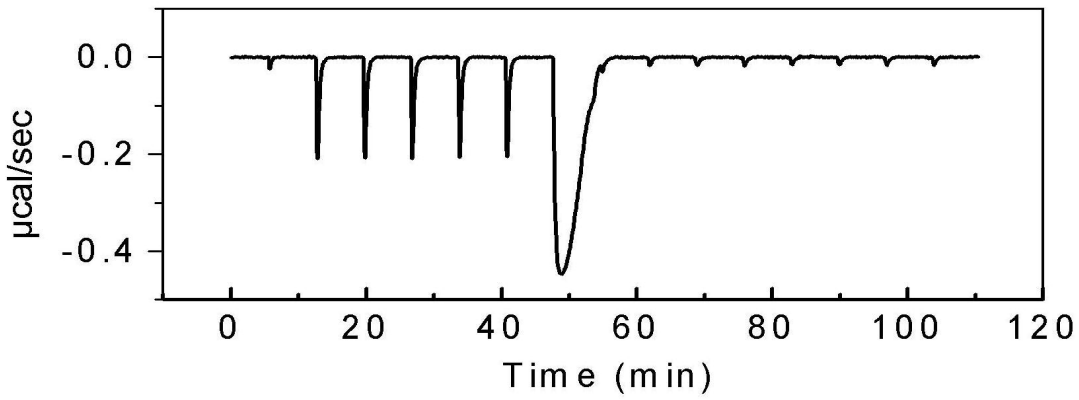

Figure 22. Titration of BirA with biotin under conditions of total association at partial saturation. The experiment was performed in Standard Buffer at 20 ºC. A 2 µM BirA solution was titrated with a 20 µM biotin stock. The first 2 µL injection was followed by 5 x 5 µL injections, a 1 x 150 µL injection, and finally 8 x 5 µL injections. The average integrated heat of the last 8 injections was subtracted from the integrated heat of injections 2 thru 6 to obtain a dilution-corrected binding enthalpy.

There are several advantages associated with this method. First, in contrast to the single-point saturation method previously employed, the standard precaution is taken that eliminates the uncertainty in the volume of the first injection due to possible leakage during loading of the syringe into the calorimeter. Second, the single point method and a full titration provide only one estimate of the binding enthalpy, while five estimates can be obtained in a single experiment using the modified method. A final advantage of the method is that, in contrast to the full titration method in which two parameters, the equilibrium constant and the enthalpy of binding are resolved in nonlinear least-squares analysis of the data, only the enthalpy value is obtained from this method. As a result less uncertainty is associated with the enthalpy values obtained from the method. All

enthalpies used in the determination of heat capacity changes and linked protonation events for binding of each ligand to the biotin repressor were measured using this method.

a. Linkage of Protonation to Binding

In order to estimate the linkage of protonation to binding of each ligand to BirA, the dependence of the binding enthalpy on the ionization enthalpy of the buffer was measured. The composition of the buffers utilized in the experiments was 200 mM KCl, 2.5 mM $MgCl_2$, with either 10 mM Tris or MOPS as the buffering agent. Data were analyzed using Equation (8), to estimate the number of protons taken up or released upon binding of each ligand to BirA (Table 6)

Results of the measurements indicate a broad range of dependencies of binding enthalpies on the ionization enthalpy of the buffer. The binding enthalpy for the BirA·btnOH-AMP interaction is independent of the ionization enthalpy of the buffer ($\Delta H_{bind,Tris}$ = -9.9 ± 0.3 kcal/mol *vs.* $\Delta H_{bind,MOPS}$ = -9.6 ± 0.2 kcal/mol) and is characterized by an nH^+ value of zero. Binding of the weak effectors, biotin and btnSA, is coupled to the release of protons from the BirA-effector complex, and by contrast, bio-5'-AMP binding is linked to the uptake of protons by the complex. In all cases the magnitude of the effect is small.

Table 6. Heat Capacity Changes and Linkage of Protonation to Binding.

Ligand	ΔC°_{p} (cal/mol K)[a]	nH^{+b}
biotin	-206 (±12)	-0.14 (±0.04)
btnSA	-395 (±16)	-0.44 (±0.08)
btnOH-AMP	-363 (±14)	0.04 (±0.05)
bio-5'-AMP	-183(±22)	0.34 (±0.05)

a- The heat capacities were determined from the slope of a linear least-squares analysis of the temperature dependence of the enthalpy for binding of each ligand to BirA in 10 mM Tris-HCl, 200 mM KCl, 2.5 mM $MgCl_2$. The pH of the buffer was adjusted to 7.50 ± 0.02 at the experimental temperature. Ten measurements of ΔH°_{b} were obtained at each temperature. *b*- The linkage of protonation to binding was determined from the slope of a linear least-squares analysis of the dependence of the binding enthalpy on the buffer ionization enthalpy. Ten measurements of the binding enthalpy were performed for each binding reaction in Tris and MOPS.

b. Changes in Heat Capacity.

In order to determine the heat capacity change associated with each binding reaction, the temperature dependence of the binding enthalpy was measured. Dimerization of each complex of BirA bound to biotin, btnOH-AMP, or btnSA is relatively weak, and thus dimerization made no contribution to the measured enthalpies of binding of these ligands to the protein. As indicated above, the contribution of dimerization to the measurements of the enthalpy of bio-5'-AMP binding was of potential concern. However, results of measurements of the dependence of the equilibrium dimerization constant for this complex on temperature indicate that the process becomes weaker as temperature is decreased. Thus, limiting the measurements of the enthalpy

changes associated with bio-5'-AMP binding from 5-20 ºC eliminated concern about the contribution from the dimerization enthalpy. The results of these measurements are summarized in Figure 23. Linear least-squares analysis of the dependence of binding enthalpy on experimental temperature yielded the heat capacities displayed in Table 6. The results indicate that all four binding interactions are characterized by negative heat capacity changes. The magnitudes of the changes are small and no correlation exists between the magnitude of the heat capacity change and the magnitude of the allosteric effect induced by each ligand.

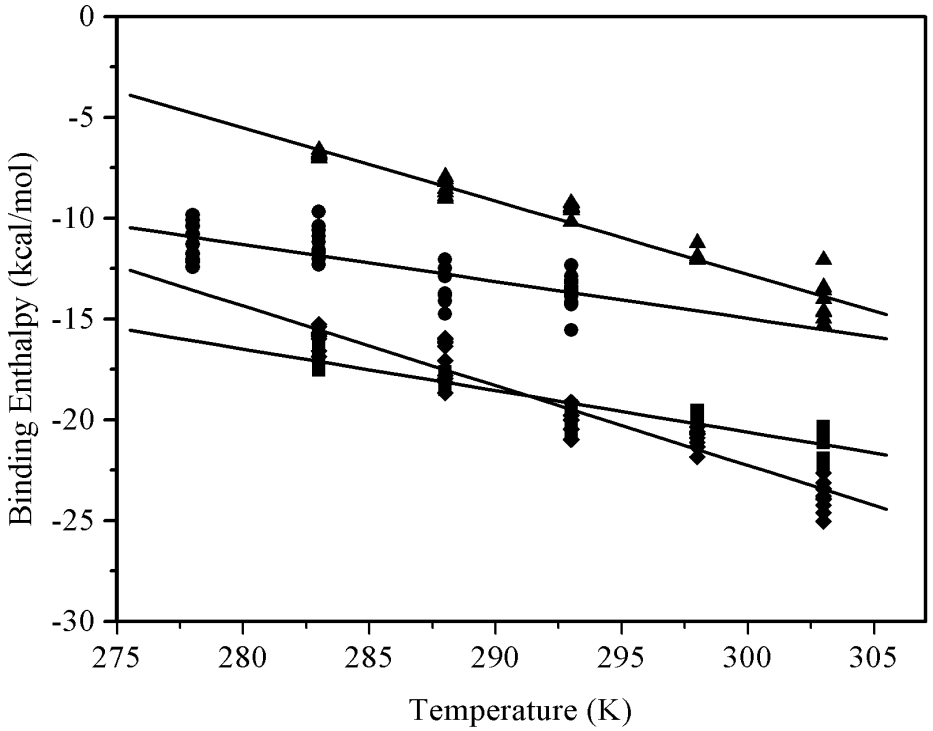

Figure 23. Determination of the Heat Capacity changes for binding of ligands to BirA. A plot of the temperature dependence of the binding enthalpy for (■) biotin, (♦) btnSA, (▲) btnOH-AMP, and (●) bio-5'-AMP. Experiments were performed under the conditions described in Figure 22 at the temperatures indicated.

D. Discussion

Combined results of solution and structural analysis of the biotin regulatory system indicates an allosteric model in which binding of bio-5'-AMP to BirA drives the self-assembly of the repressor to enhance its affinity for DNA. Results of a recent investigation into the allosteric response associated with binding of *d*-biotin, bio-5'-AMP, and two adenylate analogs (btnSA and btnOH-AMP) to the repressor indicate that the four ligands fall into two classes: weak effectors and strong effectors. Binding of the strong effectors results in an enhancement in the dimerization energetics of the repressor and this enhancement is quantitatively reflected in the total assembly energetics of the transcription repression complex. In contrast, *d*-biotin and btnSA weakly enhance dimerization and uncoupling of the dimerization and DNA binding processes is observed for both ligands. In the context of all the experimental data collected thus far, this uncoupling suggests that the function of BirA as a transcription repressor is mediated by more than just the dimerization interface. In order to completely understand the allosteric mechanism in the biotin regulatory system, it is necessary to elucidate the changes that occur in the monomer upon ligand binding. The activation of the monomer for dimerization upon effector binding must play a critical role in the mechanism for allosteric regulation of the repressor.

The thermodynamic measurements presented in this work were designed to investigate the potential differences in binding of the four effectors to the repressor monomer with the goal of obtaining insight into the allosteric activation process. All four ligands bind tightly to BirA with equilibrium dissociation constants in the nanomolar to

picomolar concentration range. The Gibbs free energy for *d*-biotin binding determined by direct titration of –9.89 (±0.04) kcal/ mol, agrees well with that previously determined using kinetic fluorescence methods (*68*) and titration calorimetry (*101*). BtnSA also binds BirA with an affinity in the nanomolar range of concentration. Tight binding of bio-5'-AMP and btnOH-AMP necessitated use of the displacement titration method. The Gibbs free energy for binding of bio-5'-AMP obtained with this method is -13.9 ± 0.4 kcal/mol, a value in close agreement with that calculated previously from results of kinetic measurements (*68*). The ester analog binds BirA with a Gibbs free energy that is intermediate between that measured for *d*-biotin and bio-5'-AMP. These latter results demonstrate the utility of the displacement titration method for measuring high affinity association reactions.

It is instructive to consider the energetics of binding of the four ligands in the context of the structure of the biotin-bound repressor. In this structure, the biotin moiety is largely excluded from solvent in a pocket on one face of the beta sheet of the central domain. The residues of the 112-128 loop fold to form a lid over the binding pocket. This folded loop is stabilized by the formation of several hydrogen bonding interactions between the main chain and side chain residues of the loop and the ureido functional group of biotin, and by a main-chain arginine amide hydrogen (R118) with the biotin carboxylate. Three glycine side chains interact with the thiophene ring and a tryptophan side chain stacks against the valerate chain of biotin. It is likely that the remaining three effectors possess similar binding interactions between the biotin moiety and the protein. Therefore, it is surprising that btnSA binds BirA with the same affinity as does biotin

despite the addition of the sulfamoyl adenosine appendage that provides more functionalization for potential hydrogen bonding and π-stacking interactions. Binding of btnSA to BirA is 4 kcal/mol less favorable than binding of bio-5'-AMP and 2 kcal/mol less favorable than binding of btnOH-AMP. The sulfamoyl group of btnSA may therefore be *non* complementary to the binding site of BirA since the phosphate ester and the mixed anhydride linker of the other two adenylates provides them with a higher affinity. Alternatively, the reduced affinity relative to btnOH-AMP and bio-5'-AMP reflects the absence of the charged phosphate at the linker region between the biotin and adenosine moieties. Binding of bio-5'-AMP to BirA is 2 kcal/mol more favorable than is binding of btnOH-AMP, which differs structurally from bio-5'-AMP only by the absence of the carbonyl group at the terminus of the valerate chain on biotin. This result implies that the carbonyl group at this position plays an important role in binding.

The binding affinity can be further analyzed by dissecting out the components of the Gibbs free energy. As was described earlier, the four effectors fall into two classes with respect to their efficacy in promoting BirA dimerization. Interestingly, in addition to their allosteric efficacy, the enthalpic and entropic components of the binding energy for the four BirA complexes can also be divided into two classes (Figure 24). The weak allosteric effectors bind to BirA with relatively large favorable enthalpy changes while the strong effectors bind with relatively moderate enthalpy changes. Furthermore, the weak effectors bind to BirA with significant unfavorable entropy changes while entropy moderately enhances binding by the strong effectors.

It is interesting that similar enthalpic changes result from binding of both weak effectors to BirA. If the same contacts are made between the protein and the biotin moiety of btnSA that are made in the BirA·biotin complex, one might expect a larger enthalpic change for btnSA binding due to the additional enthalpic potential associated with the sulfamoyl-adenosine moiety. The absence of an additional enthalpic gain for binding of btnSA relative to binding biotin may be that an expected additional enthalpy of binding the sulfamoyl adenosine portion of btnSA is offset by the absence of the carboxylate functional group of biotin which is engaged in a hydrogen bond with R118 in the crystal structure. The strong allosteric effectors contain the adenosine functionality as well, but bind with a smaller enthalpic contribution to the free energy than does binding of biotin and btnSA. Again, one would expect that the addition of the adenosine group would result in a larger enthalpic contribution to binding. It is also worth noting that binding of bio-5'-AMP is 2 kcal/mol more favorable than binding of btnOH-AMP and that that difference in free energy is exactly the difference in the enthalpic component to binding. This suggests that the carbonyl of the valerate chain is utilized in binding of bio-5'-AMP, but is not available in btnOH-AMP to provide an additional 2 kcal/mol of favorable enthalpy. When compared to the weak effectors, it appears that there is an enthalpic cost associated with binding of strong effectors to BirA.

Allosteric Activation of the Biotin Repressor

	Strong Effector		Weak Effector	
Ligands:	bio-5'-AMP	btnOH-AMP	biotin	btn-SA
ΔH_b° (kcal/mol):	-12.3 (±0.9)	-9.9 (±0.3)	-19.2 (±0.1)	-19.9 (±0.3)
ΔG°_{dim} (kcal/mol):	-6.8 (±0.1)	-5.9 (±0.1)	-4.1 (±0.2)	-4.0 (±0.1)

Figure 24. A comparison of binding enthalpy and allosteric response.

The unfavorable entropy changes for binding of biotin and btnSA are consistent with the notion that loops in the protein become organized in the course of ligand binding. Organization of the loops concomitant with binding restricts the number of conformational and translational degrees of freedom that the loop can explore. This restriction is entropically unfavorable for the protein and for the bound ligand. The small favorable entropic contributions associated with binding of btnOH-AMP and bio-5'-AMP are inconsistent with a binding process that is dominated by the known folding of the protein loops which should be entropically costly. However, in general, a process that favors entropy is the release of ordered water molecules at a protein-solvent interface into the bulk solution as residues that had been previously solvated become buried within the hydrophobic core of the protein. If favorable desolvation entropy is a driving force in the formation of the strong effector complexes with BirA, then it would be consistent with a disorder-to order transition in the protein where hydrophobic surface area is buried and bound water molecules are released into bulk solution upon binding of the strong

effectors. This ordering may be an overall entropically favorable process that requires an additional enthalpic contribution which is not realized in the complexes of BirA bound by the weak effectors.

Changes in heat capacity associated with binding of the four ligands are small and negative. The values determined from these measurements for biotin binding and bio-5'-AMP binding are in good agreement with those reported previously (*101, 109*). However there is no correlation observed between the magnitude of the heat capacity change and the magnitude of the efficacy of the ligand in promoting dimerization of the repressor. Heat capacity changes are often interpreted in terms of burial of hydrophobic and polar surface area. This interpretation works well for describing protein folding processes and rigid body associations. For binding processes that are coupled to folding an estimate of the contribution of folding to the heat capacity change that occurs upon binding can be made. However, the fact that we know that the biotin repressor undergoes structural changes upon small ligand binding and that no structure of the liganded repressor monomer is available, precludes a structural interpretation of the measured heat capacity changes.

In order to relate the thermodynamic parameters to allosteric activation it is necessary to correlate structural changes in the repressor that occur upon binding of the effector to the energetics of self-association of the liganded monomer. In comparing the X-ray structures of the biotin bound-dimer and the apo monomer, the structural differences are localized to three of the four flexible surface loops. However, biotin is a

weak allosteric activator of dimerization and the structure of the monomer bound to bio-5'-AMP is probably distinct from that of the monomer bound by *d*-biotin. First, the two complexes are functionally different with respect to dimerization. Second, results of partial proteolysis and hydroxyl-radical probing of apoBirA, BirA-biotin, and BirA-bio-5'-AMP indicate that these complexes are structurally distinct. The 233-236 surface loop of BirA that remains disordered in the biotin-bound structure is increasingly protected from cleavage in going from the apo form, to biotin-bound, to adenylate-bound. Finally, results of studies with BirA mutants that have had the N-terminal domain deleted are consistent with an inter-domain interaction between the DNA binding and central domains (*110*).

The distinct thermodynamic signatures for binding of the strong and weak activators reinforce the idea that the adenylate-bound repressor is structurally distinct from the biotin-bound repressor. Moreover, the conformational transition associated with the activation of the monomer for dimerization must be enthalpically costly. Binding of the two strong allosteric activators is characterized by a moderate enthalpy relative to binding of the weak allosteric activators. The enthalpically costly conformational transition is "paid for" by the binding enthalpy that would have otherwise been realized through formation of bonds between the protein and the ligand. This is why strong activators bind with more modest enthalpies. The loss in binding enthalpy is offset by a favorable entropic term for binding by the strong effectors. The source of this favorable entropic term may reflect changes in the protein or solvent and remains to be investigated.

IV. Crystallization of BirA·btnOH-AMP

A. Introduction

The biotin repressor, BirA, is the central component of the biotin regulatory system in *E. coli* (Figure 26). The 35.3 kDa protein has a twofold responsibility in facilitating retention of biotin in the cell and in regulating the transcription of the operon encoding the *d*-biotin biosynthetic enzymes (*52, 70, 71*). Biotin is retained in *E. coli* as a coenzyme that is covalently linked, in a two-step process, to a single biotin-dependent carboxylase (*70*). BirA functions as an enzyme by catalyzing this covalent modification of the Biotin Carboxyl Carrier Protein (BCCP), a subunit of acetyl-CoA carboxylase. The first step of the reaction is the synthesis of the adenylate of biotin, biotinyl-5'-AMP (bio-5'-AMP), from the substrates *d*-biotin and ATP (*54*). The second step is the catalytic transfer of the biotin moiety from the BirA·bio-5'-AMP complex to the ε-amino group of a specific lysine residue within the carrier protein. This process results in the regeneration of the apo enzyme and the formation of the biotinated carrier protein.

$$\text{BirA} + \textit{d}\text{-biotin} + \text{ATP} \rightarrow \text{BirA}\cdot\text{biotinyl-5'-AMP} + PP_i \qquad (1)$$

$$\text{BirA}\cdot\text{biotinyl-5'-AMP} + \text{apoBCCP} \rightarrow \text{apoBirA} + \text{holoBCCP} + \text{AMP} \qquad (2)$$

As a transcription regulator, two BirA·bio-5'-AMP monomers self-associate to bind site-specifically to *bio*O, a 40-base pair imperfect inverted palindromic DNA sequence (*57, 58, 72*). Formation of this protein-DNA complex represses transcription initiation at two divergent overlapping promoters. Therefore, in this system, bio-5'-AMP serves as both

the active intermediate in BirA-catalyzed biotin transfer and as the corepressor in transcription repression.

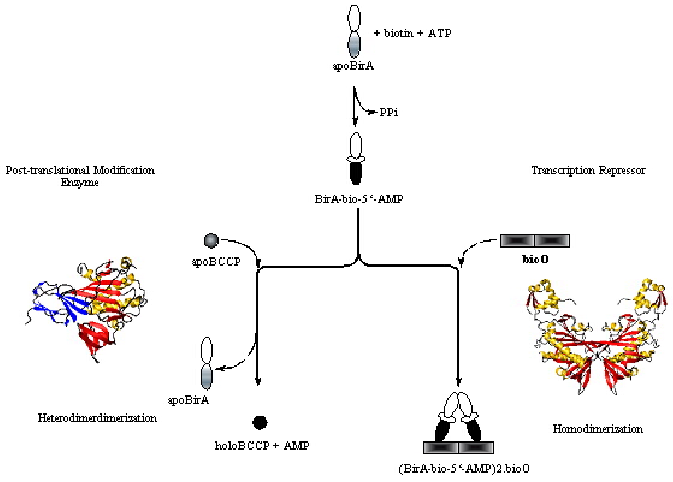

Figure 25. A schematic representation of the biotin regulatory system. BirA·bio-5'-AMP switches between functioning as a transcription repressor and as a biotin ligase.

Research efforts on the biotin regulatory system are directed toward an understanding of the mechanism of allosteric activation of the repressor. The prevailing model is supported by an abundance of biological data, results of detailed kinetic and thermodynamic investigations, and three-dimensional structures of apoBirA and BirA·biotin (*57-65*). The model asserts that binding of the corepressor drives an allosteric transition in BirA, whereby flexible surface loops of the central domain become ordered (Figure 26). The ordering of these loops results in the stabilization of the homodimer; the active form of the repressor for DNA binding (*58, 59, 62*). An increase in the population of the dimeric repressor results in a higher occupancy of the operator site, which leads to repression of transcription. The BirA·bio-5'-AMP co-complex is a critical species in the activation process of the biotin regulatory system. However, no

structural data is yet available for this complex which is vital in understanding how a small molecule effector activates the repressor for dimerization and DNA binding.

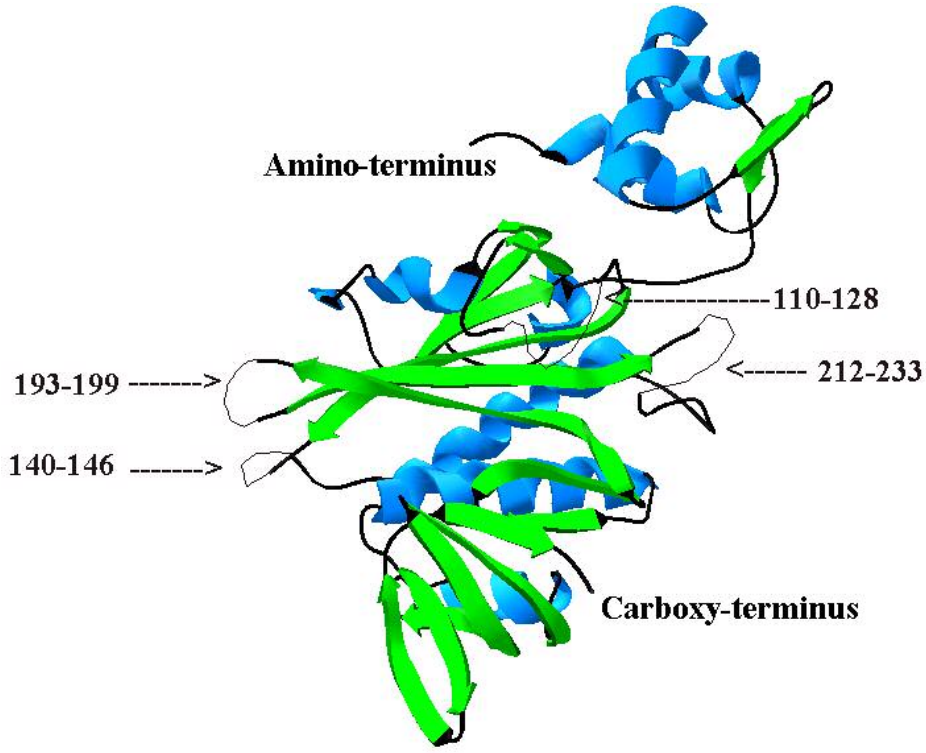

Figure 26. A model of the three-dimensional structure of apoBirA determined by X-ray crystallography. The residues contained within four partially disordered loops are indicated by the arrows. The model was generated using Deep View/ Swiss-PdbVeiwer (v. 3.7) and the Protein Data Bank file 1BIA as input.

A second focus of research is the identification of the mechanism of control of the functional switch of holoBirA from transcription repressor to biotin ligase. The existing model was formulated through efforts in structural modeling (*76*) and is supported by results obtained from biophysical solution studies of BirA and BCCP mutants (*53, 60, 71, 77, 111, 112*). The model states that the same face of BirA is utilized in formation of the

protein-protein interfaces in both the holoBirA·apoBCCP and holoBirA dimer assemblies (Figures 27 and 28) (*76*). Therefore, these processes are mutually exclusive. Heterodimer formation results in the depletion of the supply of holoBirA monomers available for homodimerization. A decrease in the population of the repressor dimer results in expression of the biotin operon.

Crystals of BirA bound to a non-labile analog of bio-5'-AMP, biotinol-AMP (btnOH-AMP), have recently been obtained and are currently the subject of X-ray diffraction studies. While btnOH-AMP is not the physiological corepressor, it serves as a competent mimic of bio-5'-AMP structurally and functionally (Figure 29). First, instead of a labile anhydride linker, a stable phosphate ester links the biotin and AMP moieties. Initial biochemical studies have indicated that the analog binds BirA with high affinity and with a thermodynamic profile similar to bio-5'-AMP. Additionally, like bio-5'-AMP, btnOH-AMP is a strong allosteric effector of BirA dimerization (*99*). Moreover, the enhanced dimerization energetics matches the enhanced assembly energetics of the $[BirA \cdot btnOH\text{-}AMP]_2$-DNA repression complex. Finally, the analog was shown to be an inactive substrate in the BirA-catalyzed biotin transfer reaction to BCCP87. For these reasons, the structure of BirA·btnOH-AMP is expected to be analogous to the structure of the physiologically relevant holorepressor complex. Information gained in this study will undoubtedly prove useful in further refinement of the existing models describing the allosteric activation of the biotin repressor and the functional switch of the ligase.

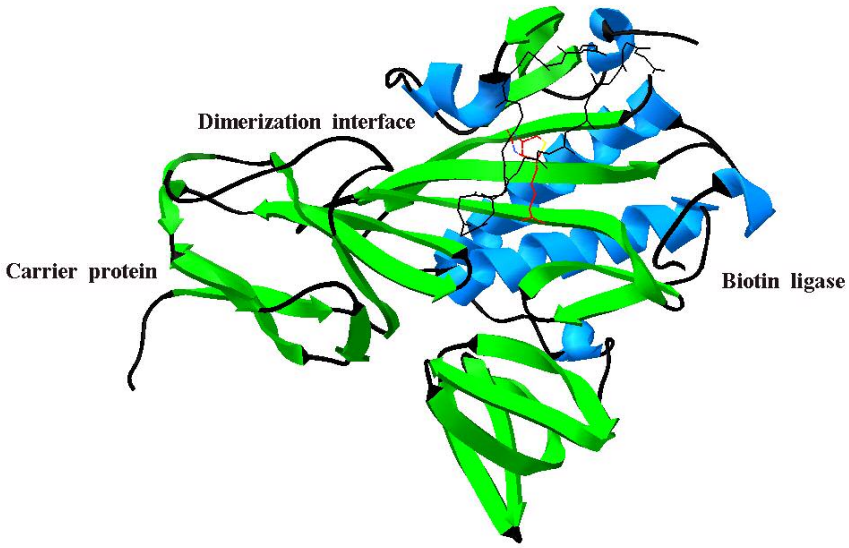

Figure 27. A model of the BirA·BCCP heterodimer interaction. The same β-sheet of the central domain of BirA that is utilized in homodimerization is utilized in heterodimerization with the carrier protein. The figure was generated utilizing Deep View/ Swiss-PdbVeiwer (v. 3.7) and the Protein Data Bank file 1K67 as input.

The three-dimensional structure obtained for the BirA·btnOH-AMP complex will represent the first published report regarding the structure of the repressor when bound to a strong allosteric activator. Previous attempts at structure determination of BirA-bio-5'-AMP have proven difficult due to the lability of the adenylate. Therefore, only structures of BirA bound by *d*-biotin and biotinyl lysine are presently available. The model of BirA·btnOH-AMP will allow for the first time the identification of the physical location of the adenylate portion of the corepressor and any contacts it makes with protein residues. This information is critical in determining how the addition of the adenosine ring or the phosphate linker moiety to the effector results in a significantly enhanced dimerization affinity of the repressor. Results of partial proteolysis and hydroxyl radical

protein footprinting experiments (*61*, *68*) indicate that the biotin adenylate is involved in ordering of the remaining 212-233 surface loop. Binding of the substrate biotin is less effective at protecting the loop from cleavage and in driving dimerization of BirA, and in the BirA·biotin crystal structure this loop remains disordered. It is possible this property of the adenylate plays some role in the enhancement of dimerization of the repressor.

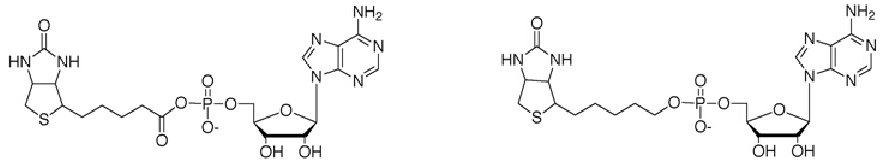

Figure 28. Structures of strong activators of BirA function. While the overall structures of the effectors are similar, bio-5'-AMP contains a labile mixed anhydride linker between the biotin and AMP moieties, and btnOH-AMP contains a stable phosphate ester linker.

Comparison of the BirA·btnOH-AMP structure with the BirA·biotin structure should prove useful for indicating any conformational differences that may be present between the two holorepressor species at the level of the homodimer. At the protein concentrations utilized for crystallization the structure of the BirA·btnOH-AMP complex is expected to be dimeric. However, results of a global analysis of sedimentation equilibrium data indicates that the adenylate is far more effective at stabilization of the homodimer than is biotin. It is not clear from these solution studies whether the differences in the dimer dissociation equilibrium constants is as a result of a structural differences in the respective ligated monomer species or if the differences are at the level of the dimer. It is important for the development of the allosteric model that the effect

ligand binding has on the structural and dynamic properties of the monomer can be dissected from the effects of dimerization and DNA binding. Comparison of the BirA·btnOH-AMP and BirA·biotin structures will indicate whether the differences in the dimerization properties of these two BirA species correlates with structural differences at the level of the dimer.

Results of this X-ray diffraction study are expected to provide structural data for the biotin repressor bound to a non-labile analog of the physiological corepressor, bio-5'-AMP. This model will be utilized to test and refine the mechanistic model describing effector-induced activation of an allosterically regulated transcription repressor. Additionally, the conditions utilized for crystallization of the BirA·btnOH-AMP complex provide a good starting point for attempting crystallization trials of the heterodimeric protein complex. This will allow for further refinement of the model proposed to control the functional switch of BirA from transcription repressor to ligase.

B. Materials and Methods

1. Chemicals and biochemicals

All chemicals utilized in the preparation of buffers were at least reagent grade. Crystallization precipitant buffers and Linbro boxes were obtained from Hampton Research (Riverside, CA). Expression and purification of the protein was as described in Brown *et al.*(*99*). Biotinol-AMP was synthesized and purified as previously described (*99*) or purchased from RNA-Tec (Leuven, Belgium). Ultra-free 4 centrifugal filters with a 5 kDa molecular weight cutoff were obtained from Millipore.

2. Crystallization of BirA·btnOH-AMP

BirA was slowly exchanged out of storage buffer [50mM Tris-HCl (pH 7.50 ± 0.02 at 4.0 ± 0.1 ºC), 200mM KCl, 5% glycerol] into crystallization exchange buffer [100 mM NaH_2PO_4/K_2HPO_4 (pH 6.50 ± 0.02 at 20.0 ± 0.1 ºC), 5 % glycerol] and concentrated to at least 30 mg/mL using an Ultra-free 4 centrifugal filter with a 5 kDa MWCO (Millipore). A BirA-btnOH-AMP stock was prepared in crystallization exchange buffer, such that $[BirA]_f$ = 20 mg/mL and $[btnOH\text{-}AMP]_f$ = 1.4 mM. Crystallization was performed utilizing the hanging drop vapor diffusion method in HR3-110 Linbro boxes. Each crystallization drop containing a mixture of 4 µL of BirA·btnOH-AMP stock and 4 µL of crystallization precipitant buffer [100 mM Tris-HCl (pH 8.0), 20 % PEG] was applied to silanized glass coverslips and placed over a reservoir containing 1 mL of the same buffer. The cover slips were sealed with a Vaseline and mineral oil mixture, and crystals grew reproducibly in 3 days at 20 ºC. In order to determine if the crystals contained protein, the crystals were washed three times with 200 µL of fresh precipitant buffer and then dissolved in 100 µl of Standard Buffer [10 mM Tris-HCl (pH 7.5 ± 0.02 at 20 ± 0.1 °C), 200 mM KCl, 2.5 mM $MgCl_2$]. The presence of BirA was confirmed by Coomassie staining of the sample electrophoresed on an SDS-PAGE gel.

C. Results

1. Crystallization conditions for BirA·btnOH-AMP

The conditions utilized for crystallization of BirA·btnOH-AMP are different than those utilized for crystallization of apoBirA and BirA·biotin (*64, 65*). For BirA·biotin, a 2.3 M phosphate buffer (NaH_2PO_4/ K_2HPO_4, pH 6.5) was utilized to precipitate protein

crystals from a BirA solution comprised of 100mM NaH_2PO_4/ K_2HPO_4, (pH 6.5), 5% glycerol at 4 ºC. The conditions used for apoBirA were the same as those used for BirA·biotin except that the crystals were grown at room temperature and in the absence of biotin. Attempts to crystallize the BirA-adenylate complex under similar conditions resulted in the formation of a few small crystals only after several months. Therefore screening trials were performed to identify more efficient and productive conditions. Trials were performed using the PEG 6K grid screen kit (Hampton Research, Riverside CA) which contains five different buffers solutions at a range of pH and precipitant concentration. The conditions that reproducibly provided several crystals in three days were 100 mM Tris (pH 8.0) and 20% PEG at room temperature.

2. Obtainment of preliminary X-ray data

Structural data was obtained for the BirA·btnOH-AMP crystals at 2.8Å resolution. An initial analysis of the data set indicates that the space group is tetragonal. Currently, molecular replacement techniques are being utilized to identify the subunit packing.

V. Summary and Prospectus

The central focus of research on the biotin regulatory system continues to be identification of how the small molecule bio-5'-AMP activates BirA for its function in transcription repression. This knowledge requires an understanding of the structural and dynamic properties of the repressor that are critical for transmission of the allosteric signal from the corepressor-binding domain to the DNA-binding domain. Here, a thermodynamic approach has been utilized to probe the equilibria governing the protein-protein, protein-ligand, and protein-DNA interactions that contribute to repressor function. Additionally, a structural investigation of the BirA·btnOH-AMP complex was initiated to obtain information about possible structural changes that occur in the repressor as a result of adenylate binding and dimerization. The combined results obtained from this effort are used to draw conclusions which further support and develop the proposed model for BirA activation.

A large body of biophysical data has been compiled from several years of detailed investigations into the biotin regulatory system and has been utilized to formulate the working model that describes how binding of bio-5'-AMP results in repression of transcription of the operon. The model indicates that the allosteric signal is transmitted through the dimerization interface. Binding of the biotin adenylate drives the self-assembly of the holorepressor which is the active form of BirA that functions in DNA binding. Therefore, bio-5'-AMP modulates the occupancy of the operator sequence by enhancing dimerization of the repressor.

While effector-induced self-assembly of the repressor leads to enhanced DNA binding, tight coupling of these processes is only observed for binding of strong allosteric effectors. This result was obtained by comparison of the relative enhancements in the energetics of dimerization and of repression complex assembly for four BirA-effector species relative to apoBirA. The magnitude of the enhancement in the total assembly energetics of the holorepressor-bioO complex is completely accounted for by the enhancement in the dimerization energetics for BirA·bio-5'-AMP and BirA·btnOH-AMP. However, tight coupling of these processes is not observed in the case of BirA·biotin and BirA·btnSA. Though an enhancement is observed for BirA dimerization and for assembly of the repression complex due to binding of the weak effectors, the magnitudes of these enhancements are not equivalent. This uncoupling of dimerization and DNA binding suggests that the dimerization interface may not be the only pathway for transmission of the allosteric signal. Therefore, changes in the protein monomer must play a critical role in the activation process.

The results of calorimetric binding measurements indicate that activation of the repressor for dimerization is an enthalpically-driven process. Four allosteric effectors are shown to form a high affinity complex with BirA ($\Delta G_b^o \approx$ -10 to -14 kcal/ mol). While binding is enthalpically favorable in each case, there is a large difference in the magnitudes of this contribution ($\Delta\Delta H_b^o \approx$ -10kcal/ mol) in relation to binding to each class of effector. High affinity binding by the strong effectors is characterized by a less favorable binding enthalpy than that obtained for binding of the weak effectors. Considering the affect of ligand binding on dimerization of the repressor, this diminished

enthalpy suggests that some of the enthalpic energy that is gained upon binding of the strong effectors is used to drive an allosteric transition in the protein monomer that stabilizes it for self-association.

Finally, an X-ray diffraction study is currently underway to obtain a structural model for the repressor bound to a competent mimic of the physiological corepressor, bio-5'-AMP. Comparison of this structure with that for BirA·biotin will be utilized for determining if binding of the effectors results in any conformational differences in the repressor at the level of the homodimer. This distinction is crucial for determining how the allosteric signal is transmitted through the repressor. Together, the crystallographic and thermodynamic data obtained from this investigation represents a modest contribution toward understanding the mechanism of effector-induced self-assembly of an allosteric gene regulatory protein.

This mechanism of activation is novel and is in contrast to that utilized by the classical regulatory systems such as the lactose repressor or the tryptophan repressor. In the classical systems, the level of occupancy of the transcription control region is modulated by the relative orientation of the DNA recognition elements of the repressor. For example, binding of an inducer sugar to the core domain of LacR drives a conformational change in the repressor whereby the hinge helix of the N-terminal domain is displaced from the minor groove of the center operator. This movement destabilizes the protein-DNA complex and results in dissociation of the repressor from the transcription control region and therefore expression of the structural genes. The details

of this mechanism are quite well established. In contrast, many transcription regulatory proteins are proposed to operate by a non-classical allosteric activation mechanism. Here, the occupancy of the transcription control region is dependent upon the level of self-association of the regulatory protein. Binding of the small molecule effector to a non-classical transcription repressor modulates the oligomeric state of the repressor which is directly reflected in the affinity of the repressor for DNA. For example, binding of divalent metal ions to DtxR drives the dimerization of the repressor and enhances the affinity of the repressor for DNA. Other examples of regulatory proteins that exhibit ligand-induced oligomerization include the tyrosine repressor (TyrR), the arginine repressor (ArgR), and the nitrogen regulatory protein C (NtrC). However, the thermodynamic and structural details of the activation process in these systems are not well defined. Therefore, research on the biotin regulatory system provides critical information that can be utilized for an understanding of many transcription regulatory proteins that operate via the non-classical allosteric mechanism.

Future efforts of research on the biotin regulatory system should include obtaining structural information for the monomer bound to an effector and for the holorepressor bound to the operator. In acquiring this data, models for each ligation-state of the biotin repressor (apo BirA, holoBirA monomer, holoBirA dimer, and holoBirA dimer-bioO) will be available for evaluating the relationship between protein structure and function. A comparison of the apoBirA structure with that of the liganded monomer will illustrate the effects that corepressor binding has on the structure of the repressor. Likewise, a comparison of the models for the holoBirA monomer and dimer may be utilized for

identifying the effects of self-association on repressor structure. Finally, a comparison of the structure of the holoBirA dimer with that of the dimer bound to bioO may illustrate the consequences of DNA binding to the repressor. The information gained in this analysis should provide details of the conformational changes that may occur in BirA that are critical in transmitting the allosteric signal from the corepressor binding domain to the N-terminal DNA binding domain.

References

1. Otwinowski, Z., Schevitz, R. W., Zhang, R. G., Lawson, C. L., Joachimiak, A., Marmorstein, R. Q., Luisi, B. F., and Sigler, P. B. (1988) *Nature **335***, 321-329.
2. Bell, C. E., and Lewis, M. (2000) *Nat. Struct. Biol. **7***, 209-214.
3. Braun, V. (1997) *Biol. Chem. **378***, 779-786.
4. Gallegos, M. T., Schleif, R., Bairoch, A., Hofmann, K., and Ramos, J. L. (1997) *Microbiol. Mol. Biol. Rev. **61***, 393-410.
5. Beckett, D. (2001) *J. Mol. Biol. **314***, 335-352.
6. Huffman, J. L., and Brennan, R. G. (2002) *Curr. Opin. Struct. Biol. **12***, 98-106.
7. Brennan, R. G., and Matthews, B. W. (1989) *J. Biol. Chem. **264***, 1903-1906.
8. Gerhart, J. C. (1962) *J. Biol. Chem. **237***, 891-896.
9. Changeaux, J. P. (1961) *Cold Spring Harbor Symp. Quant. Biol. **26***, 313-318.
10. Koshland, D. E., Jr. (1958) *Proc. Natl. Acad. Sci. U. S. A. **44***, 98-104.
11. Koshland, D. E., Jr., Nemethy, G., and Filmer, D. (1966) *Biochemistry **5***, 365-385.
12. Monod, J., Changeux, J. P., and Jacob, F. (1963) *J. Mol. Biol. **6***, 306-329.
13. Monod, J., Wyman, J., and Changeux, J. P. (1965) *J. Mol. Biol. **12***, 88-118.
14. Jacob, F., and Monod, J. (1961) *J. Mol. Biol. **3***, 318-356.
15. Gilbert, W., and Maxam, A. (1973) *Proc. Natl. Acad. Sci. U. S. A. **70***, 3581-3584.
16. Oehler, S., Eismann, E. R., Kramer, H., and Muller-Hill, B. (1990) *EMBO J. **9***, 973-979.
17. Friedman, A. M., Fischmann, T. O., and Steitz, T. A. (1995) *Science **268***, 1721-1727.

18. Lewis, M., Chang, G., Horton, N. C., Kercher, M. A., Pace, H. C., Schumacher, M. A., Brennan, R. G., and Lu, P. (1996) *Science **271***, 1247-1254.

19. Falcon, C. M., Swint-Kruse, L., and Matthews, K. S. (1997) *J. Biol. Chem. **272***, 26818-26821.

20. Falcon, C. M., and Matthews, K. S. (1999) *J. Biol. Chem. **274***, 30849-30857.

21. Barry, J. K., and Matthews, K. S. (1999) *Biochemistry **38***, 3579-3590.

22. Zhang, R. G., Joachimiak, A., Lawson, C. L., Schevitz, R. W., Otwinowski, Z., and Sigler, P. B. (1987) *Nature **327***, 591-597.

23. Lawson, C. L., and Carey, J. (1993) *Nature **366***, 178-182.

24. Schevitz, R. W., Otwinowski, Z., Joachimiak, A., Lawson, C. L., and Sigler, P. B. (1985) *Nature **317***, 782-786.

25. Lawson, C. L., Zhang, R. G., Schevitz, R. W., Otwinowski, Z., Joachimiak, A., and Sigler, P. B. (1988) *Proteins **3***, 18-31.

26. Arrowsmith, C., Pachter, R., Altman, R., and Jardetzky, O. (1991) *Eur. J. Biochem. **202***, 53-66.

27. Zhang, H., Zhao, D., Revington, M., Lee, W., Jia, X., Arrowsmith, C., and Jardetzky, O. (1994) *J. Mol. Biol. **238***, 592-614.

28. Zhao, D., Arrowsmith, C. H., Jia, X., and Jardetzky, O. (1993) *J. Mol. Biol. **229***, 735-746.

29. Jin, L., Yang, J., and Carey, J. (1993) *Biochemistry **32***, 7302-7309.

30. Reedstrom, R. J., and Royer, C. A. (1995) *J. Mol. Biol. **253***, 266-276.

31. Schmitt, M. P., and Holmes, R. K. (1993) *Mol. Microbiol. **9***, 173-181.

32. Schmitt, M. P., Twiddy, E. M., and Holmes, R. K. (1992) *Proc. Natl. Acad. Sci. U. S. A.* ***89***, 7576-7580.

33. Tao, X., Boyd, J., and Murphy, J. R. (1992) *Proc. Natl. Acad. Sci. U. S. A.* ***89***, 5897-5901.

34. Tao, X., and Murphy, J. R. (1992) *J. Biol. Chem.* ***267***, 21761-21764.

35. Qiu, X., Pohl, E., Holmes, R. K., and Hol, W. G. (1996) *Biochemistry* ***35***, 12292-12302.

36. Qiu, X., Verlinde, C. L., Zhang, S., Schmitt, M. P., Holmes, R. K., and Hol, W. G. (1995) *Structure* ***3***, 87-100.

37. Schiering, N., Tao, X., Zeng, H., Murphy, J. R., Petsko, G. A., and Ringe, D. (1995) *Proc. Natl. Acad. Sci. U. S. A.* ***92***, 9843-9850.

38. Ding, X., Zeng, H., Schiering, N., Ringe, D., and Murphy, J. R. (1996) *Nat. Struct. Biol.* ***3***, 382-387.

39. Pohl, E., Qui, X., Must, L. M., Holmes, R. K., and Hol, W. G. (1997) *Protein Sci.* ***6***, 1114-1118.

40. Pohl, E., Holmes, R. K., and Hol, W. G. (1998) *J. Biol. Chem.* ***273***, 22420-22427.

41. Pohl, E., Holmes, R. K., and Hol, W. G. (1999) *J. Mol. Biol.* ***292***, 653-667.

42. White, A., Ding, X., vanderSpek, J. C., Murphy, J. R., and Ringe, D. (1998) *Nature* ***394***, 502-506.

43. Love, J. F., vanderSpek, J. C., Marin, V., Guerrero, L., Logan, T. M., and Murphy, J. R. (2004) *Proc. Natl. Acad. Sci. U. S. A.* ***101***, 2506-2511.

44. Twigg, P. D., Parthasarathy, G., Guerrero, L., Logan, T. M., and Caspar, D. L. (2001) *Proc. Natl. Acad. Sci. U. S. A.* ***98***, 11259-11264.

45. Wang, G., Wylie, G. P., Twigg, P. D., Caspar, D. L., Murphy, J. R., and Logan, T. M. (1999) *Proc. Natl. Acad. Sci. U. S. A.* ***96***, 6119-6124.

46. Spiering, M. M., Ringe, D., Murphy, J. R., and Marletta, M. A. (2003) *Proc. Natl. Acad. Sci. U. S. A.* ***100***, 3808-3813.

47. Brinkman, A. B., Ettema, T. J., de Vos, W. M., and van der Oost, J. (2003) *Mol. Microbiol.* ***48***, 287-294.

48. Tani, T. H., Khodursky, A., Blumenthal, R. M., Brown, P. O., and Matthews, R. G. (2002) *Proc. Natl. Acad. Sci. U. S. A.* ***99***, 13471-13476.

49. Leonard, P. M., Smits, S. H., Sedelnikova, S. E., Brinkman, A. B., de Vos, W. M., van der Oost, J., Rice, D. W., and Rafferty, J. B. (2001) *EMBO J.* ***20***, 990-997.

50. Willins, D. A., Ryan, C. W., Platko, J. V., and Calvo, J. M. (1991) *J. Biol. Chem.* ***266***, 10768-10774.

51. Chen, S., Rosner, M. H., and Calvo, J. M. (2001) *J. Mol. Biol.* ***312***, 625-635.

52. Cronan, J. E., Jr. (1989) *Cell* ***58***, 427-429.

53. Barker, D. F., and Campbell, A. M. (1981) *J. Mol. Biol.* ***146***, 469-492.

54. Lane, M. D., Rominger, K. L., Young, D. L., and Lynen, F. (1964) *J. Biol. Chem.* ***239***, 2865-2871.

55. Jitrapakdee, S., and Wallace, J. C. (2003) *Curr. Protein Pept. Sci.* ***4***, 217-229.

56. Rodriguez-Melendez, R., and Zempleni, J. (2003) *J. Nutr. Biochem. 14*, 680-690.

57. Prakash, O., and Eisenberg, M. A. (1979) *Proc. Natl. Acad. Sci. U. S. A.* ***76***, 5592-5595.

58. Abbott, J., and Beckett, D. (1993) *Biochemistry* ***32***, 9649-9656.

59. Eisenstein, E., and Beckett, D. (1999) *Biochemistry* ***38***, 13077-13084.

60. Kwon, K., Streaker, E. D., Ruparelia, S., and Beckett, D. (2000) *J. Mol. Biol.* ***304***, 821-833.

61. Streaker, E. D., and Beckett, D. (1999) *J. Mol. Biol.* ***292***, 619-632.

62. Streaker, E. D., and Beckett, D. (2003) *J. Mol. Biol.* ***325***, 937-948.

63. Streaker, E. D., Gupta, A., and Beckett, D. (2002) *Biochemistry* ***41***, 14263-14271.

64. Wilson, K. P., Shewchuk, L. M., Brennan, R. G., Otsuka, A. J., and Matthews, B. W. (1992) *Proc. Natl. Acad. Sci. U. S. A.* ***89***, 9257-9261.

65. Weaver, L. H., Kwon, K., Beckett, D., and Matthews, B. W. (2001) *Proc. Natl. Acad. Sci. U. S. A.* ***98***, 6045-6050.

66. Kwon, K., and Beckett, D. (2000) *Protein Sci.* ***9***, 1530-1539.

67. Chapman-Smith, A., Mulhern, T. D., Whelan, F., Cronan, J. E., Jr., and Wallace, J. C. (2001) *Protein Sci.* ***10***, 2608-2617.

68. Xu, Y., Nenortas, E., and Beckett, D. (1995) *Biochemistry* ***34***, 16624-16631.

69. Lim, W. A. (2002) *Curr. Opin. Struct. Biol.* ***12***, 61-68.

70. Cronan, J. E., Jr. (1989) *Cell* ***58***, 427-429.

71. Barker, D. F., and Campbell, A. M. (1981) *J. Mol. Biol.* ***146***, 451-467.

72. Otsuka, A., and Abelson, J. (1978) *Nature* ***276***, 689-694.

73. Koradi, R., Billeter, M., and Wuthrich, K. (1996) *J. Mol. Graph.* ***14***, 51-55, 29-32.

74. Chapman-Smith, A., Morris, T. W., Wallace, J. C., and Cronan, J. E., Jr. (1999) *J. Biol. Chem.* ***274***, 1449-1457.

75. Cronan, J. E., Jr. (1988) *J. Biol. Chem.* ***263***, 10332-10336.

76. Weaver, L. H., Kwon, K., Beckett, D., and Matthews, B. W. (2001) *Protein Sci.* ***10***, 2618-2622.

77. Reche, P. A., Howard, M. J., Broadhurst, R. W., and Perham, R. N. (2000) *FEBS Lett.* ***479***, 93-98.

78. Fersht, A. (1985) *Enzyme structure and mechanism*, 2nd ed., W.H. Freeman, New York.

79. Safro, M., and Mosyak, L. (1995) *Protein Sci.* ***4***, 2429-2432.

80. Artymiuk, P. J., Rice, D. W., Poirrette, A. R., and Willet, P. (1994) *Nat Struct Biol* ***1***, 758-760.

81. Cusack, S., Berthet-Colominas, C., Hartlein, M., Nassar, N., and Leberman, R. (1990) *Nature* ***347***, 249-255.

82. Ueda, H., Shoku, Y., Hayashi, N., Mitsunaga, J., In, Y., Doi, M., Inoue, M., and Ishida, T. (1991) *Biochim. Biophys. Acta* ***1080***, 126-134.

83. Belrhali, H., Yaremchuk, A., Tukalo, M., Larsen, K., Berthet-Colominas, C., Leberman, R., Beijer, B., Sproat, B., Als-Nielsen, J., Grubel, G., and et al. (1994) *Science* ***263***, 1432-1436.

84. Bernier, S., Dubois, D. Y., Therrien, M., Lapointe, J., and Chenevert, R. (2000) *Bioorg. Med. Chem. Lett.* ***10***, 2441-2444.

85. Forrest, A. K., Jarvest, R. L., Mensah, L. M., O'Hanlon, P. J., Pope, A. J., and Sheppard, R. J. (2000) *Bioorg. Med. Chem. Lett.* ***10***, 1871-1874.

86. Nenortas, E., and Beckett, D. (1996) *J. Biol. Chem.* ***271***, 7559-7567.

87. Kristinsson, H., Nebel, K., O'Sullivan, A. C., Struber, F., Winkler, T. & Yamaguchi, Y. (1994) *Tetrahedron* ***50***, 6825-6838.

88. Soai, K. O. A. (1986) *J. Org. Chem.* ***51***, 4000-4005.

89. Tener, G. M. (1961) *J. Am. Chem. Soc.* ***83***, 159-168.

90. Johnson, M. L., Correia, J. J., Yphantis, D. A., and Halvorson, H. R. (1981) *Biophys. J.* ***36***, 575-588.

91. Laue, T. M. (1995) *Methods Enzymol.* ***259***, 427-452.

92. Brenowitz, M., Senear, D. F., Shea, M. A., and Ackers, G. K. (1986) *Methods Enzymol.* ***130***, 132-181.

93. Fritsch, E. F., Lawn, R. M. & Maniatis, T. (1980) *Cell* ***19***, 959-972.

94. Johnson, M. L., and Faunt, L. M. (1992) *Methods Enzymol.* ***210***, 1-37.

95. Xu, Y., and Beckett, D. (1994) *Biochemistry* ***33***, 7354-7360.

96. Sekine, S., Nureki, O., Dubois, D. Y., Bernier, S., Chenevert, R., Lapointe, J., Vassylyev, D. G., and Yokoyama, S. (2003) *EMBO J.* ***22***, 676-688.

97. Cusack, S., Yaremchuk, A., and Tukalo, M. (2000) *EMBO J.* ***19***, 2351-2361.

98. Heacock, D., Forsyth, C. J., Kiyotaka, S. & Musier-Forsyth, K. (1996) *Bioorg. Chem.* ***24***, 273-289.

99. Brown, P. H., Cronan, J. E., Grotli, M., and Beckett, D. (2004) *J. Mol. Biol.* ***337***, 857-869.

100. Sigurskjold, B. W. (2000) *Anal. Biochem.* ***277***, 260-266.

101. Xu, Y., Johnson, C. R., and Beckett, D. (1996) *Biochemistry* ***35***, 5509-5517.

102. Pierce, M. M., Raman, C. S., and Nall, B. T. (1999) *Methods* ***19***, 213-221.

103. Christensen, J. J., Hansen, L.D., Izattm R.M., Eds. (1976).

104. Sigurskjold, B. W., Berland, C. R., and Svensson, B. (1994) *Biochemistry* ***33***, 10191-10199.

105. Leavitt, S., and Freire, E. (2001) *Curr. Opin. Struct. Biol.* ***11***, 560-566.

106. Jelesarov, I., and Bosshard, H. R. (1999) *J. Mol. Recognit.* ***12***, 3-18.

107. Velazquez-Campoy, A., Kiso, Y., and Freire, E. (2001) *Arch. Biochem. Biophys.* ***390***, 169-175.

108. Bains, G., and Freire, E. (1991) *Anal Biochem* ***192***, 203-206.

109. Kwon, K., Streaker, E. D., and Beckett, D. (2002) *Protein Sci.* 11, 558-570.

110. Xu, Y., and Beckett, D. (1996) Biochemistry 35, 1783-1792.

111. Reche, P., and Perham, R. N. (1999) EMBO J. 18, 2673-2682.

112. Buoncristiani, M. R., Howard, P. K., and Otsuka, A. J. (1986) Gene 44, 255-261.